NACA RM A54J22

RESEARCH MEMORANDUM

THE PRESSURE-RECOVERY AND PROPELLER-FORCE CHARACTERISTICS OF A PROPELLER-SPINNER-COWLING COMBINATION EMPLOYING NACA 4-(5)(05)-037 SIX- AND EIGHT-BLADE DUAL-ROTATION PROPELLERS WITH AN NACA 1-SERIES D-TYPE COWL

By Robert I. Sammonds and Robert M. Reynolds

Ames Aeronautical Laboratory
Moffett Field, Calif.

NATIONAL ADVISORY COMMITTEE
FOR AERONAUTICS
WASHINGTON
January 27, 1955

NATIONAL ADVISORY COMMITTEE FOR AERONAUTICS

RESEARCH MEMORANDUM

THE PRESSURE-RECOVERY AND PROPELLER-FORCE CHARACTERISTICS OF A PROPELLER-SPINNER-COWLING COMBINATION EMPLOYING NACA 4-(5)(05)-037 SIX- AND EIGHT-BLADE DUAL-ROTATION PROPELLERS WITH AN NACA 1-SERIES D-TYPE COWL

By Robert I. Sammonds and Robert M. Reynolds

SUMMARY

An investigation has been conducted to determine the effect of both six- and eight-blade dual-rotation propellers on the internal-flow characteristics of an NACA 1-series D-type cowl, and the effect of the cowl on the characteristics of the propellers. The pressure recoveries at the cowl inlet and the characteristics of the propellers were measured at Mach numbers from 0.13 to 0.84, inlet velocity ratios from 0.27 to 1.08, advance ratios from 0.80 to 7.29, and propeller blade angles from 40° to 70°. Included are results of surveys, with the propellers removed, of the local velocity distributions ahead of the cowl, measured in the planes of both the front and rear components of the dual-rotation propeller, for an NACA 1-46.5-085 spinner, and in the plane of a single-rotation propeller, for the shorter NACA 1-46.5-047 spinner. All tests of the dual-rotation propeller-spinner-cowling combination were conducted with the model at an angle of attack of 0° and at a Reynolds number of 1.0 million per foot (1.3 million based on the maximum cowl diameter).

With the propeller removed, the ram-recovery ratios for the spinner-cowling combination were greater than 0.96 at inlet velocity ratios above 0.51 and were not affected by compressibility.

Operation of either the six- or eight-blade dual-rotation propeller ahead of the cowl, at maximum efficiency for a given blade angle, resulted in lower recoveries than those for the cowling with the propeller removed. Also, pressure recoveries for the six-blade propeller-spinner-cowling combination were higher than those for the cowl with the eight-blade propeller, although the recoveries for the cowl with either dual-rotation propeller were lower than those for a similar cowl with a four-blade single-rotation propeller.

At the design Mach number of 0.80, inlet velocity ratio of 0.50, and advance ratio of 4.2 and the near-design blade angle of 65°, the maximum efficiencies for the six- and eight-blade dual-rotation propellers with the cowl were 75 and 76 percent, respectively.

The maximum efficiencies of the six- and eight-blade dual-rotation propellers when operating in the presence of the cowl were higher, at all comparable conditions, than those for the isolated dual-rotation propeller-spinner combinations.

The effect of inlet velocity ratio on the propeller characteristics was small.

INTRODUCTION

The successful application of the turbine-propeller-type power plant is dependent, in part, on the combined efficiency of the propeller and air-induction system.

Considerable research has been conducted to determine the effect of propeller operation and propeller-spinner-juncture configuration on the internal-flow characteristics of an NACA D-type cowl and the effect of the cowl on the propeller characteristics (refs. 1 to 6). Investigations also have been conducted to determine the internal-flow characteristics of a single-rotation NACA E-type cowl (refs. 7 and 8). However, the major portion of these investigations has been carried out with regard to single-rotation propellers of current design suitable for turbine-propeller powerplant installations (refs. 1 to 4). In contrast, the data available in regard to dual-rotation propellers are limited primarily to the effect of propeller operation and propeller-spinner-juncture configuration on the internal-flow characteristics of the NACA D-type cowl (refs. 5 and 6).

Because of the many significant advantages of the dual-rotation propeller as compared to the single-rotation propeller (i.e., reduced diameter, higher efficiency, absence of reaction torque, and less noise), an investigation has been conducted in the Ames 12-foot pressure wind tunnel to determine the effect of both six- and eight-blade dual-rotation propellers on the internal-flow characteristics of an NACA D-type cowl and the effect of the cowl on the propeller characteristics. One phase of the investigation, the determination of the aerodynamic characteristics of the six- and eight-blade propellers in the absence of the cowl, has been reported in reference 9.

In the phase of the investigation reported herein, tests were made with the cowling-spinner combination alone (propeller removed) and with the cowling-spinner combination in conjunction with both six- and eight-blade dual-rotation propellers.

NOTATION

a	speed of sound[1]
B	number of blades
b	blade width
C_P	power coefficient, $\dfrac{P}{\rho n^3 D^5}$
C_T	thrust coefficient, $\dfrac{T}{\rho n^2 D^4}$
c_{l_d}	blade-section design lift coefficient
D	propeller diameter
H	total pressure[1]
$\dfrac{H_1-p}{H-p}$	ram-recovery ratio
h	maximum thickness of blade section
J	advance ratio, $\dfrac{V_o}{nD}$
M	Mach number, $\dfrac{V}{a}$
M_t	tip Mach number, $M\sqrt{1+\left(\dfrac{\pi}{J}\right)^2}$
n	propeller rotational speed
P	power

[1]As used herein, values of a, H, p, V, and ρ appearing without subscripts refer to conditions in the wind-tunnel air stream at a datum velocity that has been corrected for blockage by the cowling but is uncorrected for wind-tunnel-wall constraint on the propeller slipstream. (See ref. 2.)

p static pressure[2]

R propeller-tip radius

r radius from center of rotation

T thrust

U local velocity in propeller plane

V air-stream velocity[2]

V_o equivalent free-air velocity (air-stream velocity corrected for tunnel-wall constraint on the propeller slipstream)

$\frac{V_1}{V}$ inlet velocity ratio

β propeller blade angle at 0.75 R

$\Delta\beta$ difference between the blade angles for the front and rear components of the dual-rotation propellers

β_d design propeller-blade-section angle

η efficiency, $\frac{C_T}{C_P} J$

ρ mass density of air[2]

Subscripts

1 ram-recovery rake location

F front component of dual-rotation propeller

R rear component of dual-rotation propeller

a apparent (applied to propeller characteristics when operating ahead of the cowl)

---

[2]See footnote 1 on page 3.

MODEL AND APPARATUS

The model used in this investigation consisted of an NACA 1-62.8-070 D-type cowl in combination with an NACA 1-46.5-085 spinner and NACA 4-(5)(05)-037 six- and eight-blade dual-rotation propellers. (See refs. 10 and 11 for explanation of cowling-spinner and propeller designations, respectively.) A photograph of the model mounted on the 1000-horsepower dynamometer in the Ames 12-foot pressure wind tunnel is shown in figure 1. A sketch of the general model arrangement, showing the principal model dimensions, is shown in figure 2.

Design Conditions

The model investigated simulates a propeller-cowling-spinner combination for a turboprop installation having the following design requirements:

Altitude, ft	35,000
Mach number (cruise)	0.80
Horsepower	5600
Engine air flow, lb/sec	40
Propeller diameter, ft	
Six-blade dual	19
Eight-blade dual	18
Advance ratio	4.2
Inlet velocity ratio	0.5

Spinner-Cowling Combination

The NACA 1-62.8-070 D-type cowl and the NACA 1-46.5-085 spinner were selected, on the basis of the design requirements, in accordance with the method of reference 10. The cowling selected was the same as that described in reference 1, except that the diameter of the model was increased to accommodate the larger diameter spinner required to enclose the dual-rotation propeller-hub assembly. An NACA 1-series inner liner was incorporated at the inner lip, as recommended in reference 10, to delay the separation of the air flow from the inner lip at high inlet velocity ratios. Coordinates for the cowling-spinner combination are shown in table I.

Propellers and Propeller-Spinner Juncture

The NACA 4-(5)(05)-037 six- and eight-blade dual-rotation propellers were those described in reference 9. The blade-form curves for the propellers are shown in figure 3. Except for total solidity, the six- and eight-blade dual-rotation propellers were identical.

The propeller-spinner junctures shown in figure 4 are of the platform type, identical to those recommended in reference 5 and used with the NACA 1-46.5-085 spinner reported in reference 9. A sketch and the coordinates of the platform are shown in figure 5. The surfaces of the platform and propeller blade that bound the gap were formed by rotating the surface element defined by the platform coordinates, tabulated in figure 5, about the axis of the propeller blade in order that the gap between the platform and the blade remain unchanged as the blade angle is varied. The platforms were set to aline with the propeller blade sections when the blade angle of the front component of the dual-rotation propeller was set at 65°.

1000-Horsepower Dynamometer

The 1000-horsepower dynamometer used for this investigation was the dynamometer described in detail in reference 11, modified for use in testing dual-rotation propellers by the installation of a gearbox within the dynamometer housing and a torquemeter on each of two concentric propeller drive shafts as described in reference 9. These two torquemeters were similar in design and operation to the torquemeter described in reference 11 but had one half the capacity and twice the sensitivity.

Instrumentation

The instrumentation of the model was identical to that described in reference 1 and consisted of four shielded total-pressure rakes and two static-pressure rakes. Each rake was composed of eight tubes disposed radially across the duct in such a manner that each total-pressure tube was in the center of an area equal to one thirty-second of the total duct area. Calibration of these total-pressure rakes indicated that the error in the measured impact pressure was probably less than 1.0 percent at angles of attack up to 40° for Mach numbers up to 0.85. No attempt was made to calibrate the static-pressure rakes as the measured static pressures were considered to be within the accuracy required for the calculations of inlet velocity ratio.

The survey rake used to determine the local velocities in the propeller plane consisted of 24 static-pressure tubes at the radii listed in table II.

TESTS AND REDUCTION OF DATA

Tests

In the investigation reported herein, tests were made with the cowling-spinner combination alone (propeller removed) and with the cowling-spinner combination in conjunction with both six- and eight-blade dual-rotation propellers. With the propeller removed, measurements were made of the pressure recoveries at the cowl inlet and the velocities in the plane of each component of the propeller at inlet velocity ratios from 0.27 to 1.09 and for Mach numbers from 0.30 to 0.84. With the propeller installed and operating, measurements were made of the pressure recovery at the cowl inlet and the thrust, torque, and rotational speed of both dual-rotation propellers for blade angles from 40° to 70°, Mach numbers from 0.30 to 0.84, and inlet velocity ratios from 0.27 to 1.08, as listed in table III.

For all propeller tests, the difference between the front and rear propeller blade angles ($\beta_F-\beta_R$) was 0.8° (design $\Delta\beta$).

Surveys of the velocity distributions in the plane of the propeller, with the propeller removed, were made for the single-rotation spinner-cowling combination (NACA 1-46.5-047 spinner, NACA 1-62.8-070 D-type cowl) reported in reference 1.

All tests of the dual-rotation propeller-spinner-cowling combination were made with the model at an angle of attack of 0° and at a Reynolds number of 1.0 million per foot (1.3 million based on the maximum cowl diameter). The velocity surveys near the single-rotation spinner-cowling combination were made at a Reynolds number of 1.8 million, based on the maximum cowl diameter.

Mach Number

The Mach numbers given in this report are the average Mach numbers over the disc area of the propeller, determined by velocity surveys in the presence of the dynamometer body with the cowl removed, as reported in reference 11. The Mach number (and the corresponding dynamic pressure) was corrected for the wind-tunnel blockage due to the cowl by the method of reference 12, but in no case did this correction exceed 1 percent.

Tunnel-Wall Corrections

The air-stream velocity (and, consequently, propeller advance ratio and efficiency) was corrected for the wind-tunnel-wall constraint on the propeller slipstream by the method of reference 13. For Mach numbers of 0.30 and above, at all of the test blade angles, this correction did not exceed 2 percent and was less than 4 percent at a Mach number of 0.13.

Flow Surveys

The inlet velocity ratio, calculated in accordance with the method of reference 14, can be readily converted to mass-flow ratio by use of figure 4 of reference 14.

The ram-recovery ratio presented as a function of radial location in the duct is the arithmetic average of the recoveries from the four total-pressure tubes at each of the eight radial locations. All other values of ram-recovery ratio were computed from an arithmetic average of the readings from all 32 total-pressure tubes, which is equivalent to an area-weighted average.

The local velocities in the propeller plane were corrected for the rake calibration and for the radial velocity gradient in the tunnel (ref. 11) due to the influence of the dynamometer body. However, no attempt was made to correct the static-pressure readings near the surface of the spinner for flow angularity, and, as a result, the values of local velocity presented herein for the low inlet velocity ratios may be somewhat in error.

Thrust and Torque

The thrust, torque, and rotational speed of the propellers were measured in a manner similar to that reported in reference 11. The thrust, as used herein, is the algebraic difference between the longitudinal force produced by the propeller-spinner combination operating in the presence of the cowl and the longitudinal force produced by the spinner alone (also in the presence of the cowl) at the same air velocity, density, and inlet velocity ratio. The method of determining the propeller thrust is discussed in detail in references 2 and 11. The total torque presented for the dual-rotation propellers is the sum of the torques measured for the front and rear components of the propeller.

Analysis of the accuracy of the separate measurements of thrust, torque, and air-stream velocity, as in reference 11, indicates that errors in the propeller efficiencies reported herein are probably less than 2 percent.

RESULTS AND DISCUSSION

The results of this investigation are presented in figures 6 through 24. An index of these figures is presented in table III and gives the model configuration and the range of the variables for each figure. Additional values of the velocity ratios in the plane of the front and rear components of the dual-rotation propeller and the single-rotation propeller, with the propellers removed, are tabulated in table II.

Internal-Flow Characteristics

<u>Spinner-cowling combination with propeller removed.</u>- Examination of the ram-recovery ratios presented in figure 6 for the NACA 1-62.8-070 D-type cowl in combination with an NACA 1-46.5-085 dual-rotation spinner indicates that the losses in recovery were a result of the boundary-layer build-up on the spinner.

The comparison in figure 7 of the averages of these data with comparable data from reference 1, for a similarly designated cowling with an NACA 1-46.5-047 spinner, shows that the recoveries obtained with the long (-085) spinner were lower for all test inlet velocity ratios (1.5 percent lower at the respective design conditions: $M = 0.80$, $V_1/V = 0.50$ for the -085 spinner, and $M = 0.80$, $V_1/V = 0.42$ for the -047 spinner). Figure 7 also shows that, because of the increase in boundary-layer thickness for a constant inlet velocity ratio due to the longer -085 spinner (13.22 inches as compared to 6.58 inches for the -047 spinner), the inlet velocity ratio required to avoid excessive losses in the duct was higher for the -085 spinner than for the -047 spinner (0.51 as compared to 0.45). A further comparison in figure 7 of the present data with those for a model of the same geometric proportions (reported in ref. 5) shows relatively good agreement (less than 1-percent difference in recovery at the design condition), except at inlet velocity ratios greater than 0.8. In regard to the data from reference 5, it may be noted that in that reference the high recoveries at inlet velocity ratios greater than 0.8 were associated with a condition of extensive laminar flow over the spinner. Differences in the spinner surface conditions between the model of reference 5 and the model reported herein (the spinner of reference 5 had a smooth, continuous, painted surface, whereas the spinner of the present investigation had machined surfaces and a discontinuity at the gap between the front and rear components) may account for the differences in recovery at the high inlet velocity ratios. It should also be noted that there were differences in the total-pressure-tube instrumentation and the location of the survey station between the two models. The model reported in reference 5 had one rake at the top vertical center line, 6 percent of the cowl diameter behind the leading edge of the cowl as compared to the present model having four rakes 90° apart, 18 percent of the cowl diameter behind the leading edge of the cowl.

The ram-recovery ratios for the present model were greater than 0.96 at inlet velocity ratios greater than 0.51 and were not affected by compressibility within the range of Mach numbers covered in this investigation (fig. 7). It can be seen from figure 6, however, that increasing the inlet velocity ratio to values greater than 0.50 resulted in a decrease in the recovery near the outer surface of the duct.

Spinner-cowling combination with propeller operating.- Examination of the data presented in figures 8 to 12 indicates that with the addition of the dual-rotation propeller to the spinner-cowling combination, the recoveries behind the operating propeller were affected not only by the spinner boundary layer, as was the case with the propeller removed, but also by the angle of attack (loading) of the platform and inner portions of the propeller blade, the air flow through the gap between the platform and the propeller blade, and other propeller interference effects.

Analysis of the data in figures 8 to 12 indicates that for a constant inlet velocity ratio, operation of the propeller at combinations of blade angles, rotational speeds, and forward speeds that increased the angle of attack (and thus the loading) of the platform and the inner portion of the blade generally resulted in increased recoveries due to the pumping action of the platform and inner portions of the blades. As can be seen from figures 8 and 9 for the low Mach numbers, recoveries in excess of 1.0 were obtained when the propellers were operated at blade angles up to 60° and at high rotational speeds. For these operating conditions, it is apparent that the pumping action of the platform and inner portions of the blade added sufficient energy to the air stream to overcome the energy losses due to the spinner boundary layer. A further analysis of the data in figures 8(a) and 9(a) indicates that at blade angles of 40° and 50° the large effect of rotational speed on the pressure recoveries results from the fact that the angle of attack of the inner portions of the blade varied over a wide range (e.g., for a $\beta_F = 40^\circ$, $J = 1.1$ to 2.0, and $r = 4$ inches the change in angle of attack was of the order of 12°). Also at these conditions of operation, the difference in the angle of attack of the platform and inner blade sections is quite large and, as can be seen from figures 11(a) and (b) for the high inlet velocity ratios, this difference in angle of attack (loading) plus the air flow through the juncture gap resulted in a relatively uneven distribution of recovery radially across the duct. At a propeller blade angle of 40° and for the advance ratios presented in figures 11(a) and (b), the platform was operating at a positive angle of attack and producing thrust; whereas the inner blade sections were operating near zero angle of attack. At the low inlet velocity ratios, the platform did not impart sufficient energy to the air stream to overcome the energy losses due to the spinner boundary layer.

Although decreasing the inlet velocity ratio at a constant Mach number, blade angle, and rotational speed also increased the angle of attack of the platform and inner portions of the blade, it is apparent from figures 8 to 12 that for a given decrease in inlet velocity ratio, the losses in energy due to the increase in spinner boundary-layer thickness were greater than the increase in energy imparted to the air stream by the change in angle of attack of the platform and inner blade sections, resulting in an over-all decrease in recovery with decreasing inlet velocity ratio.

The effect of Mach number on the pressure recoveries at the inlet is readily apparent in figure 12, in which it can be seen that for a constant blade angle, inlet velocity ratio, and advance ratio, an increase in Mach number generally resulted in a decrease in recovery, due to the compressibility effects on the platform and inner portions of the blades. However, it can also be seen from figure 12 that, for a blade angle of 60°, the inlet velocity ratio at which excessive losses occurred at the cowl inlet was lower at high Mach numbers than that at low Mach numbers.

The recovery data presented in figure 13 show that the addition of either the six- or eight-blade dual-rotation propellers to the basic cowling-spinner combination resulted in an appreciable decrease in recovery due to the interference effects of the propellers. However, figure 13 (and also figs. 8, 9, and 11) shows that for a given set of operating conditions, the recoveries for the six-blade propeller were higher for all the test conditions than those for the eight-blade propeller. This indicates that the effectiveness (relationship between pumping action and interference effects) of the platform and inner portions of the blades was higher for the six-blade propeller than for the eight-blade propeller.

Sealing the gap between the platform and propeller blade, for the blade angle at which the propeller was alined with the platform (figs. 10 and 14), resulted in higher recoveries at the cowl inlet throughout the test range of inlet velocity ratios than those for operation of the propeller with the gap open. This effect is similar to that reported in reference 6 and can be attributed to eliminating the flow through the gap. Although sealing the platform gap of the dual-rotation propeller of this report resulted in a relatively large increase in recovery, the effect of sealing the gap of the single-rotation propeller reported in reference 1, for a comparable condition, was small.

The comparison presented in figure 14 also shows that the recoveries at the respective design advance ratios and near design blade angles were generally lower for the dual-rotation propeller-spinner-cowling combination of this report than those for the single-rotation propeller-spinner-cowling combination reported in reference 1 or the single-rotation E-type cowl reported in reference 8. However, at high values of inlet velocity ratio the E-type cowl operated as a turbine, absorbing energy from the air stream, with consequent losses in recovery as compared with those for the cowl with the dual-rotation propellers. These lower recoveries obtained for the dual-rotation propeller-spinner-cowling combination resulted from the increased boundary-layer thickness due to the longer -085 dual-rotation spinner and the larger interference effects of six- and eight-blade propellers as compared to the single-rotation propeller-spinner-cowling combination or the single-rotation E-type cowl.

Propeller Characteristics

In accord with the discussion in reference 15, the characteristics of both the six- and eight-blade dual-rotation propellers operating in the presence of the cowl are presented as apparent values (figs. 16 to 23) since the determination of propulsive thrust was precluded by the fact that it was impractical, with the dynamometer arrangement used in the present investigation, to measure the increase in drag of the cowl and dynamometer parts within the influence of the propeller slipstream. Surveys of the velocities in the planes of both the front and rear components of the dual-rotation propeller with the propeller removed (table II and fig. 15) show that the cowl had a considerable effect on these velocities, especially in the plane of the rear component where at low values of inlet velocity ratio the local velocities near the surface of the spinner were reduced nearly 30 percent. As would be expected with these reduced velocities, the thrust and power coefficients for the dual-rotation propeller operating ahead of the cowl were greater than those for the isolated propeller-spinner combination of reference 9 when operating at the same advance ratio, blade angle, and Mach number, as shown in figure 20.

Power coefficients.- The power coefficients presented in figures 18 and 19, show that for $\Delta\beta = 0.8$, the front and rear components of the dual-rotation propellers did not absorb equal power when operating at the advance ratio for maximum efficiency. On the basis of the data in reference 9, it would be expected that, had the propellers been operated at the $\Delta\beta$ for equal power absorption by both components of the dual-rotation propeller at the advance ratio for maximum efficiency, the efficiencies would probably have been of the order of 2 percent higher.

Effects of solidity and of sealing the juncture gap.- The comparison in figure 21 of the characteristics of the six- and eight-blade dual-rotation propellers, on the basis of equal total activity factor, shows good agreement between the characteristics of the two propellers.

As would be expected from the data reported in references 2 and 9, operation of the propeller with the gaps between the platforms and propeller blades sealed resulted in no significant change in the propeller characteristics (fig. 22).

Maximum efficiency.- As can be seen from figure 23, the maximum efficiencies obtained for the dual-rotation propellers in the presence of the cowl were higher at all comparable Mach numbers and blade angles than those for the isolated propeller-spinner combination. At a blade angle of 65° (near design blade angle) and a Mach number of 0.80 (design Mach number), the efficiencies of the six- and eight-blade dual-rotation propellers with the cowl were 75 and 76 percent, as compared to 63 and 61 percent for the isolated condition. In comparison, the efficiencies of the four-blade single-rotation propeller, reported in references 2 and 11, at the design blade angle of 60° and the design Mach number of 0.80 were 78 and 59 percent for the cowl-on and -off conditions, respectively. It should be emphasized that the changes in maximum efficiency due to the addition of the cowl for these propellers for the design, or near design, conditions apply only thereto; that is, at a given Mach number the change in efficiency would not necessarily be the same for some other blade angle. It may be noted that on the basis of the velocity ratios presented in figure 15 and table II, the interference effects of the cowl on the maximum efficiency of the dual-rotation propeller would be expected to be somewhat less than that on the single-rotation propeller, due to the fact that the front component of the dual-rotation propeller was little affected by the flow field about the cowl (with near free-stream velocity over the entire blade); whereas the interference of the cowl on the single-rotation propeller and the rear component of the dual-rotation propeller was quite pronounced over the inner portion of the blades and of approximately the same magnitude. However, due to geometric differences between the single- and dual-rotation propellers which preclude the citing of comparisons on the basis of equal blade angle, the relative interference effects of the cowl on the maximum efficiencies of these propellers cannot be determined from the data available.

The maximum efficiencies for the cowl-on conditions reported herein and in reference 2 are presented for an inlet velocity ratio of 0.80. However, examination of the propeller characteristics in figures 16 and 17 shows that the effect of inlet velocity ratio on the thrust and power coefficients and on the propeller efficiency was small. Similarly, results presented in reference 2 show that for the four-blade single-rotation propeller, the effect of inlet velocity ratio on the propeller characteristics was also small.

CONCLUDING REMARKS

The following remarks may be made regarding the results of the subject investigation.

With the propeller removed, the ram-recovery ratios for the spinner-cowling combination were greater than 0.96 at inlet velocity ratios above 0.51 and were not affected by compressibility in the test range of Mach number.

Operation of either the six- or the eight-blade dual-rotation propeller at the advance ratio for maximum efficiency resulted in lower pressure recoveries than those for the spinner-cowling combination with the propeller removed. However, for certain off-design conditions for the propellers when the platforms and inner blade sections were highly loaded, operation of the propellers improved the pressure recoveries and for certain conditions gave pressure recoveries greater than 1.0. Also, pressure recoveries for the six-blade propeller-spinner-cowling combination were higher than those for the cowl with the eight-blade propeller, although the recoveries for the cowl with either dual-rotation propeller were lower than those for a similar cowl with a four-blade single-rotation propeller.

The pressure recoveries for the dual-rotation propeller-spinner-cowling combination with the gap between the platform and propeller blade sealed (propeller alined with platform) were higher than those for the same combination with the gap open.

The local velocities in the plane of the rear component of the dual-rotation propeller were considerably reduced by the presence of the cowl (nearly 30 percent lower than free-stream velocity near the surface of the spinner for low inlet velocity ratios), whereas the velocities in the plane of the front component were nearly free-stream.

At the design Mach number of 0.80, inlet velocity ratio of 0.50, advance ratio of 4.2, and the near design blade angle of 65°, the maximum efficiencies obtained for the six- and eight-blade dual-rotation propellers with the cowl were 75 and 76 percent, respectively.

The maximum efficiencies of the six- and eight-blade dual-rotation propellers when operating in the presence of the cowl were higher, for all comparable conditions, than those for the isolated dual-rotation propeller-spinner combinations.

The effect of inlet velocity ratio on the propeller characteristics was small.

Ames Aeronautical Laboratory
National Advisory Committee for Aeronautics
Moffett Field, Calif., Oct. 22, 1954

REFERENCES

1. Sammonds, Robert I., and Molk, Ashley J.: Effects of the Propeller-Spinner Juncture on the Pressure-Recovery Characteristics of an NACA 1-Series D-Type Cowl in Combination With a Four-Blade Single-Rotation Propeller at Mach Numbers Up to 0.83 and at an Angle of Attack of 0°. NACA RM A52D01a, 1952.

2. Reynolds, Robert M., Sammonds, Robert I., and Kenyon, George C.: An Investigation of a Four-Blade Single-Rotation Propeller in Combination With an NACA 1-Series D-Type Cowling at Mach Numbers Up to 0.83. NACA RM A53B06, 1953.

3. Molk, Ashley J., and Reynolds, Robert M.: Effects of Two Spinner Shapes on the Pressure Recovery in an NACA 1-Series D-Type Cowl Behind a Three-Blade Propeller at Mach Numbers Up to 0.80. NACA RM A53I29a, 1954.

4. Kenyon, George C., and Reynolds, Robert M.: Investigation of a Three-Blade Propeller in Combination With Two Different Spinners and an NACA D-Type Cowl at Mach Numbers Up to 0.80. NACA RM A54B18a, 1954.

5. Keith, Arvid L., Jr., Bingham, Gene J., and Rubin, Arnold J.: Effects of Propeller-Shank Geometry and Propeller-Spinner-Juncture Configuration on Characteristics of an NACA 1-Series Cowling-Spinner Combination With an Eight-Blade Dual-Rotation Propeller. NACA RM L51F26, 1951.

6. Bingham, Gene J., and Keith Arvid L., Jr.: Effects of Compressibility at Mach Numbers up to 0.8 on Internal-Flow Characteristics of a Cowling-Spinner Combination Equipped With an Eight-Blade Dual-Rotation Propeller. NACA RM L53E12, 1953.

7. Reynolds, Robert M., and Sammonds, Robert I.: Subsonic Mach and Reynolds Number Effects on the Surface Pressures, Gap Flow, Pressure Recovery, and Drag of a Nonrotating NACA 1-Series E-Type Cowling at an Angle of Attack of 0°. NACA RM A51E03, 1951.

8. Sammonds, Robert I., and Reynolds, Robert M.: Effect of Rotation of an NACA 1-Series E-Type Cowling on the Internal Flow and Force Characteristics of the Cowling at Mach Numbers Up to 0.84 and at an Angle of Attack of 0°. NACA RM A54G14, 1954.

9. Walker, John H., and Reynolds, Robert M.: Investigation of the NACA 4-(5)(05)-037 Six- and Eight-Blade, Dual-Rotation Propellers at Positive and Negative Thrust at Mach Numbers Up to 0.90, Including Some Characteristics of the NACA 4-(5)(05)-041 Two- and Four-Blade, Single-Rotation Propellers. NACA RM A54G13, 1954.

10. Nichols, Mark R., and Keith, Arvid L., Jr.: Investigation of a Systematic Group of NACA 1-Series Cowlings With and Without Spinners. NACA Rep. 950, 1949. (Formerly NACA RM L8A15)

11. Reynolds, Robert M., Buell, Donald A., and Walker, John H.: Investigation of an NACA 4-(5)(05)-041 Four-Blade Propeller With Several Spinners at Mach Numbers up to 0.90. NACA RM A52I19a, 1952.

12. Herriot, John G.: Blockage Corrections for Three-Dimensional-Flow Closed-Throat Wind Tunnels, With Consideration of the Effect of Compressibility. NACA Rep. 995, 1950. (Supersedes NACA RM A7B28)

13. Young, A. D.: Note on the Application of the Linear Perturbation Theory to Determine the Effect of Compressibility on the Wind Tunnel Constraint on a Propeller. R.A.E. TN No. Aero. 1539, British A.R.C., 1944.

14. Smith, Norman F.: Numerical Evaluation of Mass-Flow Coefficient and Associated Parameters from Wake Survey Equations. NACA TN 1381, 1947.

15. Glauert, H.: Airplane Propellers Body and Wing Interference. Vol. IV of Aerodynamic Theory, div. L, ch. VIII, W. F. Durand, ed., Julius Springer (Berlin), 1935. (CIT reprint 1943)

TABLE I. — COWLING–SPINNER COORDINATES
[Coordinates in inches]

Distance from leading edge of cowl, x_c	NACA 1-62.8-070 cowl, radius, r_c	Distance from leading edge of cowl, x_i	NACA 1-series inner lip, radius, r_i	Distance from leading edge of spinner, x_s	NACA 1-46.5-085 spinner, radius, r_s
0	4.955	0	4.955	0	0
.022	5.091	.005	4.939	.053	.240
.044	5.142	.009	4.932	.106	.337
.065	5.184	.019	4.921	.198	.460
.109	5.248	.028	4.913	.331	.599
.218	5.371	.037	4.905	.463	.721
.327	5.472	.047	4.899	.595	.830
.436	5.561	.070	4.884	.793	.977
.544	5.643	.093	4.873	1.058	1.151
.871	5.853	.117	4.863	1.454	1.380
1.198	6.032	.140	4.854	1.851	1.579
1.524	6.188	.187	4.838	2.248	1.751
1.851	6.321	.234	4.826	2.644	1.906
2.178	6.443	.280	4.816	3.173	2.095
2.613	6.590	.327	4.808	3.702	2.267
3.049	6.724	.374	4.803	4.231	2.424
3.484	6.847	.420	4.800	4.760	2.570
3.920	6.961	.467	4.799	5.289	2.704
4.356	7.065	--	--	5.818	2.827
4.791	7.161	--	--	6.347	2.939
5.227	7.249	--	--	7.140	3.091
5.880	7.367	--	--	8.198	3.265
6.751	7.503	--	--	9.255	3.398
7.840	7.630	--	--	10.313	3.501
8.711	7.703	--	--	11.371	3.571
9.800	7.761	--	--	12.429	3.612
10.889	7.778	--	--	13.222	3.617

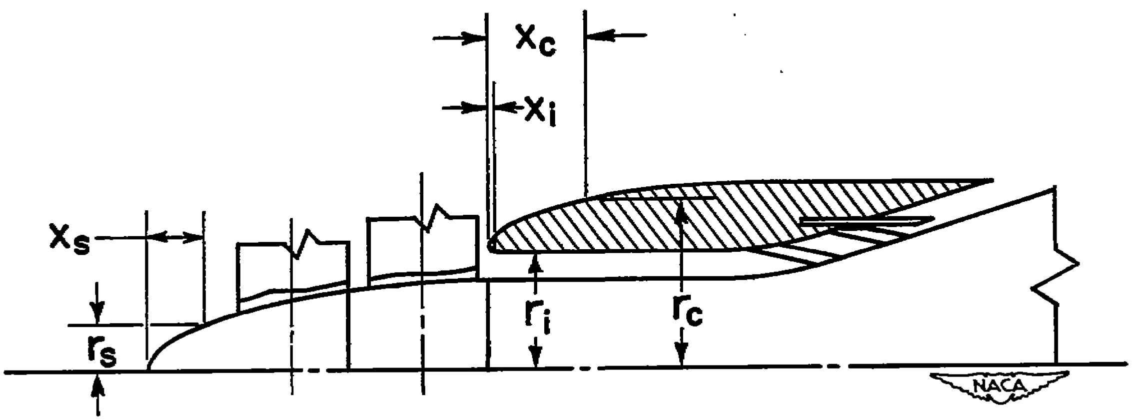

TABLE II.– LOCAL VELOCITY RATIO, U/V

(a) NACA 1-46.5-085 dual-rotation spinner, front plane of rotation

Radial station, in.	M = 0.30						M = 0.40						M = 0.60					
	Inlet velocity ratio, V_1/V						Inlet velocity ratio, V_1/V						Inlet velocity ratio, V_1/V					
	0.29	0.39	0.52	0.59	0.80	1.09	0.31	0.41	0.51	0.62	0.82	1.09	0.32	0.40	0.50	0.58	0.80	1.05
3.26	0.949	0.959	0.963	0.966	0.976	0.983	0.945	0.957	0.962	0.965	0.972	0.978	0.952	0.958	0.957	0.969	0.971	0.974
3.51	.953	.963	.966	.969	.980	.983	.947	.959	.962	.967	.975	.980	.950	.949	.954	.962	.971	.978
3.76	.949	.959	.963	.963	.973	.983	.945	.958	.959	.962	.967	.975	.947	.950	.954	.959	.964	.971
4.01	.938	.945	.952	.955	.962	.972	.933	.944	.950	.952	.956	.967	.935	.940	.945	.952	.954	.959
4.26	.945	.948	.958	.958	.965	.972	.937	.949	.952	.954	.962	.967	.938	.940	.945	.952	.955	.962
4.76	.932	.942	.948	.948	.958	.965	.925	.938	.941	.943	.951	.959	.930	.933	.936	.943	.950	.954
5.26	.934	.944	.951	.951	.954	.964	.928	.940	.943	.946	.951	.959	.931	.933	.936	.943	.947	.954
5.76	.936	.943	.946	.950	.953	.969	.928	.940	.941	.943	.951	.956	.933	.933	.936	.940	.949	.952
6.26	.933	.940	.943	.943	.950	.956	.928	.938	.941	.943	.948	.958	.933	.933	.936	.940	.947	.948
7.26	.939	.942	.945	.945	.952	.955	.930	.937	.940	.942	.947	.953	.933	.935	.936	.941	.943	.948
8.26	.938	.941	.941	.941	.944	.951	.932	.937	.940	.942	.947	.953	.928	.928	.931	.933	.938	.938
9.26	.956	.964	.964	.967	.970	.967	.952	.959	.964	.962	.964	.967	.952	.952	.954	.959	.962	.962
10.26	.959	.963	.963	.962	.963	.969	.957	.962	.962	.962	.964	.967	.958	.954	.954	.955	.957	.957
12.26	.965	.968	.968	.968	.972	.971	.962	.965	.965	.967	.967	.970	.960	.960	.958	.961	.963	.963
14.26	.971	.971	.971	.970	.971	.974	.965	.967	.970	.970	.972	.975	.962	.960	.961	.961	.965	.963
16.26	.975	.975	.975	.975	.975	.979	.968	.973	.976	.973	.973	.971	.975	.970	.972	.975	.975	.972
18.26	.979	.982	.982	.978	.982	.982	.976	.976	.978	.978	.978	.976	.979	.976	.978	.977	.976	.978
20.26	.983	.987	.987	.983	.987	.987	.981	.984	.987	.984	.984	.979	.989	.987	.989	.989	.987	.987
22.26	.983	.983	.983	.985	.980	.983	.981	.984	.989	.986	.986	.987	.989	.986	.986	.988	.988	.988
24.26	.992	.996	.992	.992	.989	.992	.986	.988	.991	.990	.990	.991	.992	.988	.988	.990	.990	.988
26.26	.991	.995	.995	.995	.991	.988	.987	.989	.992	.987	.989	.992	.996	.991	.993	.992	.993	.991
28.26	.990	.990	.990	.990	.990	.990	.986	.988	.991	.991	.988	.991	.994	.992	.991	.992	.992	.991
30.26	.990	.990	.990	.990	.987	.990	.985	.990	.993	.990	.990	.990	.993	.990	.990	.991	.991	.990
32.26	.989	.993	.989	.989	.989	.993	.984	.986	.989	.986	.986	.987	.991	.991	.991	.991	.989	.989

Radial station, in.	M = 0.70						M = 0.80						M = 0.84					
	Inlet velocity ratio, V_1/V						Inlet velocity ratio, V_1/V						Inlet velocity ratio, V_1/V					
	0.29	0.40	0.50	0.59	0.82	1.06	0.32	0.41	0.48	0.62	0.81	1.00	0.30	0.42	0.47	0.60	0.83	0.95
3.26	0.940	0.950	0.956	0.963	0.969	0.970	0.940	0.945	0.955	0.961	0.965	0.969	0.935	0.944	0.949	0.950	0.961	0.964
3.51	.941	.950	.956	.961	.967	.968	.938	.945	.947	.953	.959	.964	.933	.940	.947	.945	.961	.961
3.76	.934	.944	.950	.955	.961	.964	.934	.941	.947	.952	.960	.963	.929	.936	.942	.944	.955	.955
4.01	.928	.935	.943	.946	.952	.955	.925	.930	.938	.944	.949	.953	.919	.927	.931	.935	.946	.946
4.26	.928	.938	.943	.955	.955	.965	.926	.932	.939	.944	.952	.956	.921	.930	.935	.936	.947	.949
4.76	.919	.929	.932	.939	.945	.947	.916	.924	.928	.935	.941	.947	.911	.919	.925	.931	.936	.938
5.26	.920	.931	.934	.939	.945	.947	.918	.924	.930	.943	.944	.947	.914	.922	.926	.932	.938	.940
5.76	.919	.928	.934	.939	.945	.943	.917	.921	.930	.932	.939	.941	.910	.917	.921	.926	.932	.935
6.26	.917	.926	.934	.937	.942	.943	.917	.921	.928	.931	.937	.940	.910	.918	.922	.926	.932	.932
7.26	.920	.928	.932	.937	.940	.943	.917	.921	.926	.931	.937	.940	.912	.919	.922	.927	.931	.932
8.26	.926	.932	.937	.940	.945	.943	.922	.928	.932	.935	.943	.943	.917	.925	.929	.934	.941	.942
9.26	.943	.949	.952	.955	.957	.965	.937	.940	.948	.948	.955	.956	.933	.937	.938	.945	.952	.951
10.26	.940	.943	.947	.951	.951	.952	.934	.937	.942	.943	.947	.948	.928	.931	.933	.936	.941	.938
12.26	.949	.952	.955	.957	.958	.959	.942	.942	.946	.948	.951	.951	.934	.939	.939	.940	.946	.945
14.26	.953	.955	.955	.957	.963	.965	.942	.944	.946	.947	.949	.951	.936	.940	.939	.940	.946	.944
16.26	.967	.968	.968	.972	.969	.968	.961	.961	.962	.963	.965	.967	.953	.955	.957	.955	.958	.958
18.26	.974	.974	.974	.976	.975	.973	.968	.968	.967	.969	.969	.971	.962	.962	.963	.962	.964	.963
20.26	.983	.985	.985	.987	.985	.982	.978	.980	.980	.979	.980	.980	.970	.972	.971	.970	.972	.971
22.26	.985	.985	.985	.987	.986	.982	.981	.981	.982	.982	.983	.983	.975	.978	.975	.975	.975	.976
24.26	.984	.986	.984	.986	.985	.981	.979	.979	.980	.979	.981	.981	.974	.975	.974	.973	.971	.971
26.26	.991	.994	.991	.993	.990	.992	.985	.985	.984	.984	.985	.984	.977	.977	.979	.976	.976	.973
28.26	.992	.992	.992	.992	.992	.989	.988	.988	.989	.988	.990	.988	.978	.982	.983	.981	.980	.980
30.26	.988	.990	.990	.992	.990	.988	.989	.989	.988	.989	.990	.990	.986	.986	.986	.984	.981	.985
32.26	.988	.988	.988	.990	.988	.985	.988	.986	.986	.985	.987	.987	.981	.982	.982	.981	.980	.979

TABLE II.– LOCAL VELOCITY RATIO, U/V – Continued

(b) NACA 1-46.5-085 dual-rotation spinner, rear plane of rotation

Radial station, in.	M = 0.30						M = 0.40						M = 0.60					
	Inlet velocity ratio, V_1/V						Inlet velocity ratio, V_1/V						Inlet velocity ratio, V_1/V					
	0.31	0.41	0.52	0.61	0.81	1.09	0.32	0.40	0.48	0.63	0.82	1.08	0.33	0.42	0.50	0.59	0.80	1.08
3.78	0.735	0.802	0.818	0.828	0.862	0.902	0.737	0.787	0.805	0.828	0.855	0.897	0.719	0.755	0.799	0.814	0.847	0.883
4.03	.740	.817	.817	.830	.864	.908	.744	.792	.810	.830	.860	.897	.724	.757	.802	.814	.850	.885
4.28	.757	.807	.820	.830	.861	.901	.754	.794	.813	.830	.855	.892	.738	.764	.800	.814	.843	.878
4.53	.764	.814	.820	.830	.854	.891	.762	.794	.813	.830	.853	.889	.745	.771	.802	.818	.842	.874
4.78	.791	.824	.830	.834	.864	.891	.785	.810	.823	.833	.850	.884	.768	.785	.809	.819	.845	.874
5.28	.816	.830	.836	.839	.870	.884	.807	.824	.829	.837	.857	.878	.788	.802	.816	.826	.847	.873
5.78	.846	.859	.862	.865	.879	.893	.842	.849	.850	.860	.870	.883	.821	.828	.836	.842	.859	.876
6.28	.876	.879	.882	.882	.889	.896	.867	.872	.873	.880	.885	.898	.850	.852	.857	.862	.874	.887
6.78	.893	.893	.896	.896	.902	.909	.890	.890	.890	.895	.898	.898	.869	.873	.874	.876	.885	.895
7.78	.929	.929	.922	.925	.932	.938	.922	.917	.917	.917	.914	.920	.907	.905	.905	.905	.911	.916
8.78	.954	.951	.947	.947	.951	.948	.942	.944	.948	.944	.944	.942	.931	.928	.928	.928	.928	.931
9.78	.974	.967	.970	.967	.970	.967	.962	.964	.959	.962	.962	.957	.961	.957	.957	.957	.955	.961
10.78	.973	.973	.972	.966	.969	.966	.971	.968	.969	.963	.963	.961	.967	.964	.964	.964	.962	.966
12.78	.975	.978	.975	.975	.975	.971	.973	.973	.973	.973	.975	.970	.975	.973	.973	.972	.972	.974
14.78	.986	.986	.986	.983	.983	.983	.984	.982	.982	.984	.982	.982	.985	.984	.984	.984	.984	.987
16.78	.985	.985	.985	.982	.982	.982	.981	.983	.978	.981	.978	.978	.984	.983	.983	.985	.985	.986
18.78	.984	.984	.984	.984	.984	.984	.982	.980	.980	.980	.982	.977	.988	.990	.986	.986	.986	.990
20.78	.993	.990	.987	.987	.987	.983	.989	.989	.986	.989	.986	.984	.996	.994	.992	.990	.992	.996
22.78	.986	.982	.982	.979	.982	.979	.985	.983	.983	.985	.983	.983	.991	.989	.989	.991	.989	.995
24.78	.995	.995	.991	.988	.991	.988	.989	.987	.987	.989	.987	.987	.997	.992	.994	.994	.994	.997
26.78	.991	.995	.995	.991	.995	.991	.989	.989	.989	.992	.989	.984	.995	.995	.995	.995	.992	.997
28.78	.990	.990	.990	.987	.994	.987	.988	.991	.988	.991	.988	.986	.996	.994	.994	.994	.996	.997
30.78	.986	.986	.986	.986	.989	.986	.990	.990	.987	.987	.987	.985	.992	.990	.990	.992	.992	.995
32.78	.989	.989	.989	.989	.989	.989	.986	.986	.984	.984	.984	.981	.990	.990	.990	.990	.990	.995

Radial station, in.	M = 0.70						M = 0.80						M = 0.84					
	Inlet velocity ratio, V_1/V						Inlet velocity ratio, V_1/V						Inlet velocity ratio, V_1/V					
	0.27	0.39	0.49	0.61	0.83	1.05	0.30	0.41	0.50	0.61	0.81	1.00	0.34	0.43	0.50	0.62	0.83	0.95
3.78	0.701	0.745	0.784	0.808	0.839	0.864	0.704	0.754	0.770	0.789	0.817	0.834	0.716	0.745	0.755	0.782	0.810	0.819
4.03	.706	.750	.775	.808	.841	.864	.708	.756	.769	.785	.815	.833	.719	.745	.755	.780	.808	.815
4.28	.718	.751	.786	.805	.835	.858	.714	.754	.770	.785	.815	.827	.721	.745	.753	.778	.807	.814
4.53	.727	.756	.786	.804	.832	.853	.718	.754	.769	.783	.811	.826	.724	.745	.752	.776	.804	.812
4.78	.746	.769	.793	.808	.833	.855	.735	.762	.774	.790	.814	.827	.736	.755	.761	.781	.804	.812
5.28	.770	.786	.799	.814	.835	.850	.753	.772	.782	.793	.815	.826	.751	.762	.769	.786	.804	.810
5.78	.802	.808	.820	.826	.845	.856	.783	.795	.799	.809	.825	.831	.775	.783	.785	.799	.815	.819
6.28	.830	.834	.841	.846	.857	.865	.807	.815	.818	.825	.835	.841	.796	.803	.805	.815	.826	.828
6.78	.853	.855	.855	.861	.869	.876	.827	.833	.837	.836	.849	.853	.817	.820	.821	.827	.838	.840
7.78	.893	.891	.891	.892	.895	.898	.872	.869	.870	.870	.875	.875	.854	.855	.854	.860	.864	.864
8.78	.919	.910	.912	.912	.911	.916	.894	.894	.895	.892	.898	.899	.884	.884	.882	.886	.890	.888
9.78	.952	.943	.948	.945	.947	.948	.932	.932	.931	.927	.931	.930	.921	.920	.918	.919	.922	.919
10.78	.956	.954	.948	.952	.953	.952	.939	.936	.936	.935	.936	.935	.929	.927	.925	.925	.927	.922
12.78	.970	.966	.964	.964	.964	.964	.954	.954	.952	.950	.950	.948	.944	.943	.941	.943	.941	.941
14.78	.983	.979	.981	.981	.977	.976	.972	.969	.968	.967	.966	.966	.963	.964	.960	.963	.962	.957
16.78	.985	.982	.981	.981	.980	.978	.976	.975	.975	.970	.972	.970	.971	.968	.967	.968	.967	.963
18.78	.989	.987	.985	.987	.985	.985	.982	.981	.982	.978	.979	.978	.978	.977	.974	.975	.975	.972
20.78	.997	.990	.993	.991	.989	.990	.991	.988	.988	.983	.986	.982	.984	.982	.978	.981	.980	.976
22.78	.994	.990	.992	.989	.991	.989	.990	.988	.990	.986	.986	.985	.985	.982	.980	.981	.980	.978
24.78	.995	.991	.992	.989	.990	.991	.988	.988	.988	.983	.984	.984	.983	.984	.980	.980	.982	.976
26.78	.997	.994	.994	.993	.995	.994	.988	.991	.990	.988	.987	.987	.988	.986	.986	.987	.982	.979
28.78	.998	.997	.995	.995	.993	.994	.992	.993	.993	.989	.989	.988	.991	.989	.985	.987	.987	.982
30.78	.997	.994	.992	.992	.990	.992	.996	.996	.993	.991	.992	.991	.991	.992	.989	.990	.991	.995
32.78	.993	.992	.990	.993	.990	.989	.991	.990	.991	.985	.986	.985	.986	.985	.984	.985	.984	.978

TABLE II.– LOCAL VELOCITY RATIO, U/V – Concluded

(c) NACA 1-46.5-047 single-rotation spinner

Radial station, in.	M = 0.30					M = 0.40					M = 0.60						
	Inlet velocity ratio, V_1/V					Inlet velocity ratio, V_1/V					Inlet velocity ratio, V_1/V						
	0.39	0.61	0.80	1.00	1.30	0.39	0.63	0.81	1.03	1.30	0.29	0.35	0.50	0.59	0.78	1.00	1.32
3.47	0.820	0.902	0.929	0.956	0.986	0.815	0.904	0.927	0.952	0.983	0.836	0.852	0.871	0.883	0.912	0.936	0.959
3.72	.817	.895	.932	.949	.983	.810	.894	.917	.945	.973	.828	.845	.862	.876	.898	.928	.948
3.97	.822	.887	.914	.938	.965	.818	.888	.909	.933	.962	.826	.840	.855	.867	.893	.916	.936
4.47	.843	.887	.908	.925	.948	.838	.886	.901	.919	.942	.829	.838	.850	.859	.881	.900	.915
4.97	.859	.886	.900	.914	.930	.855	.885	.898	.908	.926	.841	.849	.855	.864	.878	.892	.907
5.47	.889	.910	.917	.924	.934	.883	.903	.908	.916	.928	.865	.869	.873	.876	.888	.895	.907
5.97	.912	.926	.929	.933	.939	.906	.915	.921	.926	.933	.890	.890	.898	.893	.902	.909	.914
6.47	.925	.932	.936	.936	.939	.921	.928	.928	.931	.939	.903	.902	.905	.907	.912	.912	.919
7.47	.955	.955	.959	.959	.959	.948	.950	.950	.948	.950	.934	.933	.931	.931	.933	.935	.936
8.47	.974	.971	.971	.968	.971	.971	.968	.968	.968	.971	.957	.955	.955	.954	.955	.955	.955
9.47	.983	.983	.980	.984	.980	.985	.982	.980	.980	.980	.974	.972	.971	.971	.969	.969	.969
10.47	.982	.979	.979	.976	.976	.982	.980	.977	.980	.980	.974	.972	.971	.969	.967	.969	.967
12.47	.998	.995	.992	.995	.992	.995	.993	.990	.990	.990	.987	.987	.986	.986	.984	.984	.984
14.47	.997	.997	.997	.997	.994	1.002	1.000	.997	.994	.997	.996	.994	.996	.992	.992	.991	.991
16.47	.995	.999	.995	.999	.992	.999	.999	.996	.993	.996	.997	.997	.995	.995	.993	.993	.993
18.47	.998	1.001	1.001	.998	.994	.999	.999	.996	.999	.996	1.000	.998	.998	.998	.998	.997	.997
20.47	1.000	1.004	1.003	1.003	1.000	1.008	1.005	1.003	1.005	1.005	1.006	1.004	1.002	1.002	.999	1.001	1.001
22.47	1.000	1.000	1.000	1.000	.997	1.007	1.004	1.002	1.002	1.004	1.005	1.005	1.003	1.001	1.001	1.001	1.001
24.47	1.003	1.006	1.002	1.006	1.002	1.006	1.003	1.003	1.003	1.006	.995	.995	.995	.992	.994	.992	.992
26.47	1.005	1.008	1.005	1.005	1.001	1.005	1.007	1.005	1.005	1.005	1.008	1.008	1.008	1.006	1.006	1.005	1.006
28.47	1.004	1.004	1.000	1.004	1.000	1.004	1.004	1.004	1.004	1.004	1.008	1.006	1.006	1.006	1.004	1.004	1.004
30.47	1.001	1.001	1.004	1.004	1.000	1.003	1.005	1.003	1.003	1.003	1.005	1.003	1.003	1.000	1.002	1.002	1.002
32.47	1.010	1.010	1.010	1.009	1.006	1.007	1.004	1.004	1.004	1.004	1.007	1.007	1.006	1.004	1.005	1.005	1.005

Radial station, in.	M = 0.70						M = 0.80						M = 0.84					
	Inlet velocity ratio, V_1/V						Inlet velocity ratio, V_1/V						Inlet velocity ratio, V_1/V					
	0.30	0.38	0.47	0.62	0.80	1.16	0.31	0.39	0.50	0.60	0.80	1.03	0.31	0.40	0.51	0.63	0.85	0.97
3.47	0.824	0.843	0.860	0.875	0.907	0.937	0.799	0.826	0.845	0.864	0.892	0.909	0.787	0.813	0.836	0.854	0.883	0.893
3.72	.815	.836	.851	.866	.900	.930	.789	.817	.836	.853	.884	.899	.776	.807	.828	.851	.877	.887
3.97	.812	.827	.843	.857	.888	.895	.784	.811	.826	.844	.872	.887	.770	.798	.818	.838	.864	.873
4.47	.810	.824	.834	.848	.874	.895	.782	.803	.819	.830	.855	.869	.771	.791	.808	.826	.846	.854
4.97	.824	.833	.840	.848	.867	.885	.794	.811	.821	.830	.849	.862	.780	.797	.809	.824	.841	.848
5.47	.848	.852	.858	.860	.879	.892	.819	.829	.834	.844	.857	.868	.802	.812	.825	.835	.848	.851
5.97	.871	.874	.880	.881	.891	.898	.841	.848	.852	.857	.867	.873	.823	.830	.837	.848	.855	.859
6.47	.885	.886	.891	.890	.897	.903	.857	.860	.862	.866	.874	.879	.840	.844	.850	.855	.860	.864
7.47	.918	.918	.919	.918	.921	.924	.892	.894	.894	.897	.900	.902	.877	.877	.879	.883	.887	.888
8.47	.948	.945	.948	.946	.948	.949	.926	.925	.925	.926	.928	.927	.911	.910	.911	.916	.915	.915
9.47	.964	.964	.963	.963	.963	.963	.948	.947	.946	.946	.948	.946	.933	.931	.933	.937	.937	.934
10.47	.963	.961	.961	.961	.961	.960	.944	.944	.943	.943	.943	.942	.933	.930	.931	.933	.931	.930
12.47	.981	.979	.979	.978	.978	.978	.967	.966	.964	.964	.963	.962	.955	.954	.953	.954	.953	.952
14.47	.984	.990	.990	.988	.988	.987	.980	.979	.977	.979	.979	.978	.971	.966	.969	.971	.968	.967
16.47	.994	.994	.993	.993	.993	.993	.985	.987	.983	.983	.984	.983	.977	.976	.976	.977	.975	.973
18.47	.997	.997	.997	.995	.996	.994	.992	.989	.989	.987	.989	.988	.986	.985	.982	.981	.980	.978
20.47	1.002	1.002	1.002	1.000	1.002	.999	.999	.996	.996	.993	.992	.993	.991	.990	.989	.987	.986	.985
22.47	1.004	1.004	1.004	1.001	1.004	1.001	.999	.999	.998	.998	.998	.995	.994	.992	.990	.993	.989	.989
24.47	.992	.992	.992	.992	.992	.989	.986	.986	.983	.982	.983	.981	.983	.979	.978	.978	.977	.973
26.47	1.006	1.006	1.006	1.004	1.006	1.002	.999	.999	.999	.999	.999	.995	.994	.992	.992	.992	.991	.987
28.47	1.007	1.007	1.007	1.005	1.005	1.002	1.002	1.002	1.000	1.002	.999	.996	.997	.994	.993	.997	.993	.991
30.47	1.003	1.003	1.005	1.003	1.005	1.002	1.004	1.002	1.001	1.001	1.000	.994	.998	.997	.996	.997	.995	.995
32.47	1.003	1.000	1.005	1.002	1.003	1.002	1.003	1.000	1.000	1.000	1.002	.998	1.000	.999	.996	.996	.996	.994

TABLE III.— INDEX OF DATA FIGURES

Figure number	Plot	Number of blades, B	Mach number, M	Propeller blade angle, β_F, deg	Inlet velocity ratio, V_1/V
			Recovery data		
6	$(H_1-p)/(H-p)$ vs. r	(a)	0.30 to 0.84	---	0.28 to 1.09
7	$(H_1-p)/(H-p)$ vs. V_1/V	(a)	0.30 to 0.84	---	0.28 to 1.09
8	$(H_1-p)/(H-p)$ vs. J	6	0.30 to 0.80	40 to 70	0.28 to 1.08
9	↓	8	0.30 to 0.84	40 to 70	0.27 to 1.03
[b]10	↓	8	0.80	65	0.31 to 0.96
11	$(H_1-p)/(H-p)$ vs. r	6,8	0.30 to 0.80	40 to 70	0.27 to 1.05
12	$(H_1-p)/(H-p)$ vs. V_1/V	6	0.30 to 0.80	40 to 70	0.28 to 1.08
	↓	8	0.30 to 0.84	40 to 70	0.27 to 1.03
[c]13	↓	(a),6,8	0.30 to 0.80	40 to 70	0.28 to 1.09
[b,d]14	↓	4,6,8	0.80	(e)	0.22 to 0.99
			Velocity surveys		
[f]15	U/V vs. r	(a)	0.30 to 0.84	---	0.29 to 1.09
			Propeller characteristics		
16	C_{T_a}, C_{P_a}, η_a, M_t vs. J	6	0.30 to 0.80	40 to 70	0.28 to 1.08
17	C_{T_a}, C_{P_a}, η_a, M_t vs. J	8	0.13 to 0.84	40 to 70	0.27 to 1.03
18	$C_{P_{a_F}}$, $C_{P_{a_R}}$ vs. J	6	0.30 to 0.80	40 to 70	0.28 to 1.08
19	$C_{P_{a_F}}$, $C_{P_{a_R}}$ vs. J	8	0.13 to 0.84	40 to 70	0.27 to 1.03
[g]20	C_{T_a}, C_T, C_{P_a}, C_P, η_a, η vs. J	6	0.80	65	0.64
[h]21	C_{T_a}, C_{P_a}, η_a vs. J	6,8	0.30 to 0.80	40 to 65	0.61 to 0.65
[b]22	C_{T_a}, C_{P_a}, η_a vs. J	8	0.80	65	0.31 to 0.96
[g,i]23	$\eta_{a_{max}}$, η_{max} vs. M	6,8	0.13 to 0.90	40 to 70	0.80

[a]Propeller removed.
[b]Effect of sealing the juncture gap.
[c]Comparison of six- and eight-blade-propeller and propeller-removed recovery data.
[d]Comparison of four-blade single-rotation, six- and eight-blade dual-rotation, and single-rotation NACA E-type-cowl recovery data.
[e]Respective near design blade angles.
[f]Velocity surveys in plane of front and rear components of the dual-rotation propeller and in the plane of a single-rotation propeller; propellers removed. (See table II for tabulated data.)
[g]Comparison of six-blade dual-rotation-propeller characteristics with cowl on and off.
[h]Comparison of six-blade and eight-blade dual-rotation-propeller characteristics; cowl on.
[i]Comparison of eight-blade dual-rotation-propeller characteristics with cowl on and off.

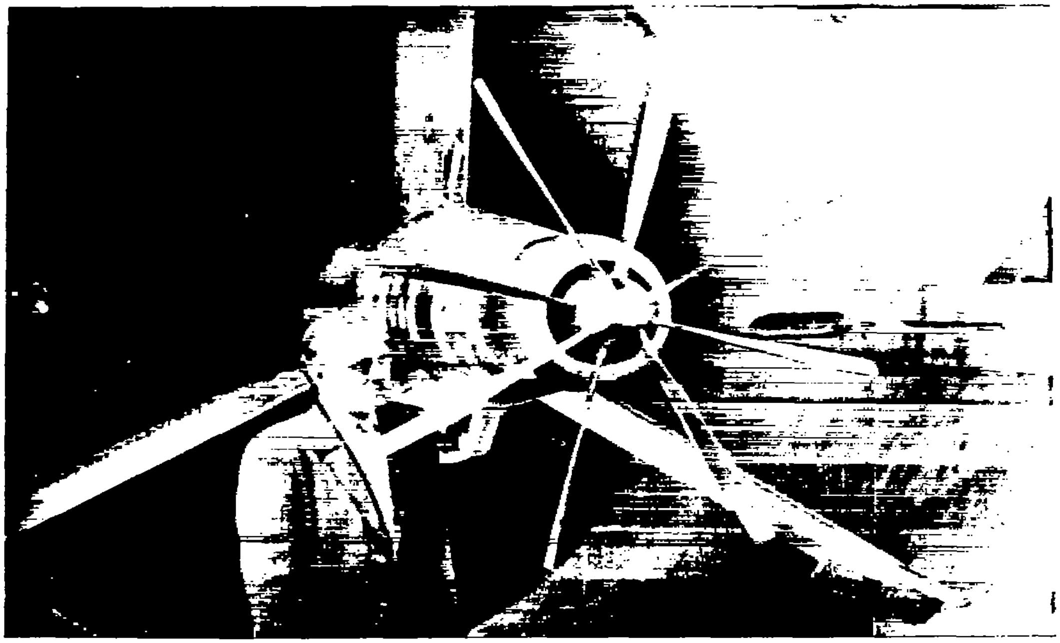

A-17903

Figure 1.– The model mounted on the 1000-horsepower propeller dynamometer in the Ames 12-foot pressure wind tunnel.

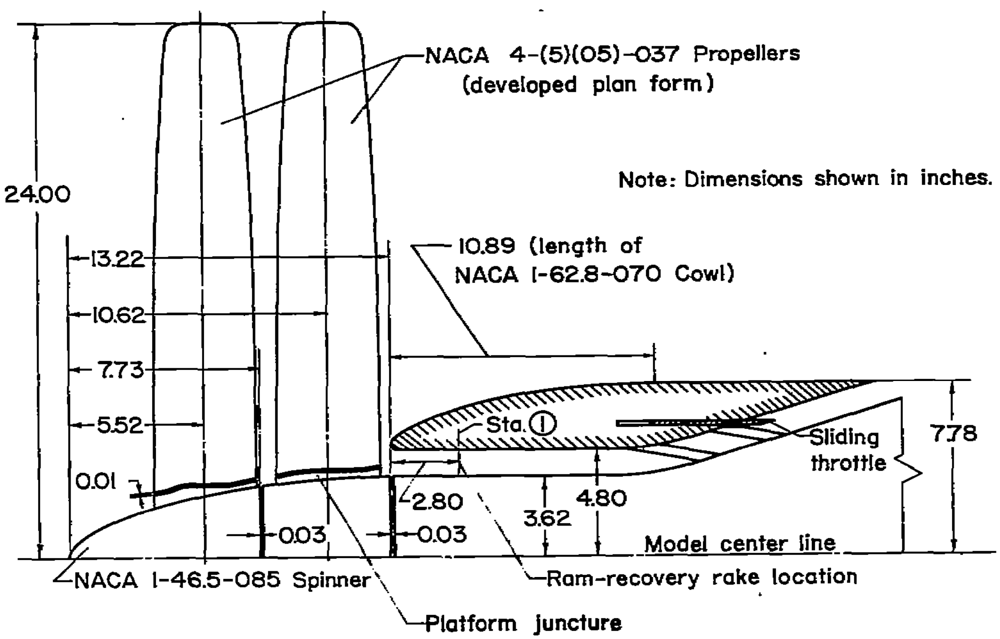

Figure 2.– Model arrangement.

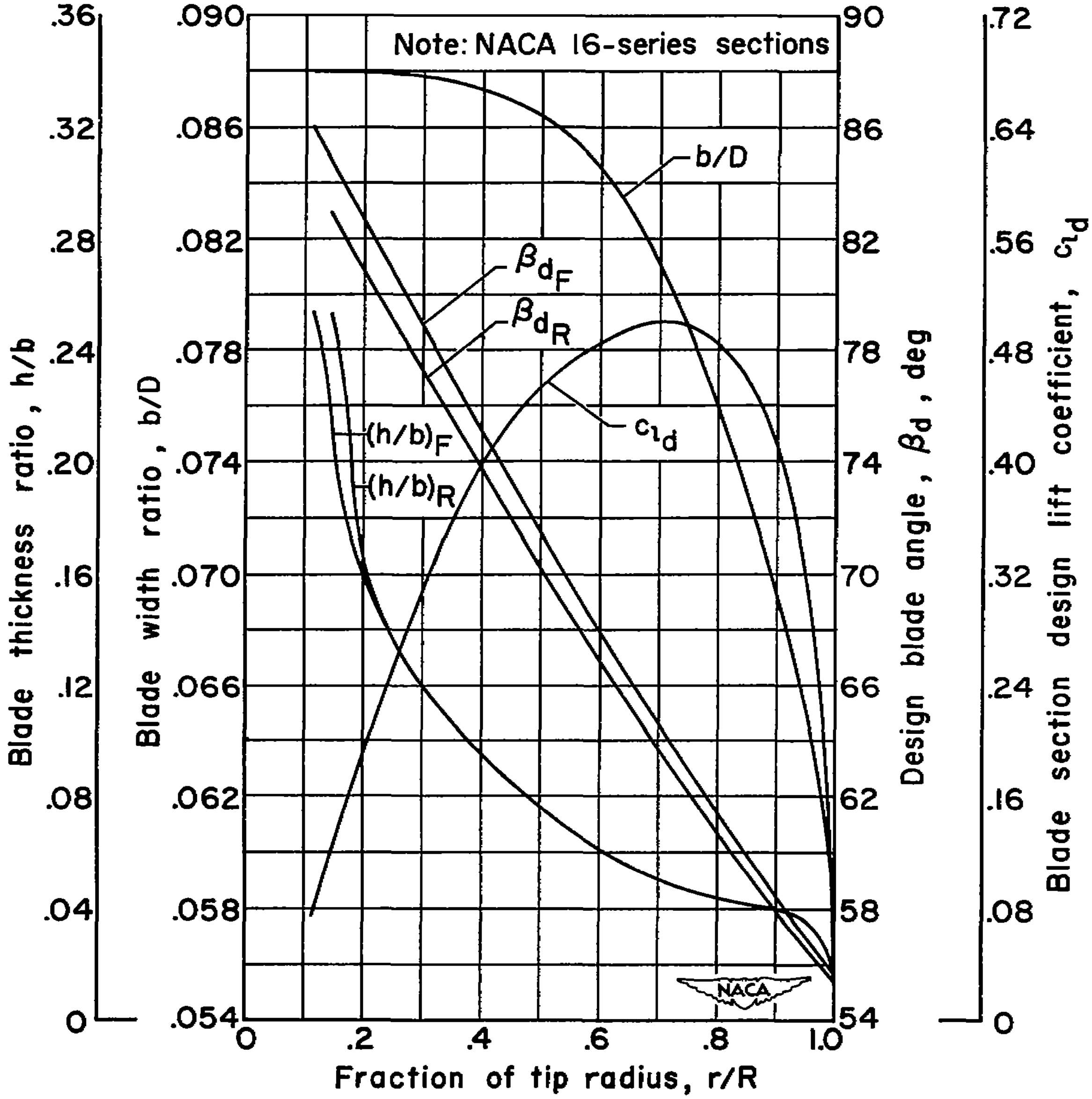

Figure 3.— Blade-form curves for the NACA 4-(5)(05)-037 six- and eight-blade dual-rotation propellers.

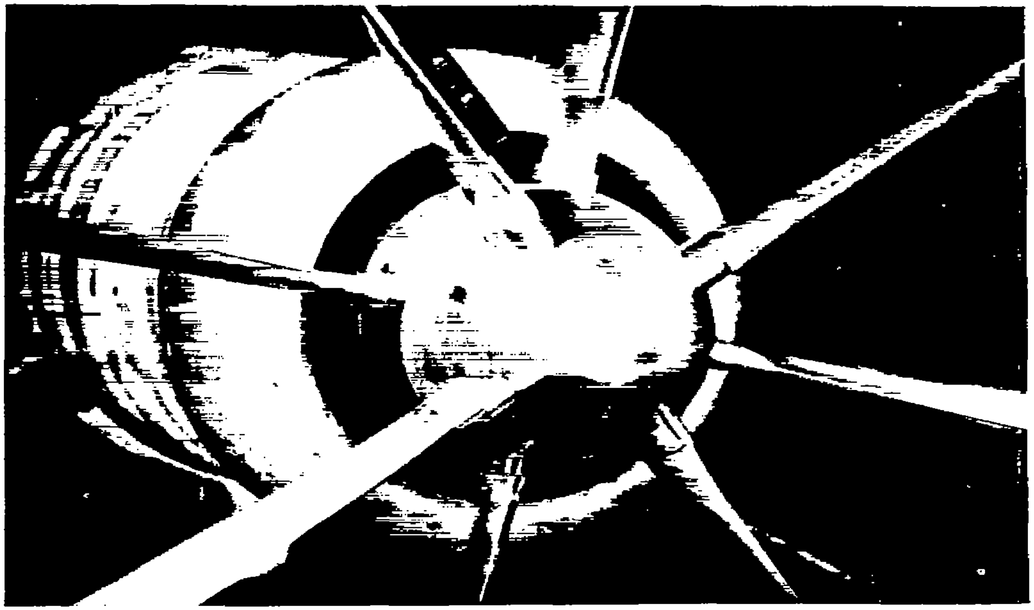

Figure 4.— Close-up of model showing platform propeller-spinner junctures.

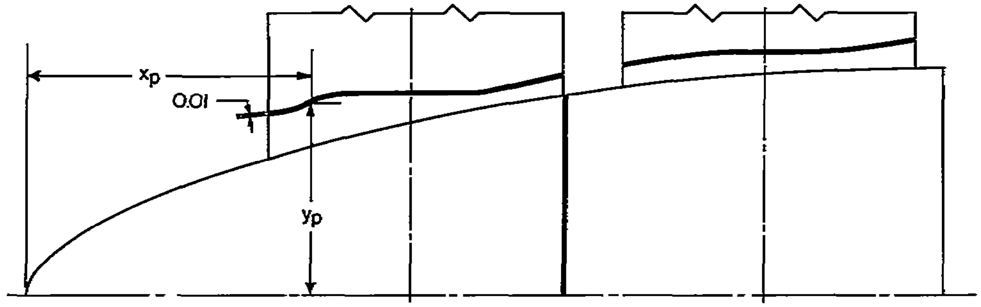

Platform coordinates			
Front		Rear	
x_p	y_p	x_p	y_p
3.482	2.890	8.582	3.655
3.720	2.924	8.820	3.695
3.920	2.992	9.220	3.760
4.320	3.167	9.620	3.825
4.720	3.220	10.020	3.860
6.520	3.220	11.420	3.860
6.920	3.317	11.820	3.890
7.320	3.411	12.220	3.950
7.706	3.502	12.806	4.040

All dimensions in inches
Platforms shown in developed plan form
Platforms aline with blades when $\beta_F = 65°$ and $\beta_R = 64.2°$

Figure 5.— Platform arrangement and coordinates.

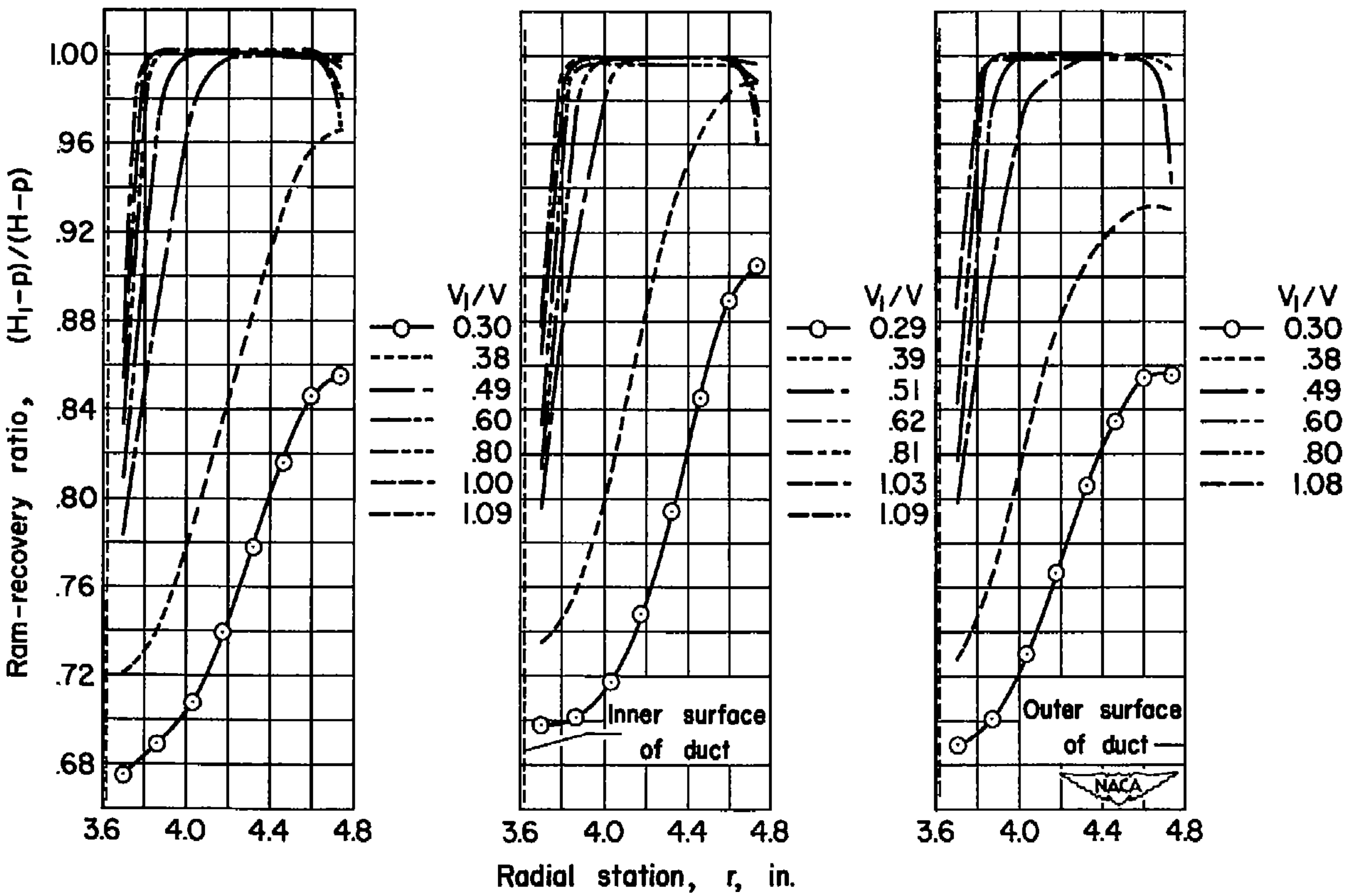

(a) M = 0.30 (b) M = 0.40 (c) M = 0.60

Figure 6.– The variation of the average ram-recovery ratio across the duct; propeller removed.

[redacted]

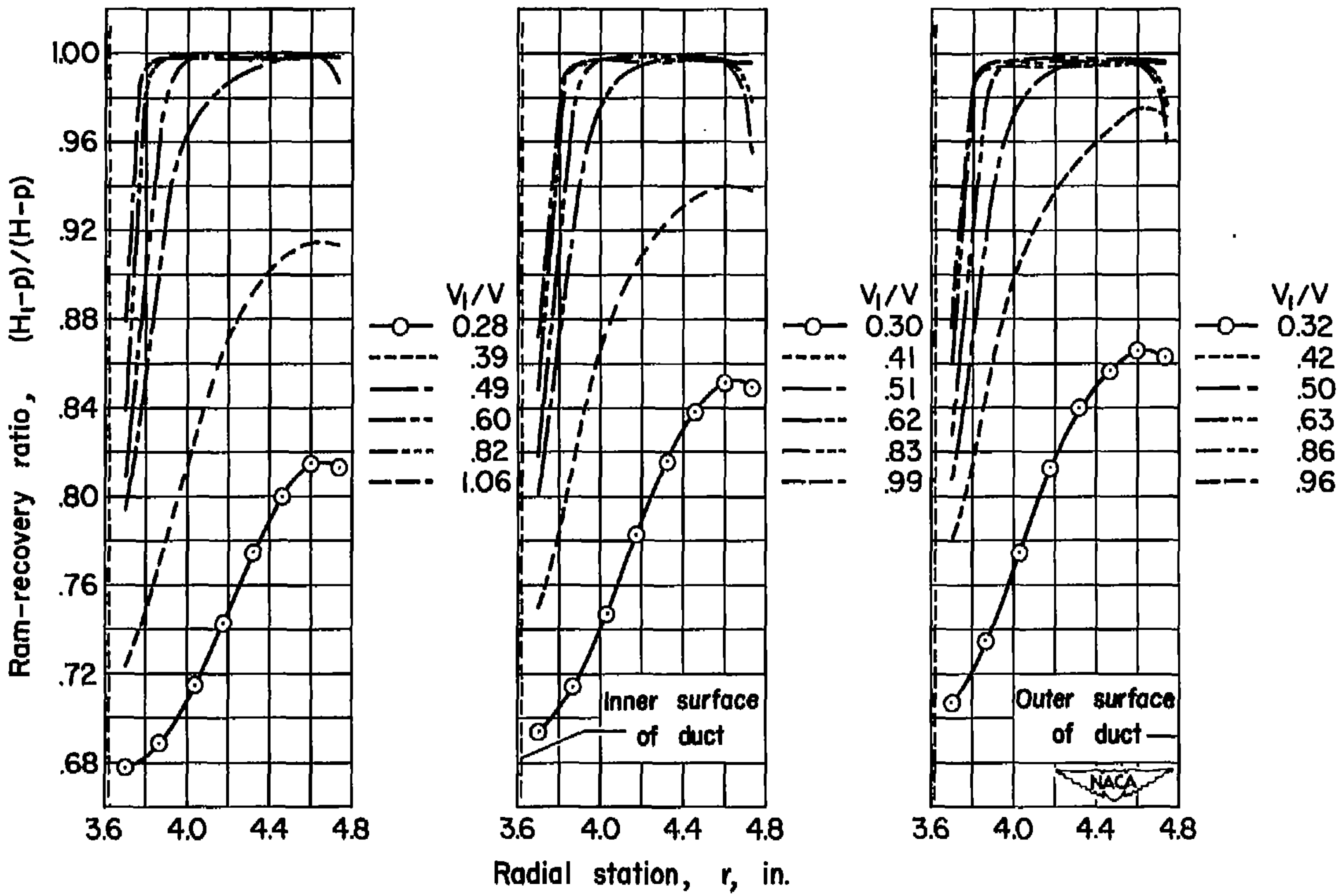

(d) M = 0.70

(e) M = 0.80

(f) M = 0.84

Figure 6.—Concluded.

[redacted]

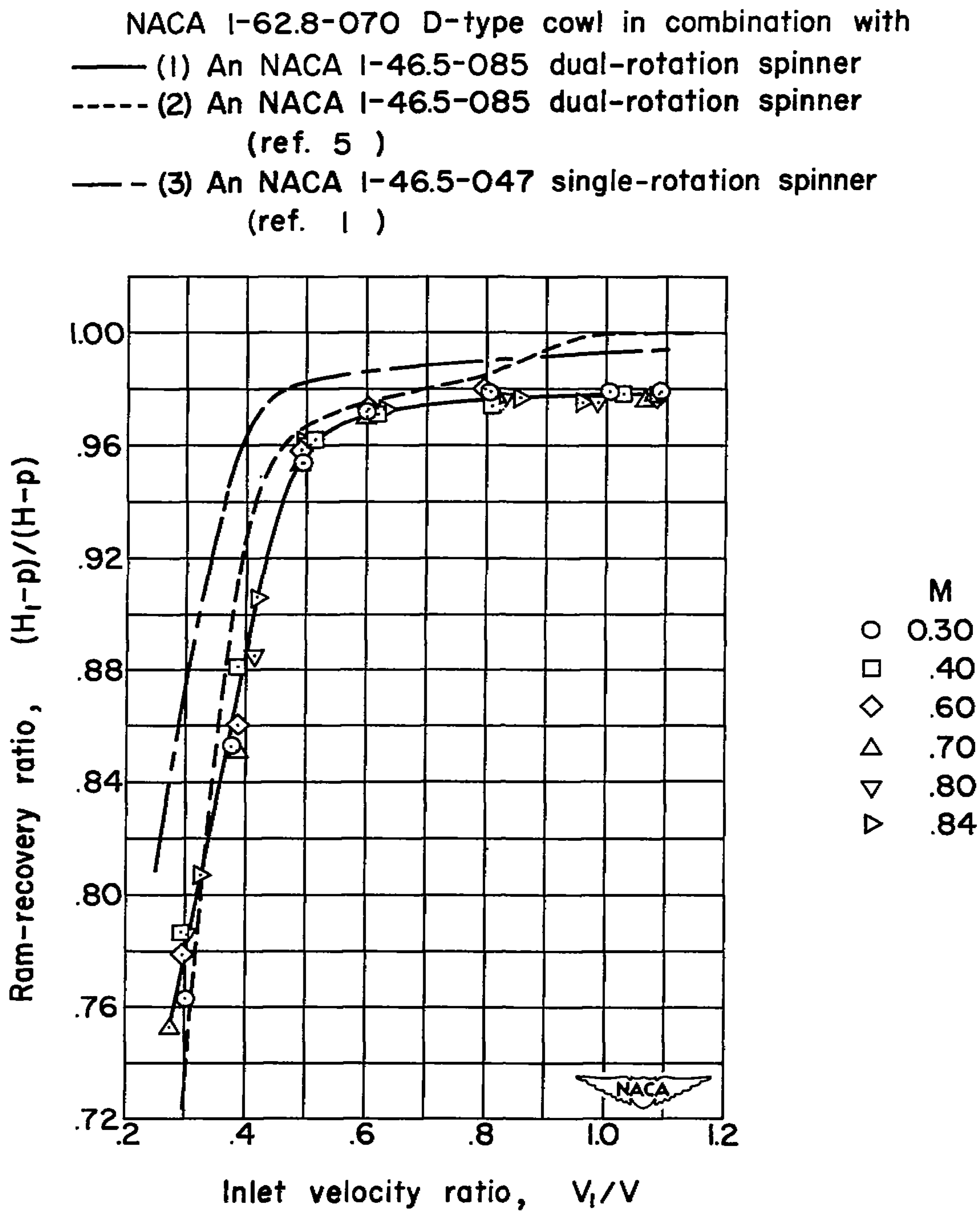

Figure 7.— The effect of inlet velocity ratio on the average ram-recovery ratio; propeller removed.

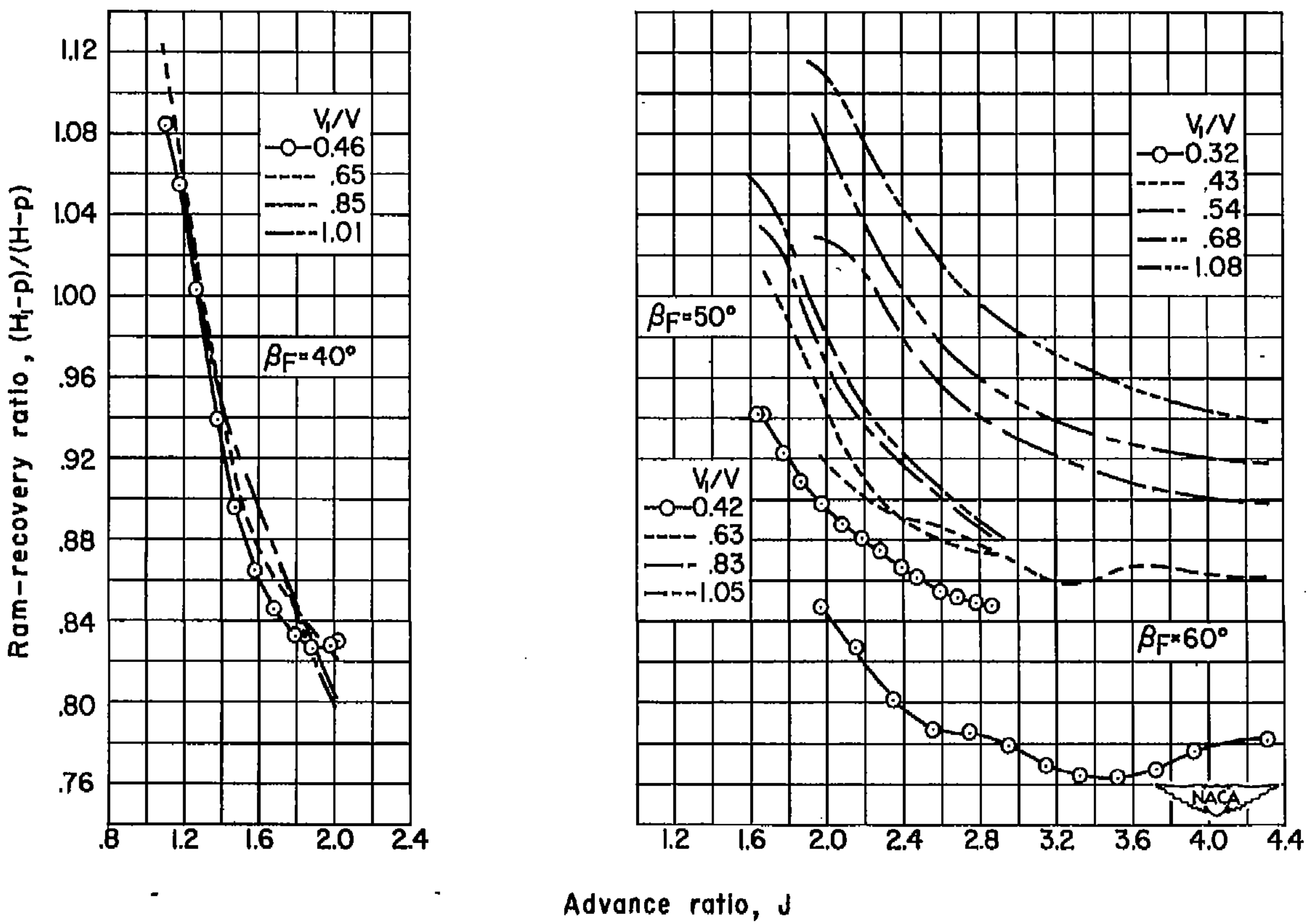

(a) M = 0.30; B = 6

(b) M = 0.40; B = 6

Figure 8.– The effect of advance ratio on the average ram-recovery ratio; propeller operating.

[redacted]

[redacted]

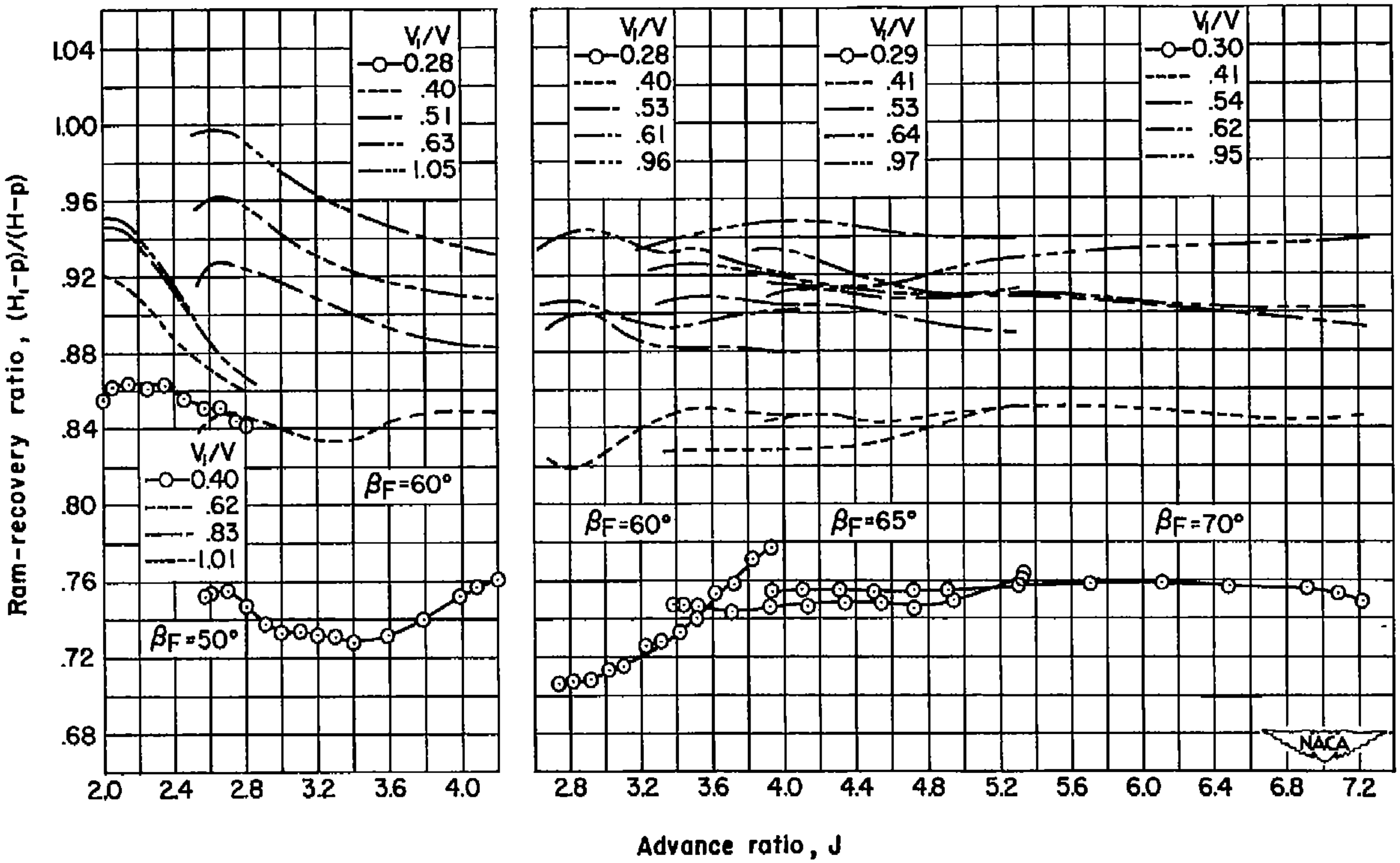

(c) M = 0.60; B = 6

(d) M = 0.80; B = 6

Figure 8.- Concluded.

[redacted]

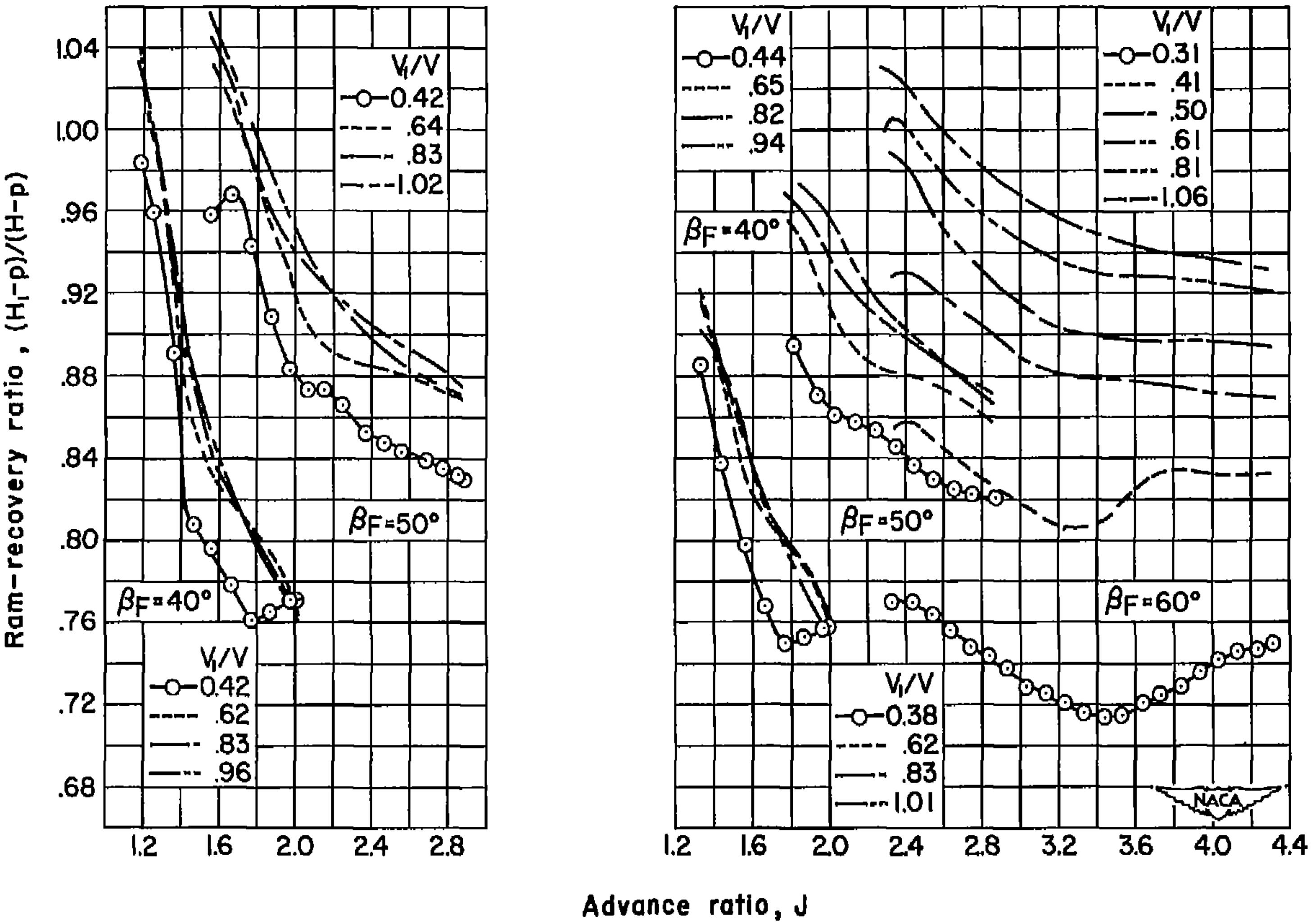

(a) M = 0.30; B = 8

(b) M = 0.40; B = 8

Figure 9.— The effect of advance ratio on the average ram-recovery ratio; propeller operating.

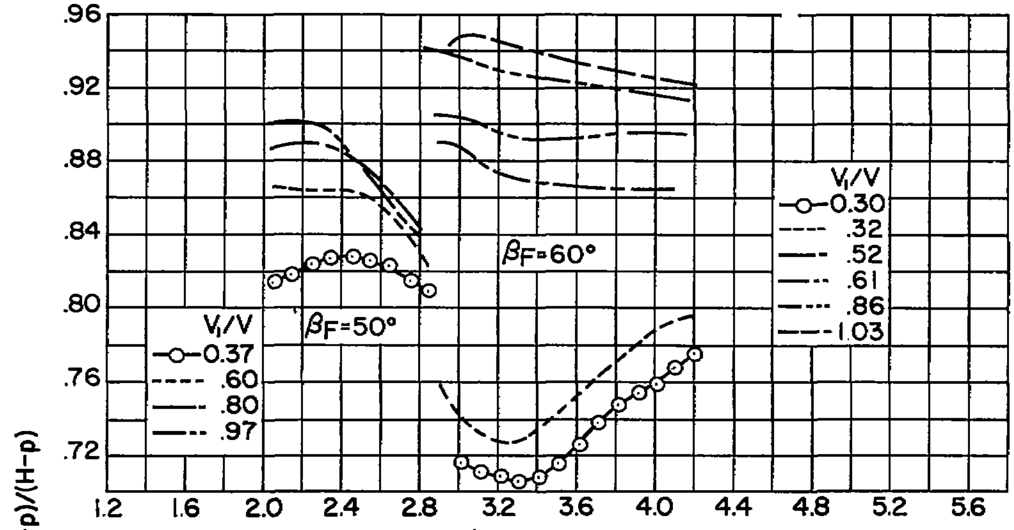

(c) M = 0.60; B = 8

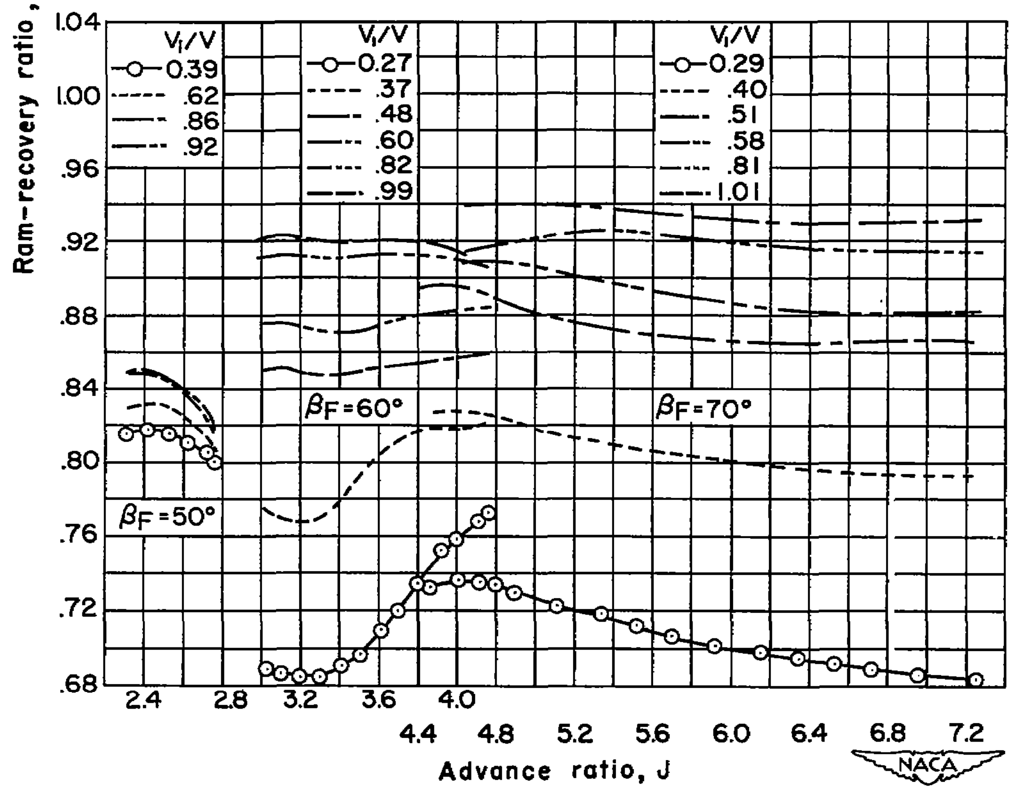

(d) M = 0.70; B = 8

Figure 9.— Continued.

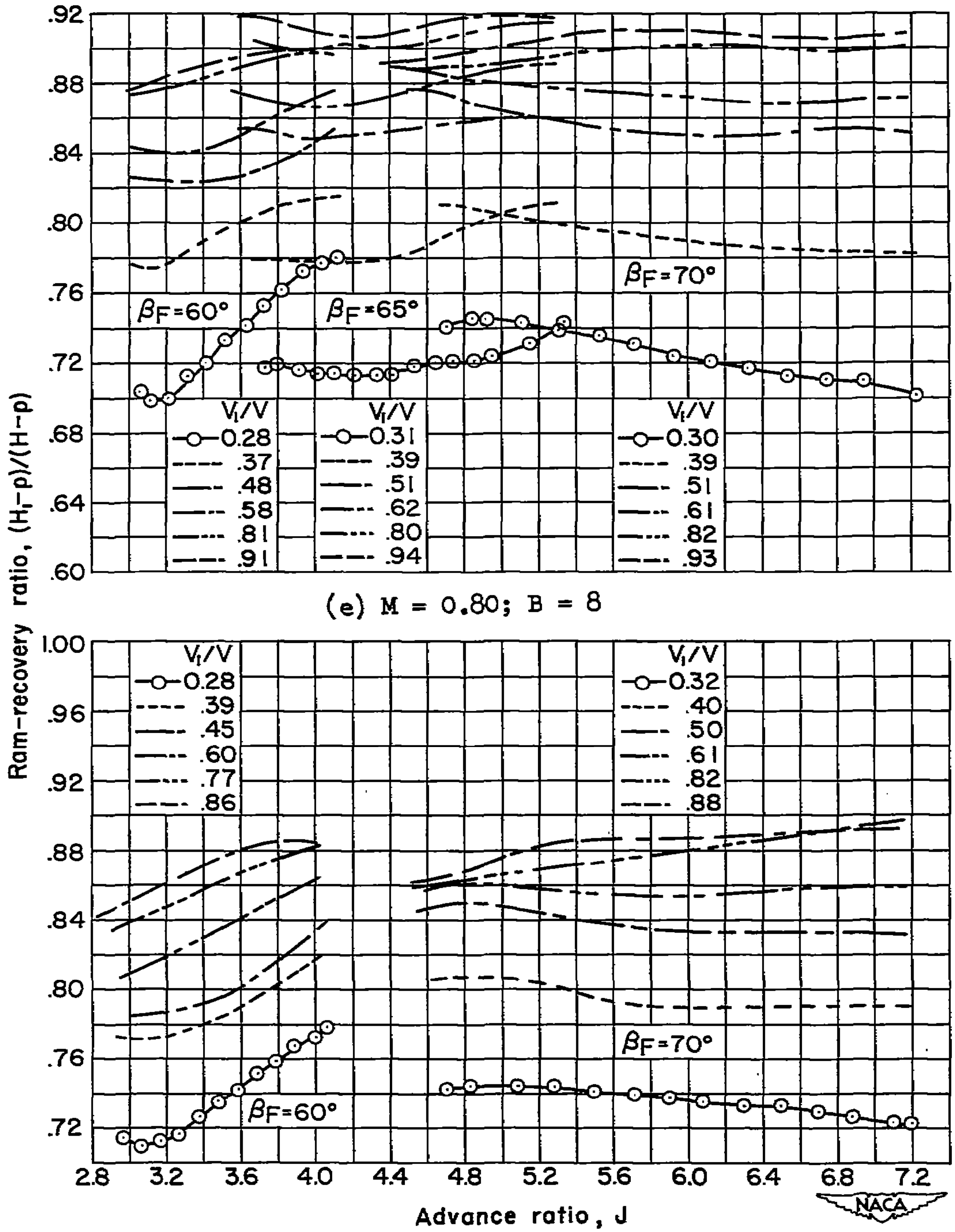

(e) M = 0.80; B = 8

(f) M = 0.84; B = 8

Figure 9.— Concluded.

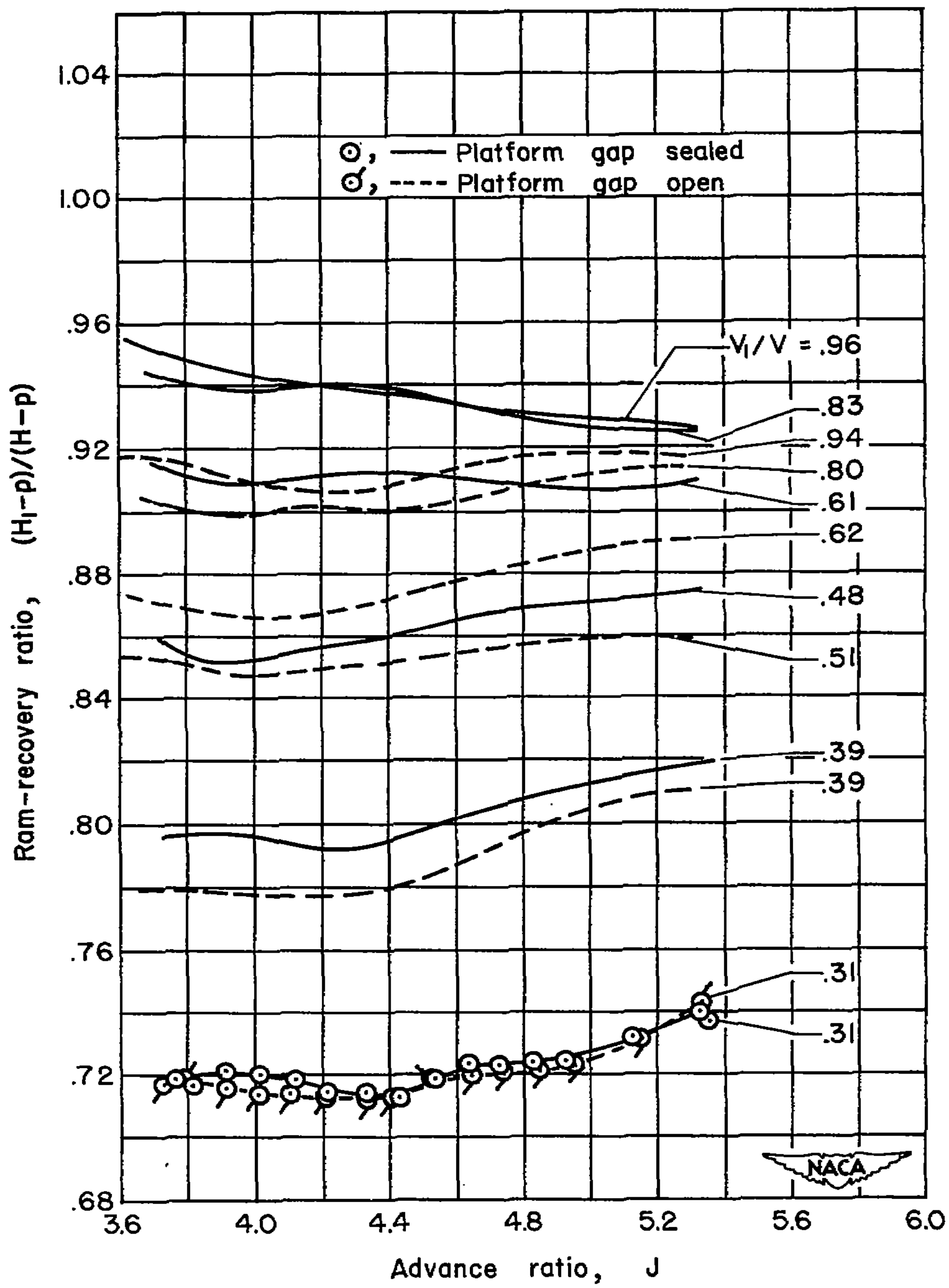

Figure 10.— The effect of sealing the propeller–platform gap on the variation of the average ram-recovery ratio with advance ratio; $M = 0.80$, $\beta_F = 65^{\circ}$, $B = 8$.

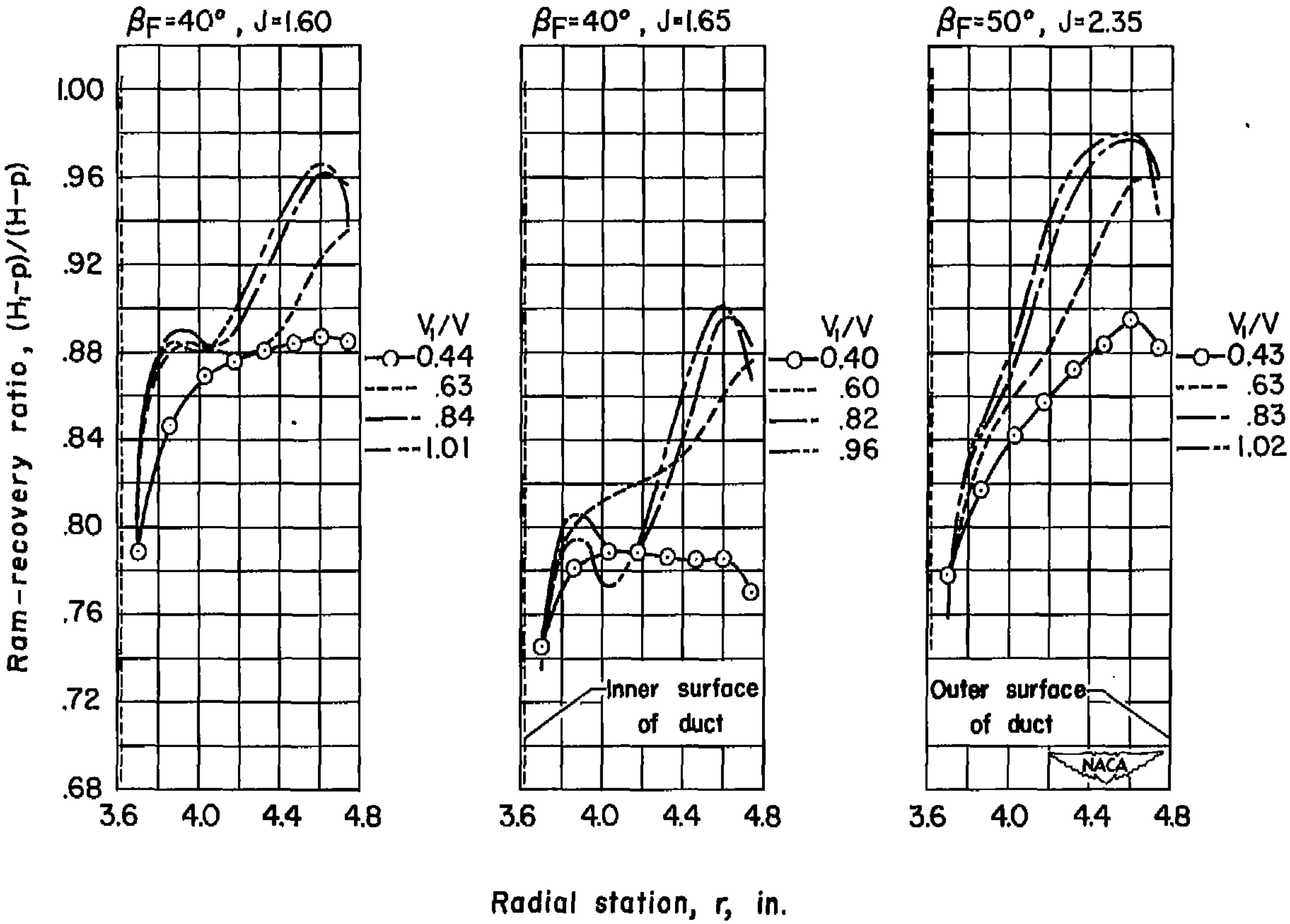

(a) M = 0.30; B = 6 (b) M = 0.30; B = 8

Figure 11.– The variation of the average ram-recovery ratio across the duct; propeller operating, J for $\eta_{a_{max}}$.

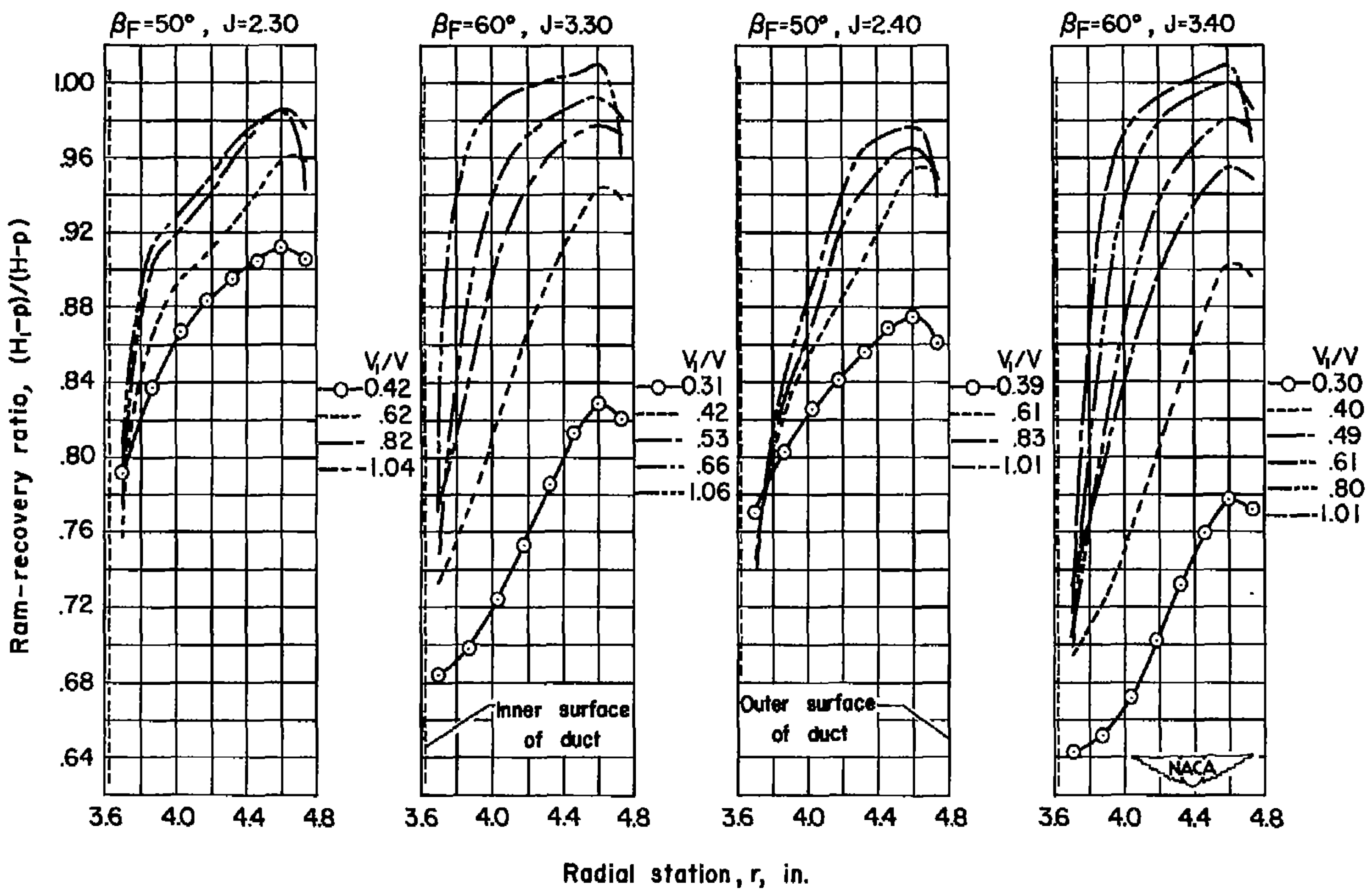

(c) M = 0.40; B = 6 (d) M = 0.40; B = 8

Figure 11.– Continued.

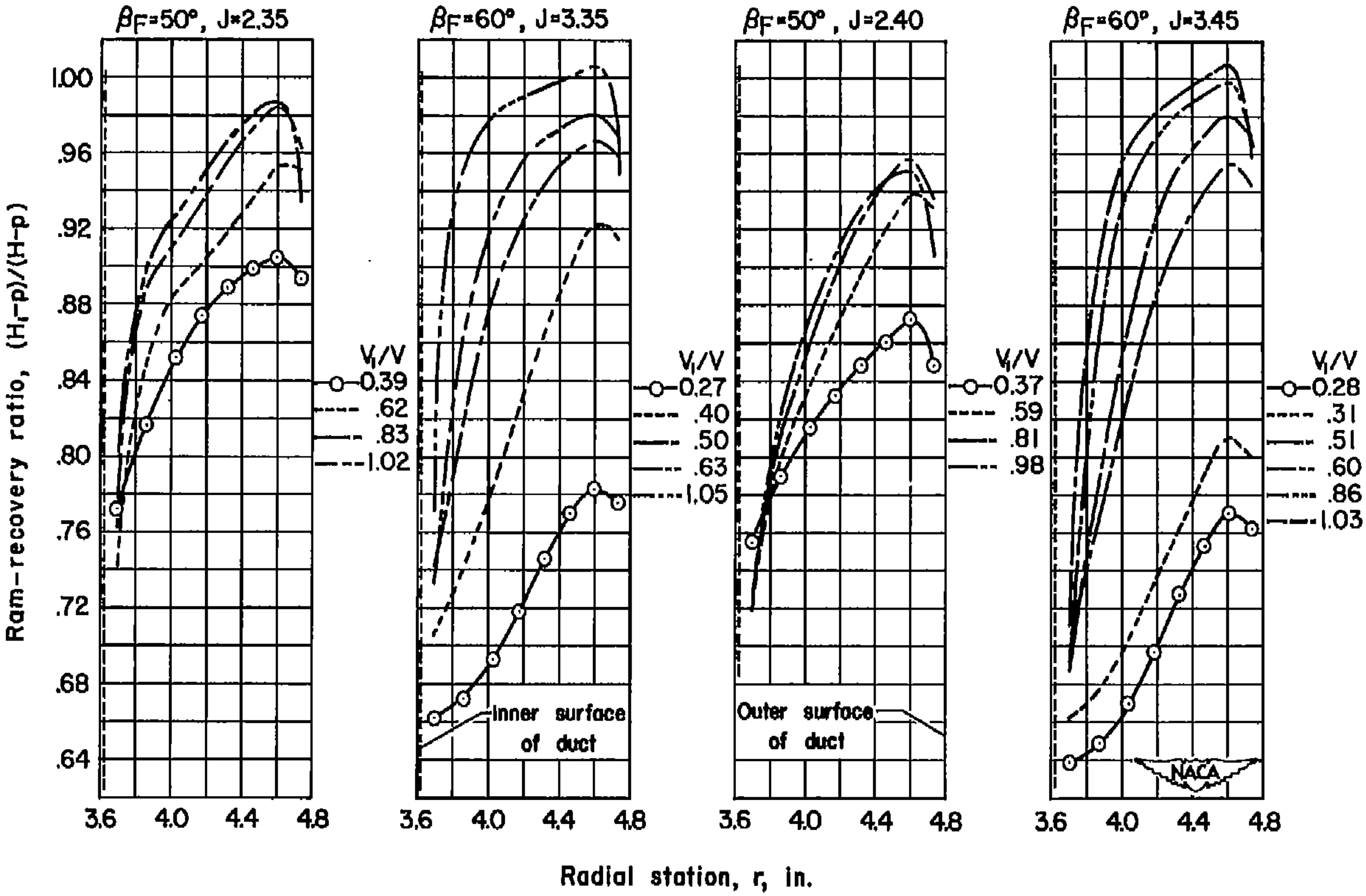

(e) M = 0.60; B = 6

(f) M = 0.60; B = 8

Figure 11.– Continued.

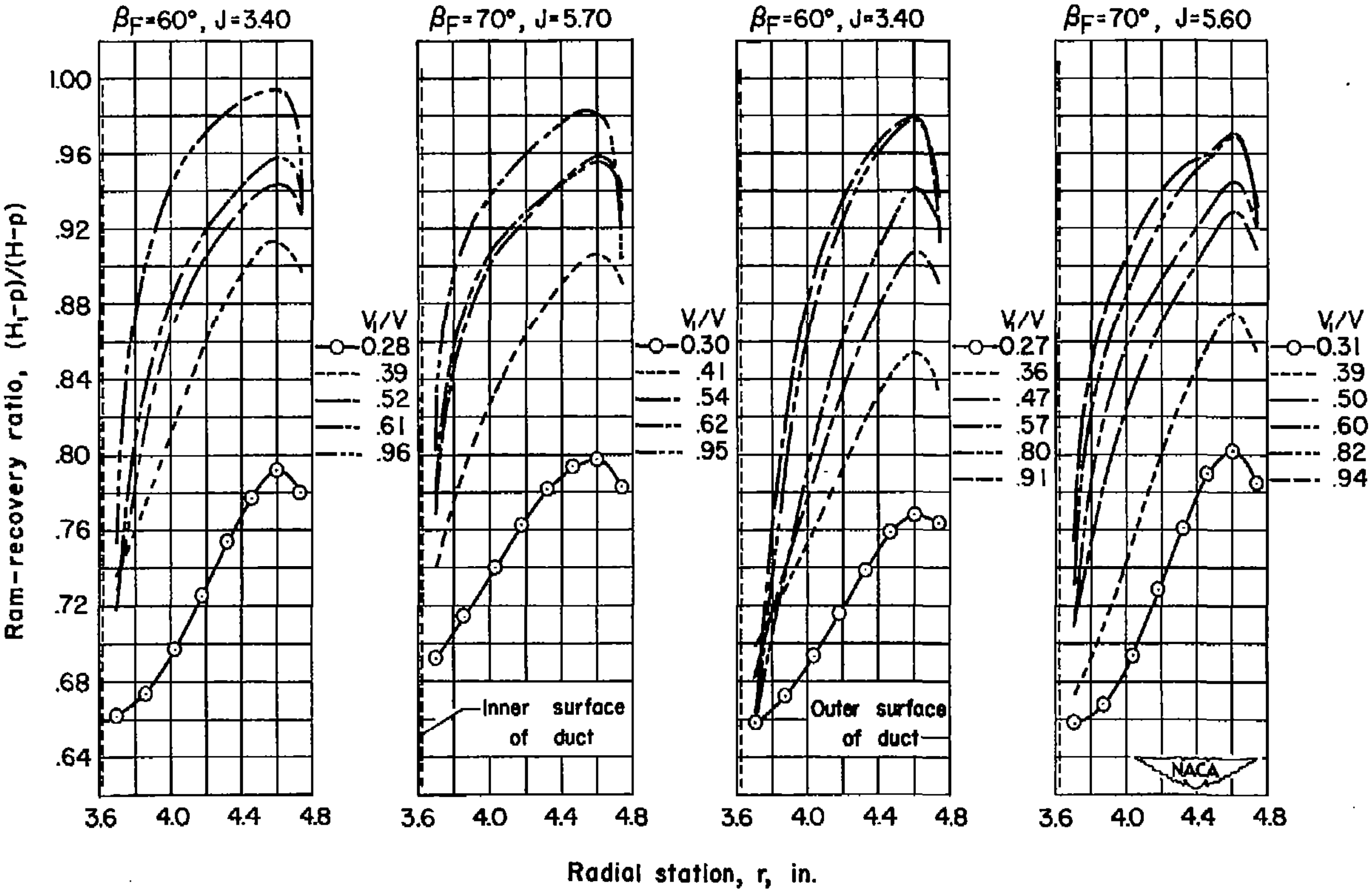

(g) M = 0.80; B = 6

(h) M = 0.80; B = 8

Figure 11.– Concluded.

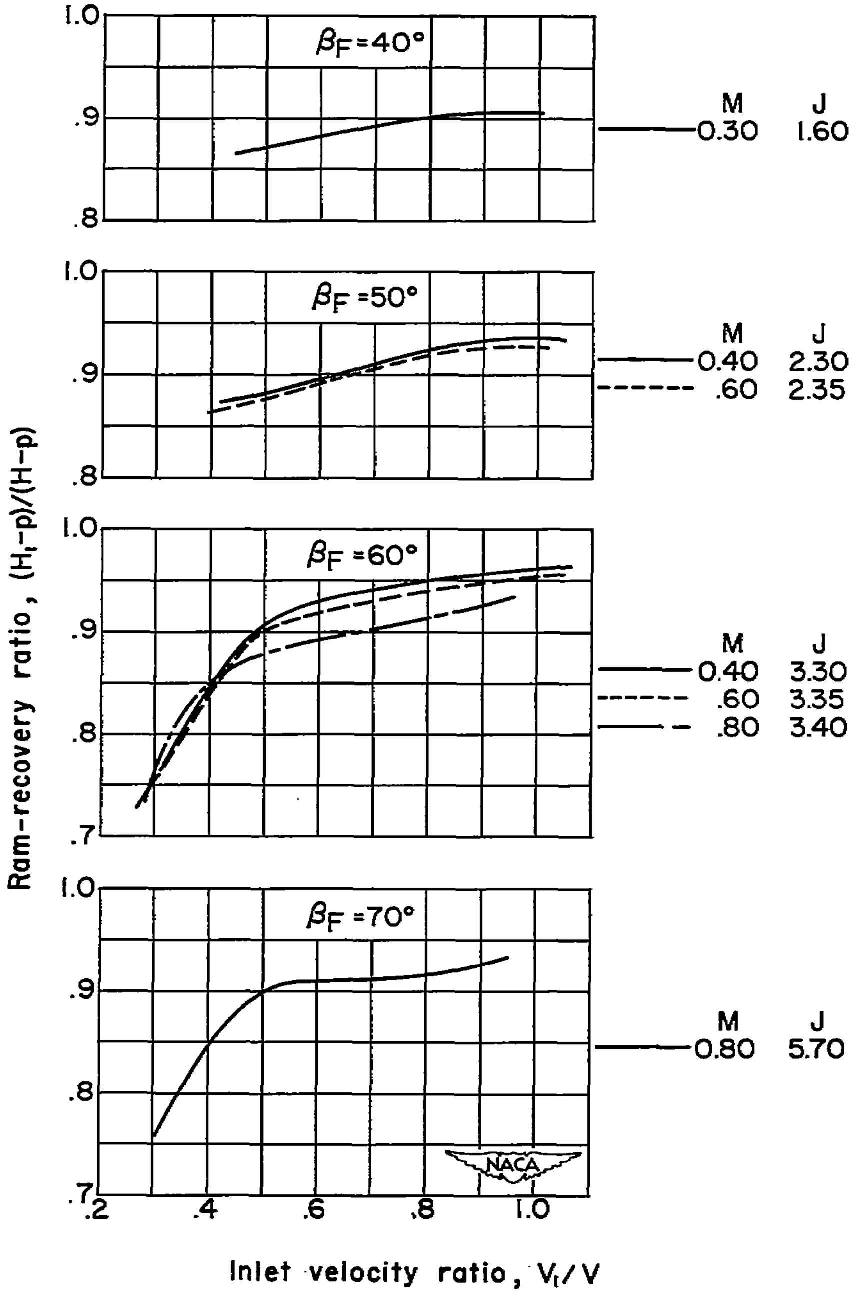

(a) B = 6

Figure 12.– The effect of inlet velocity ratio on the average ram-recovery ratio for various Mach numbers; propeller operating, J for $\eta_{a_{max}}$.

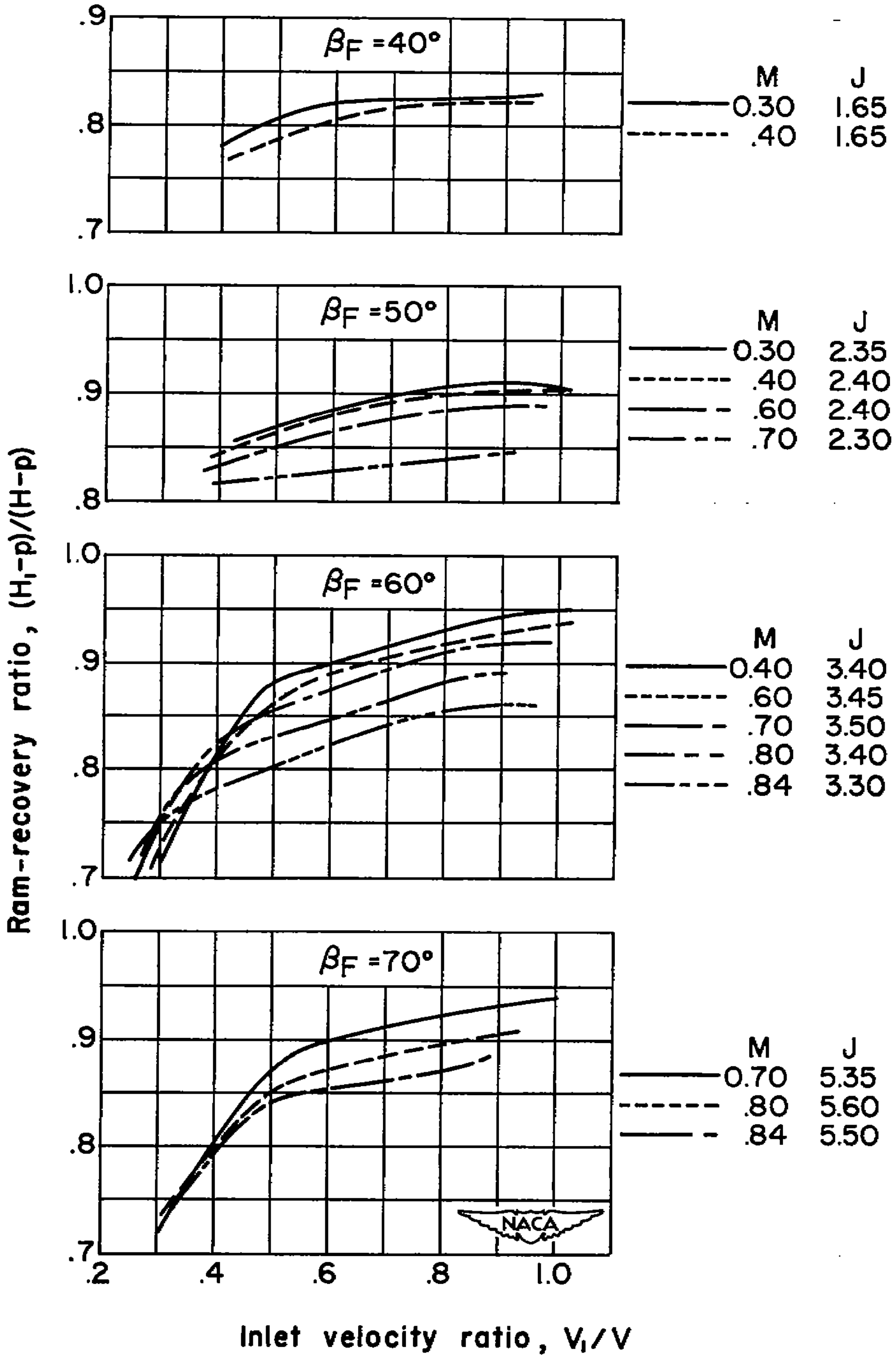

(b) B = 8

Figure 12.— Concluded.

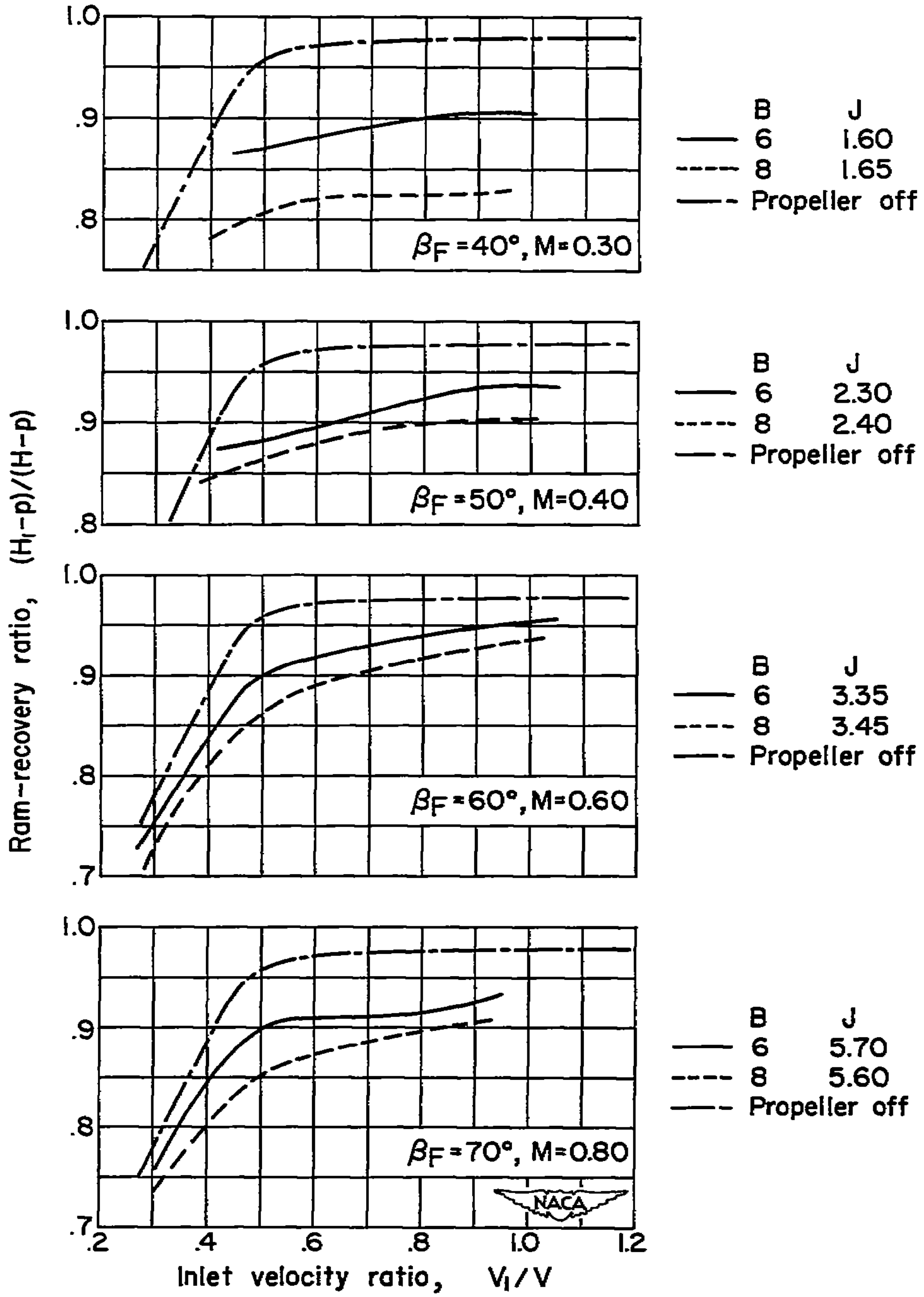

Figure 13.– Comparison of the average ram-recovery ratio for the six- and eight- blade dual-rotation propellers operating ahead of the cowl and for the propeller removed; J for $\eta_{a_{max}}$.

[redacted]

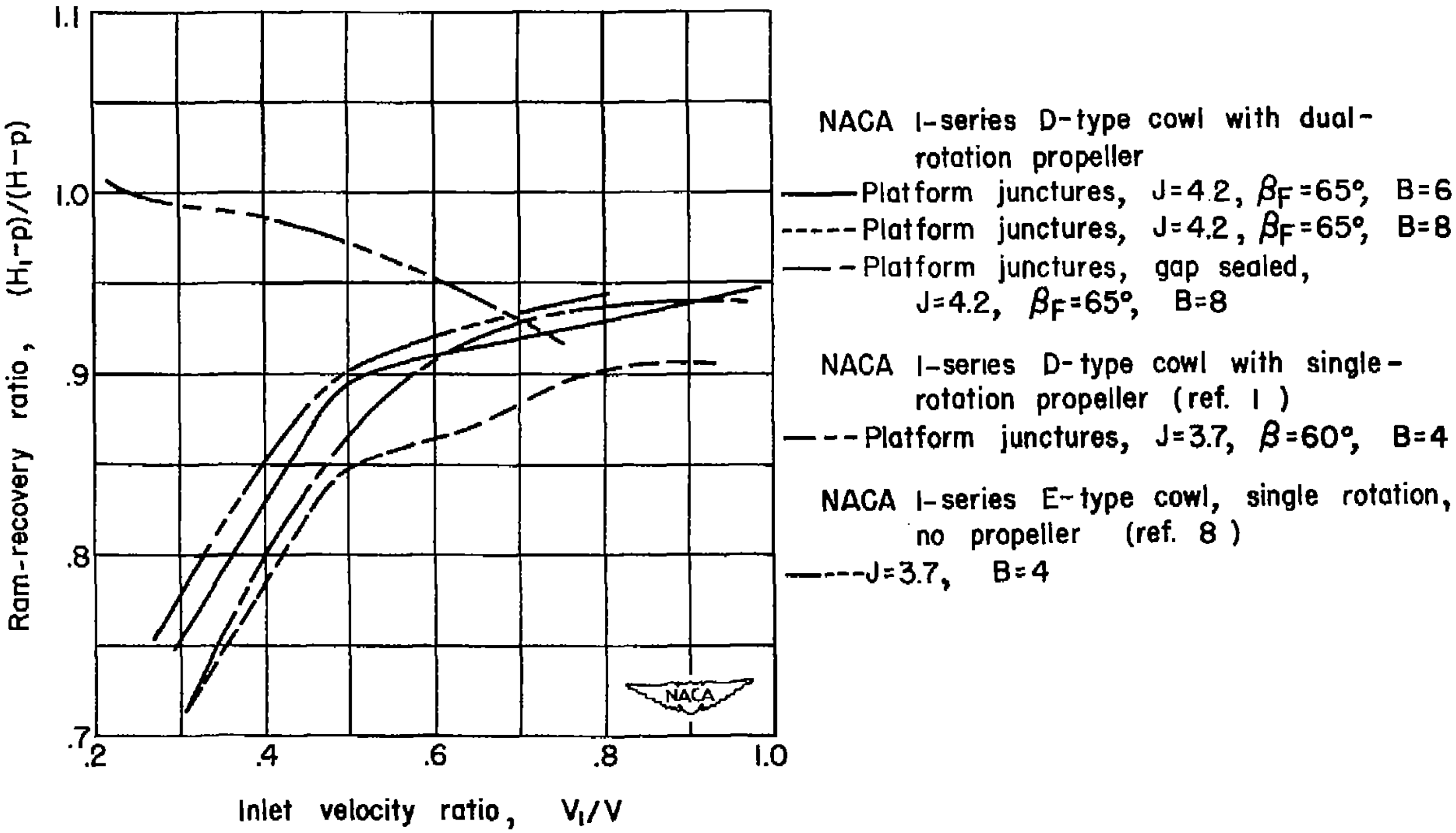

Figure 14.- Comparison of the average ram-recovery ratio for a six- and eight-blade dual-rotation propeller-spinner-cowling combination, a four-blade single-rotation propeller-spinner-cowling combination, and a single-rotation NACA 1-series E-type cowl.

[redacted]

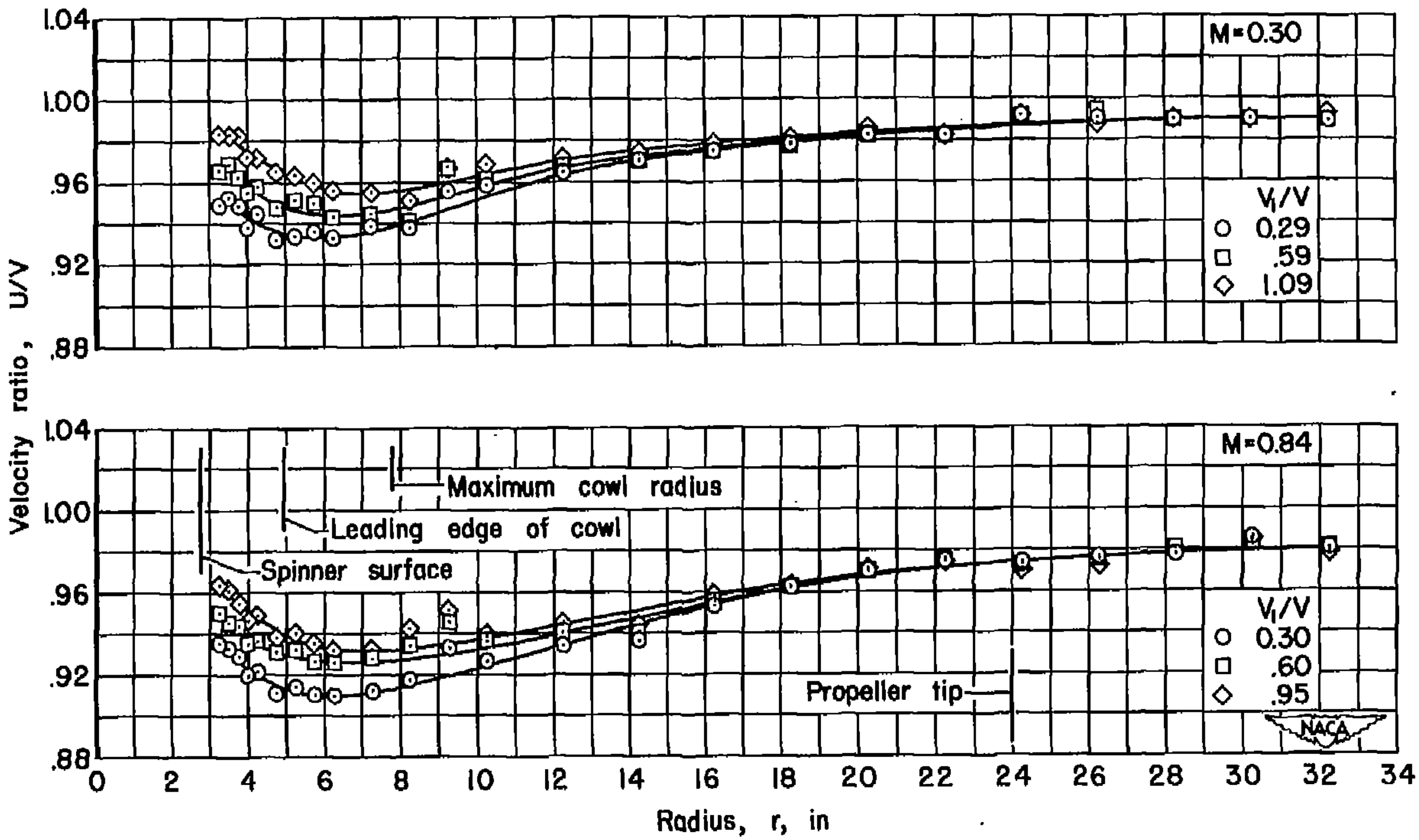

(a) NACA 1-46.5-085 dual-rotation spinner; front plane of rotation.

Figure 15.– Typical radial distributions of the local velocity ratio in the propeller plane; cowl on.

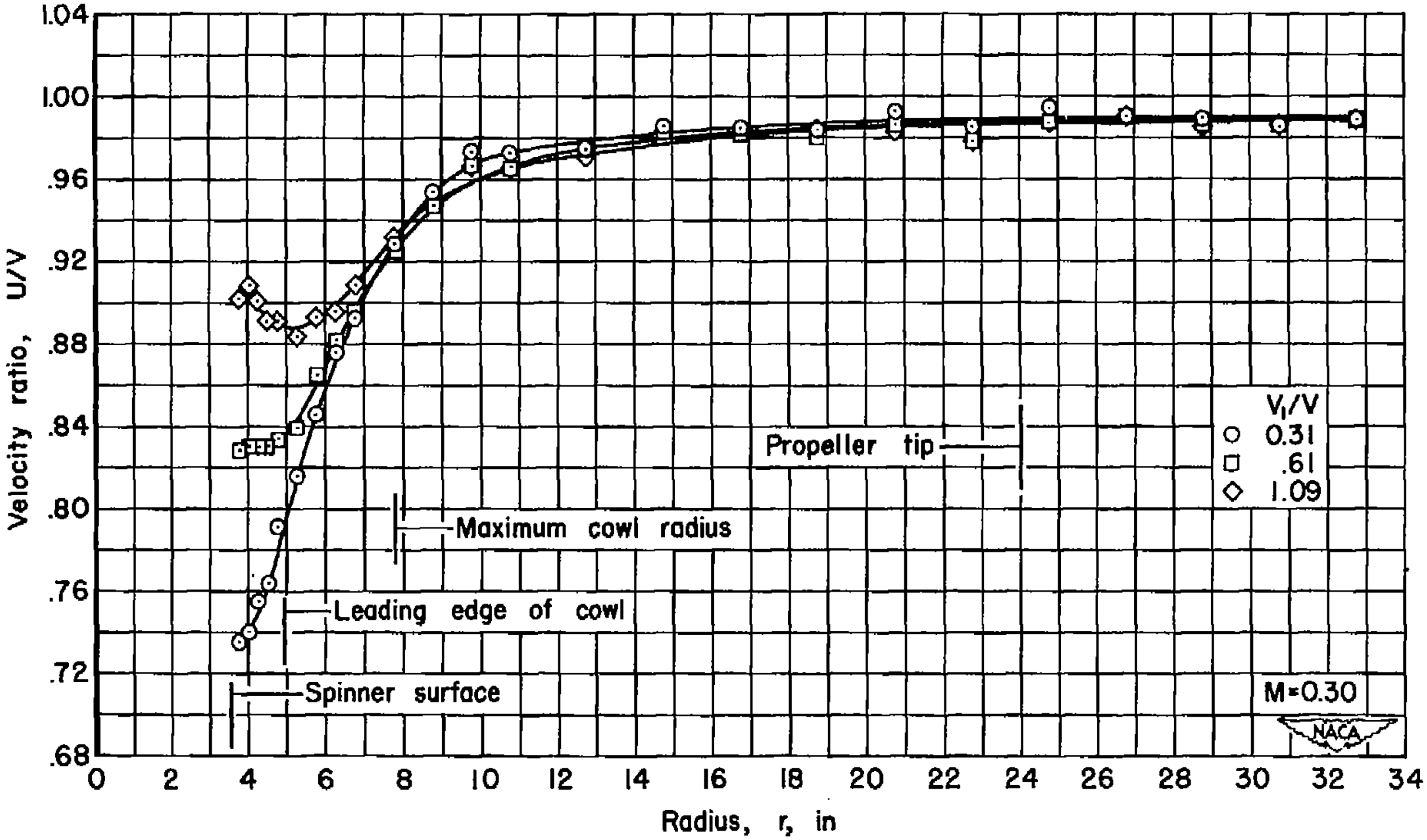

(b) NACA 1-46.5-085 dual-rotation spinner; rear plane of rotation.

Figure 15.– Continued.

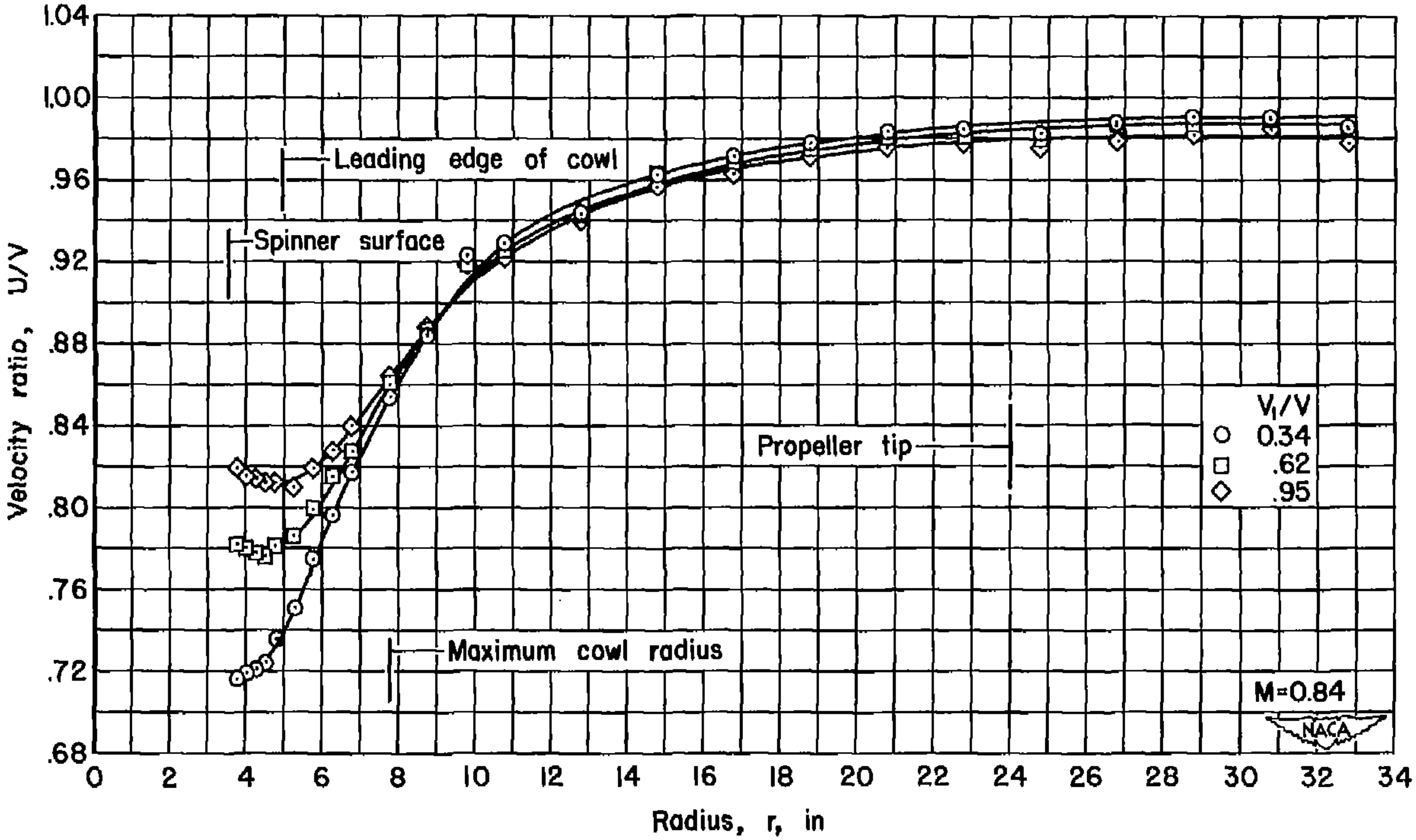

(b) NACA 1-46.5-085 dual rotation spinner; rear plane of rotation – Concluded.

Figure 15.– Continued.

[redacted]

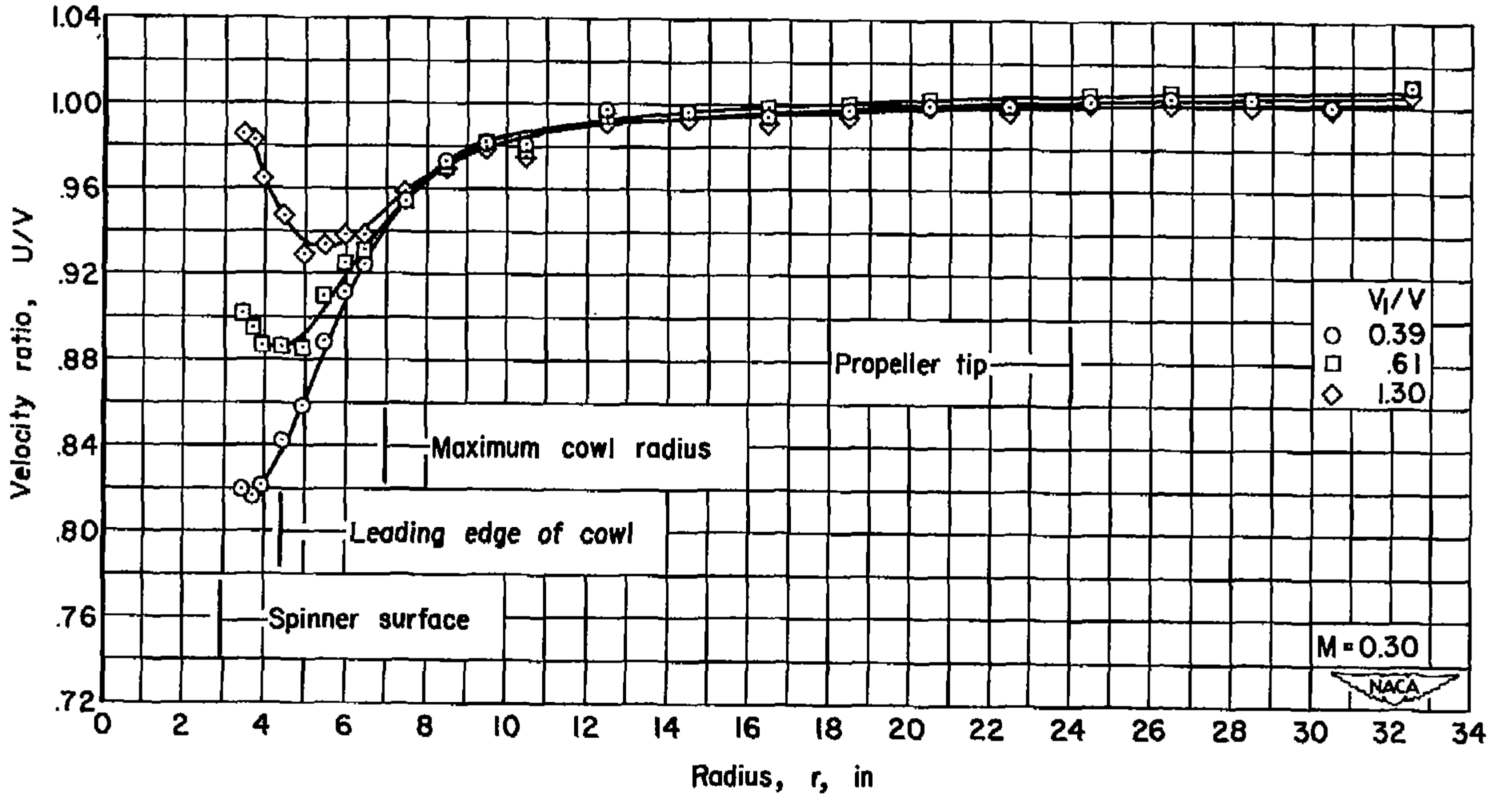

(c) NACA 1-46.5-047 single-rotation spinner.

Figure 15.– Continued.

[redacted]

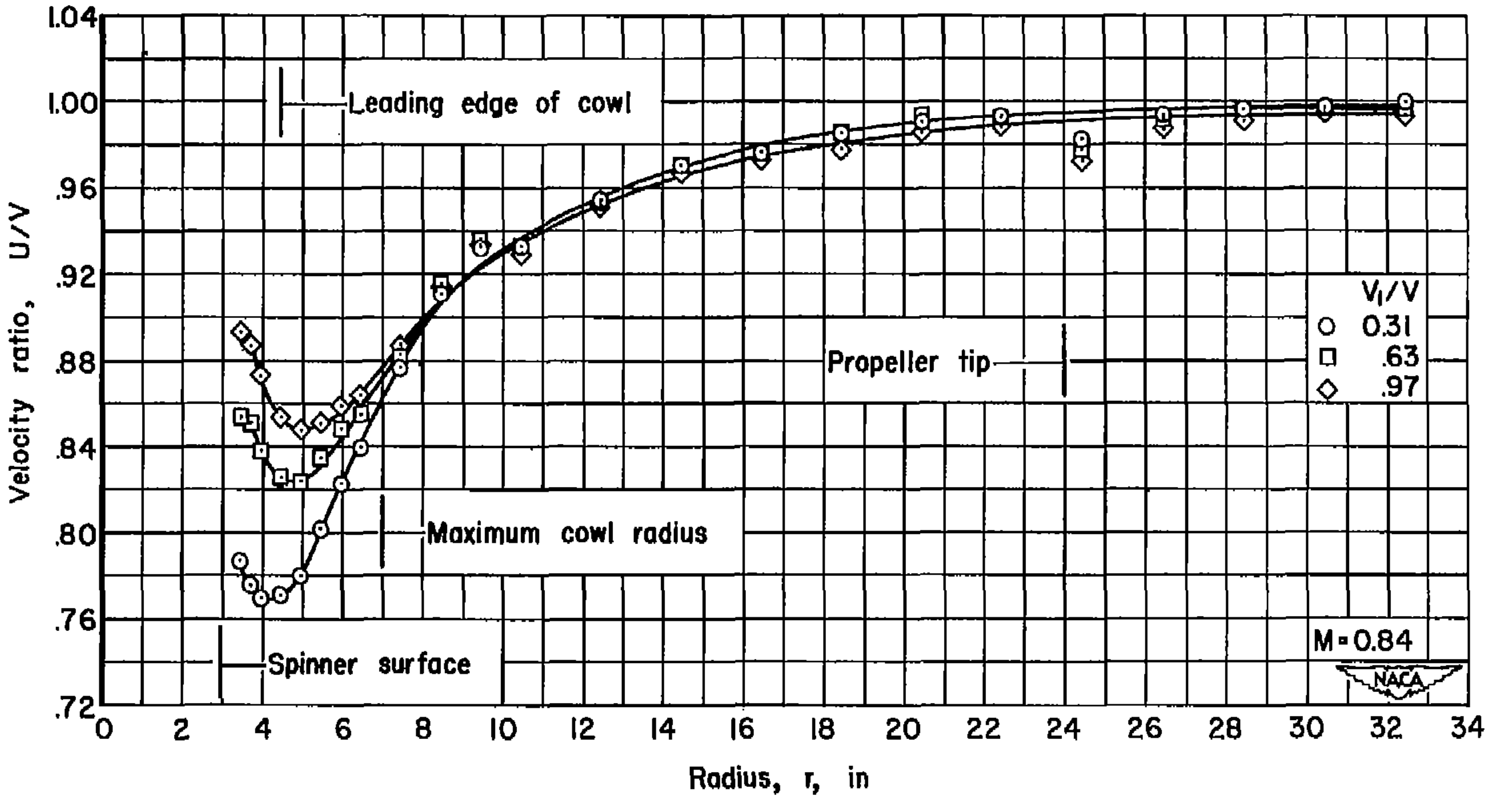

(c) NACA 1-46.5-047 single-rotation spinner – Concluded

Figure 15.– Concluded.

[redacted]

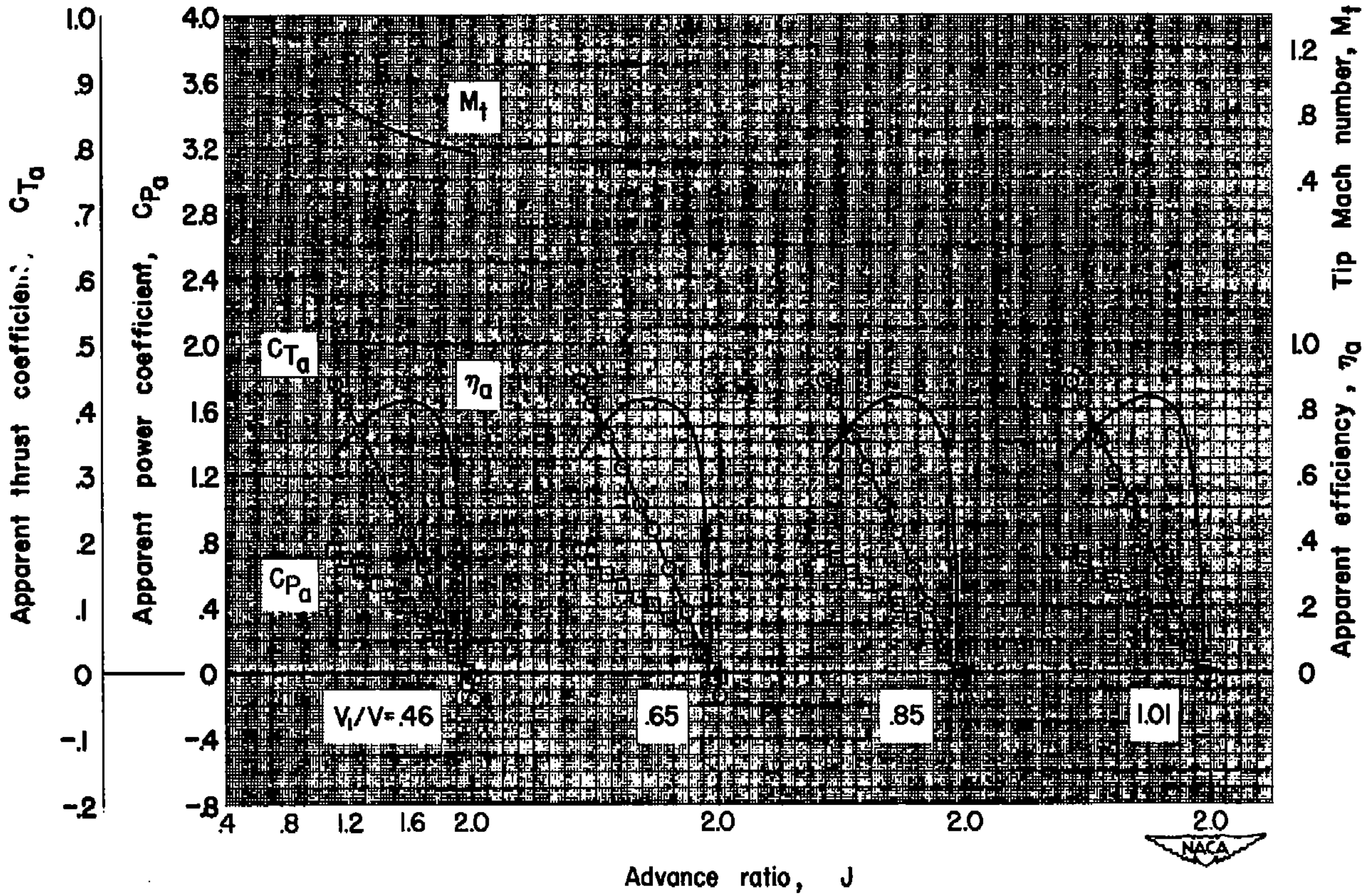

[redacted]

(a) $M = 0.30$; $\beta_F = 40°$

Figure 16.– Characteristics of the six-blade dual-rotation propeller operating in the presence of the cowl.

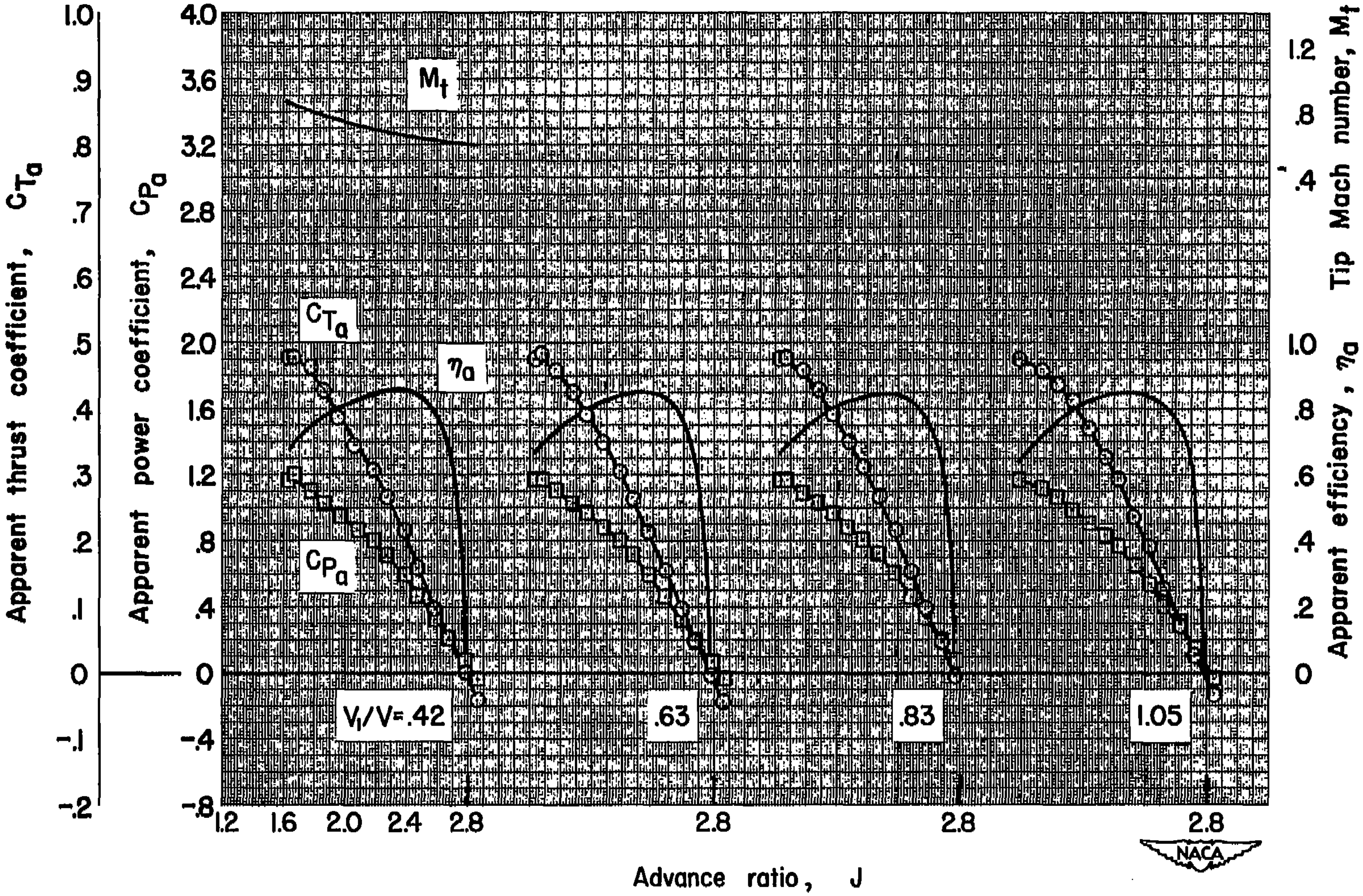

(b) $M = 0.40$; $\beta_F = 50^{\circ}$

Figure 16.– Continued.

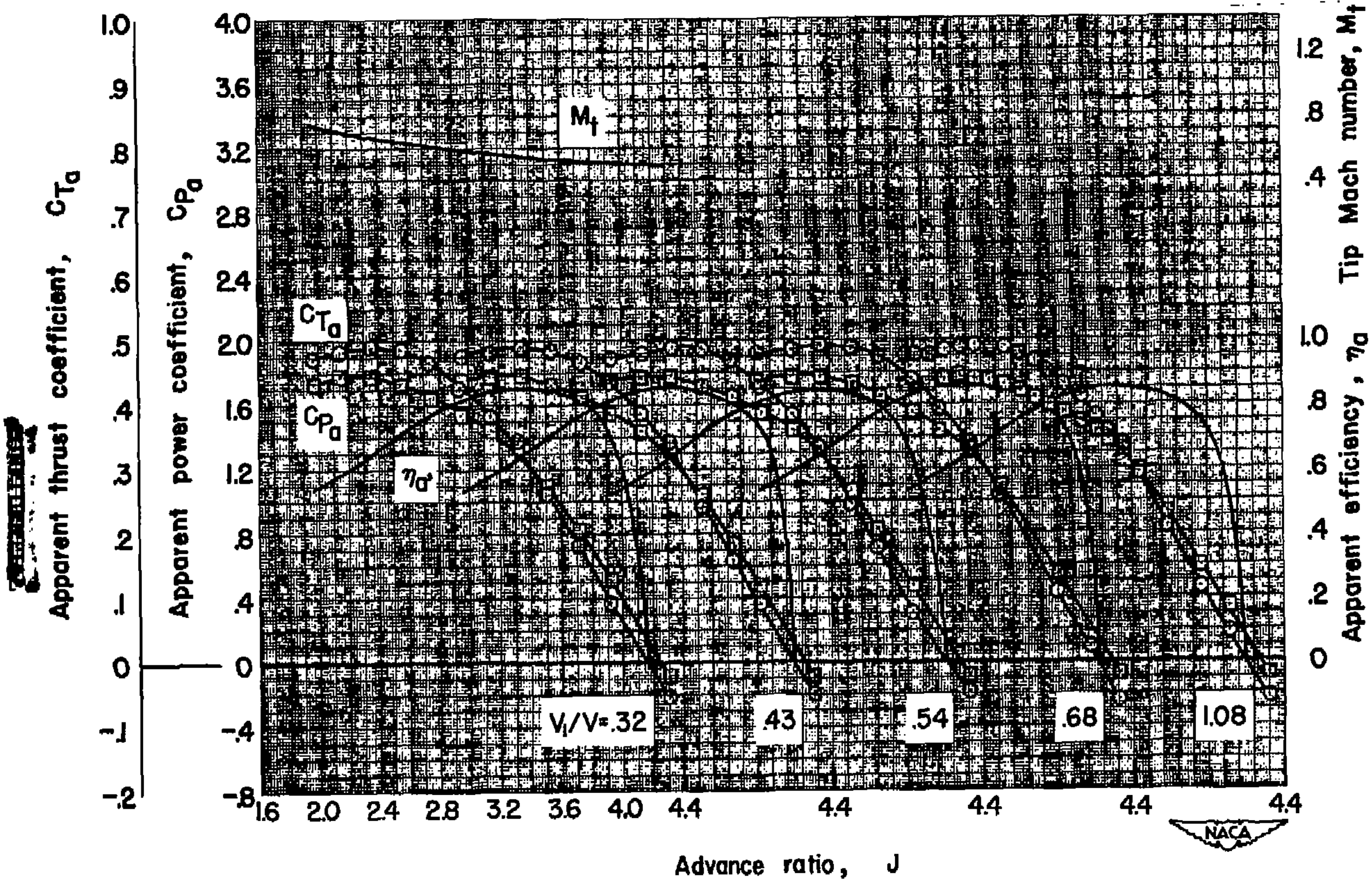

(c) $M = 0.40$; $\beta_F = 60^\circ$

Figure 16.— Continued.

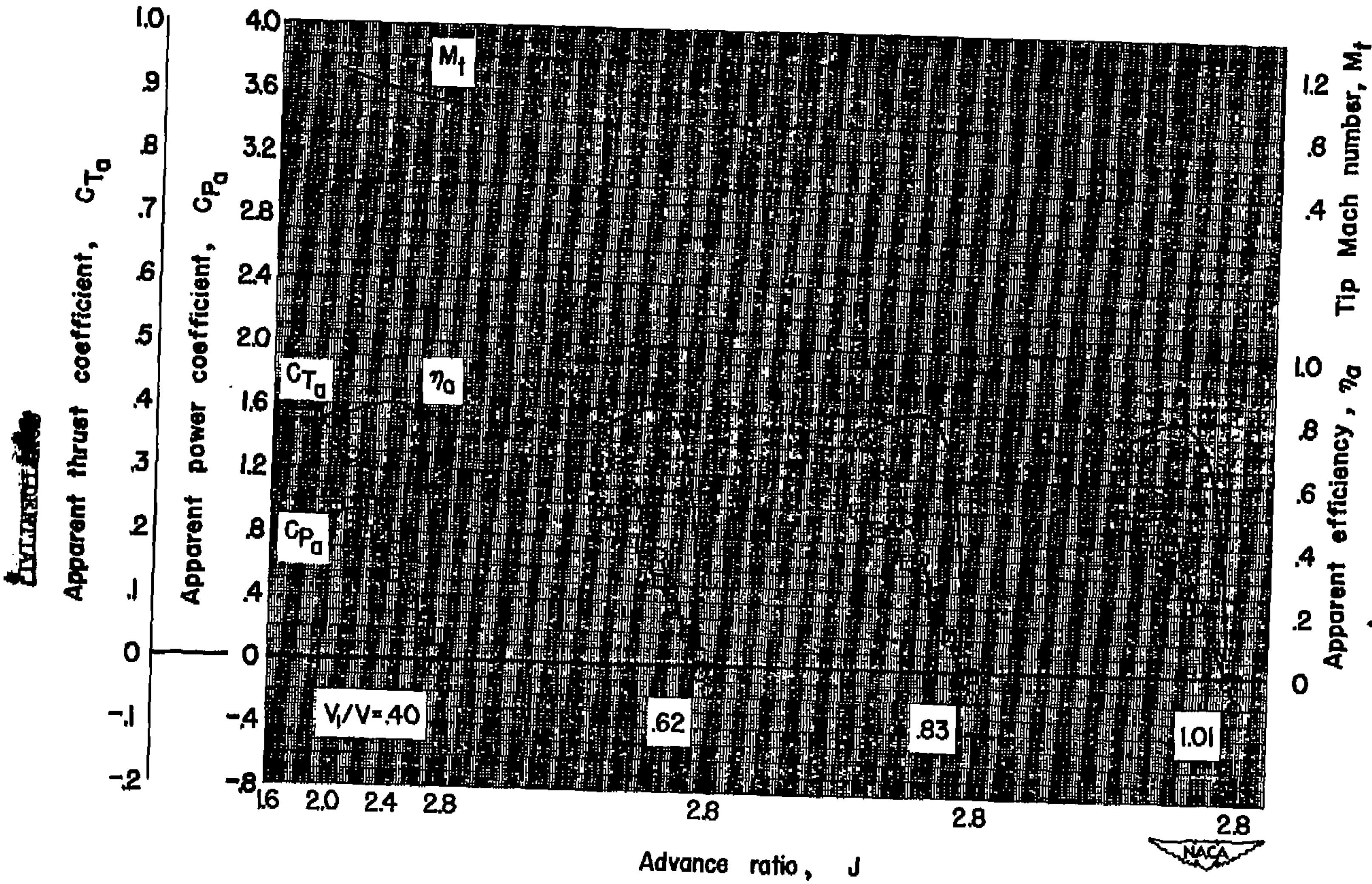

(a) M = 0.60; β_F = 50°

Figure 16.– Continued.

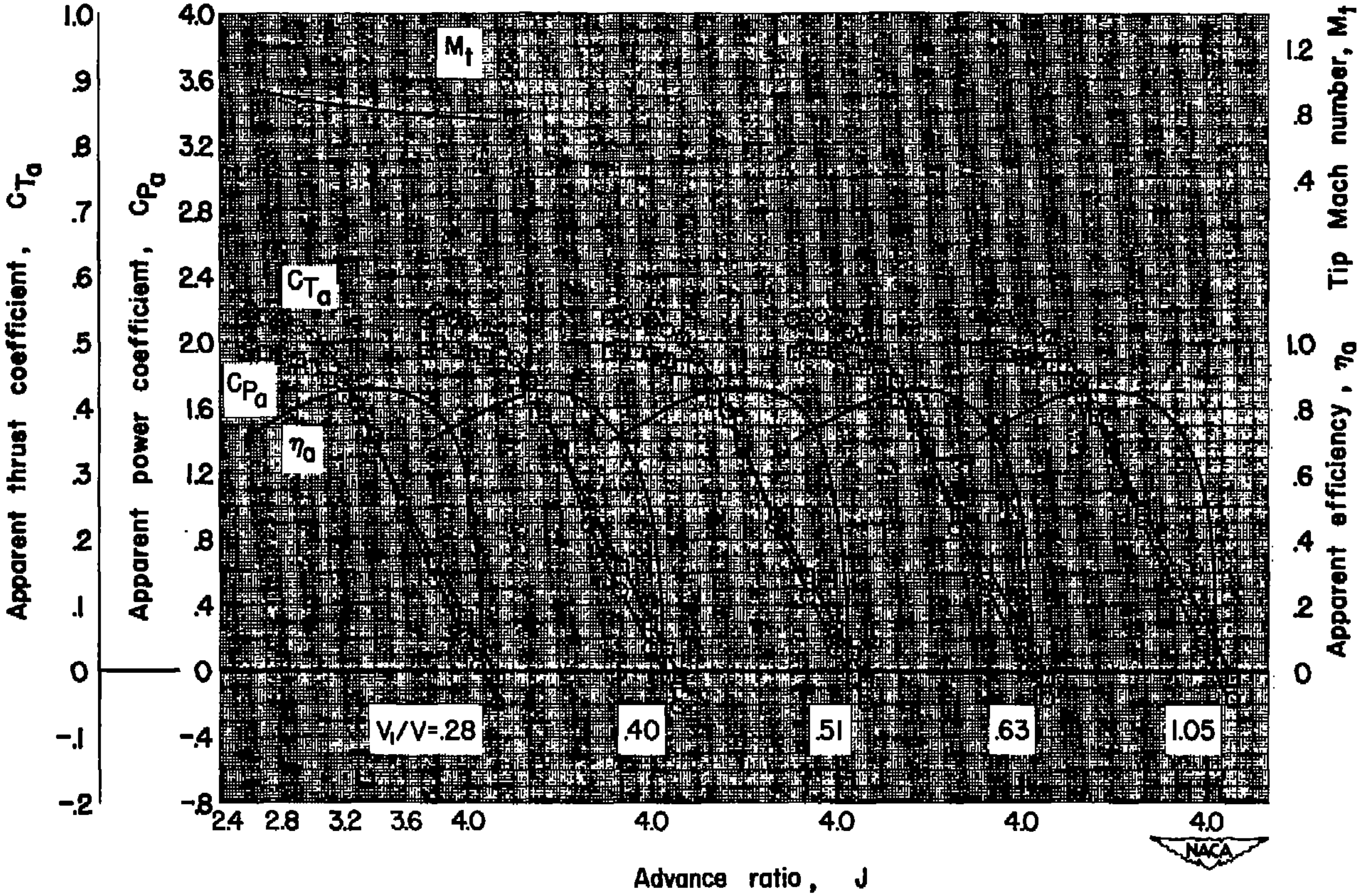

(e) $M = 0.60$, $\beta_F = 60^{\circ}$

Figure 16.– Continued.

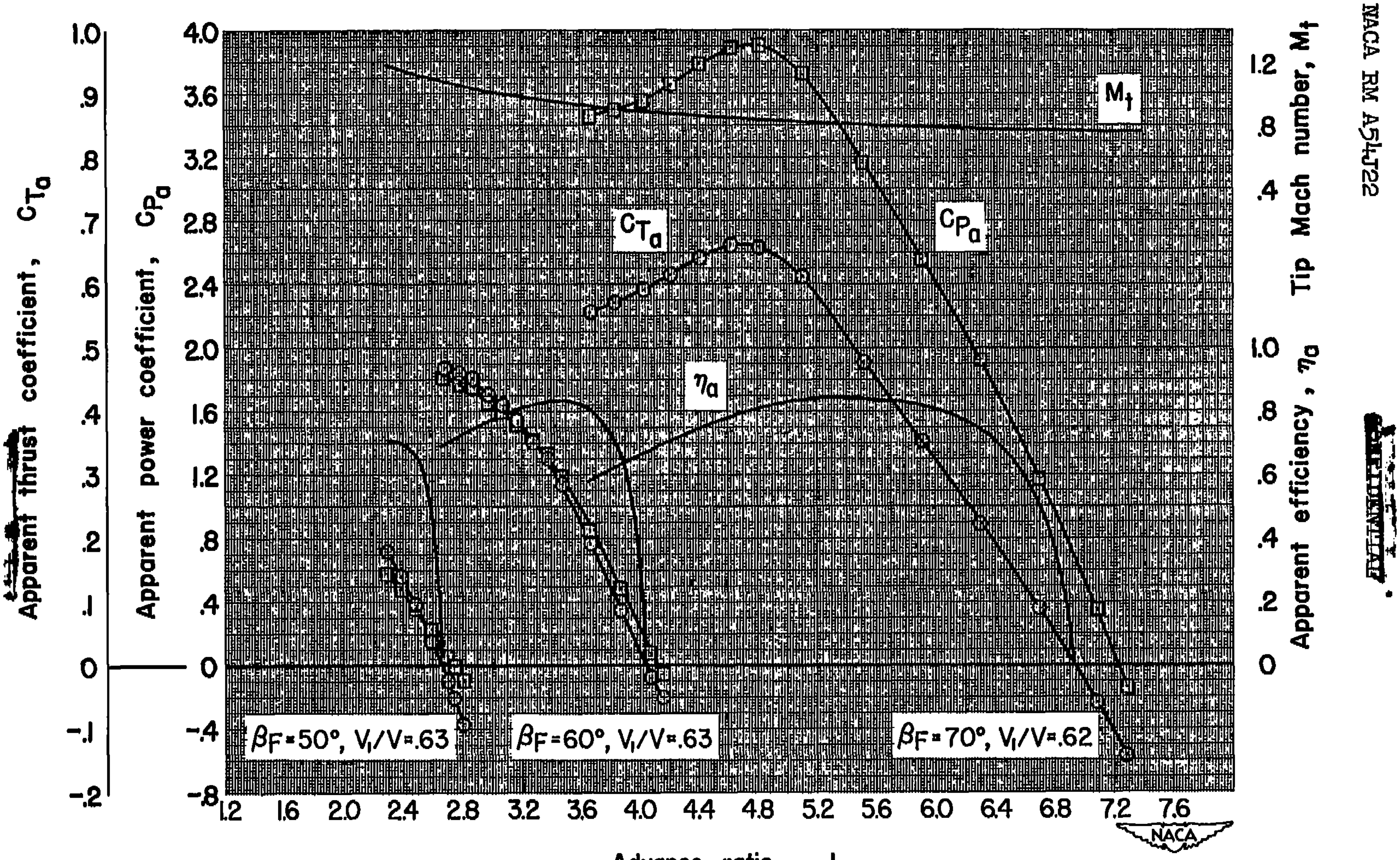

(f) M = 0.70; β_F = 50°, 60°, 70°

Figure 16.– Continued.

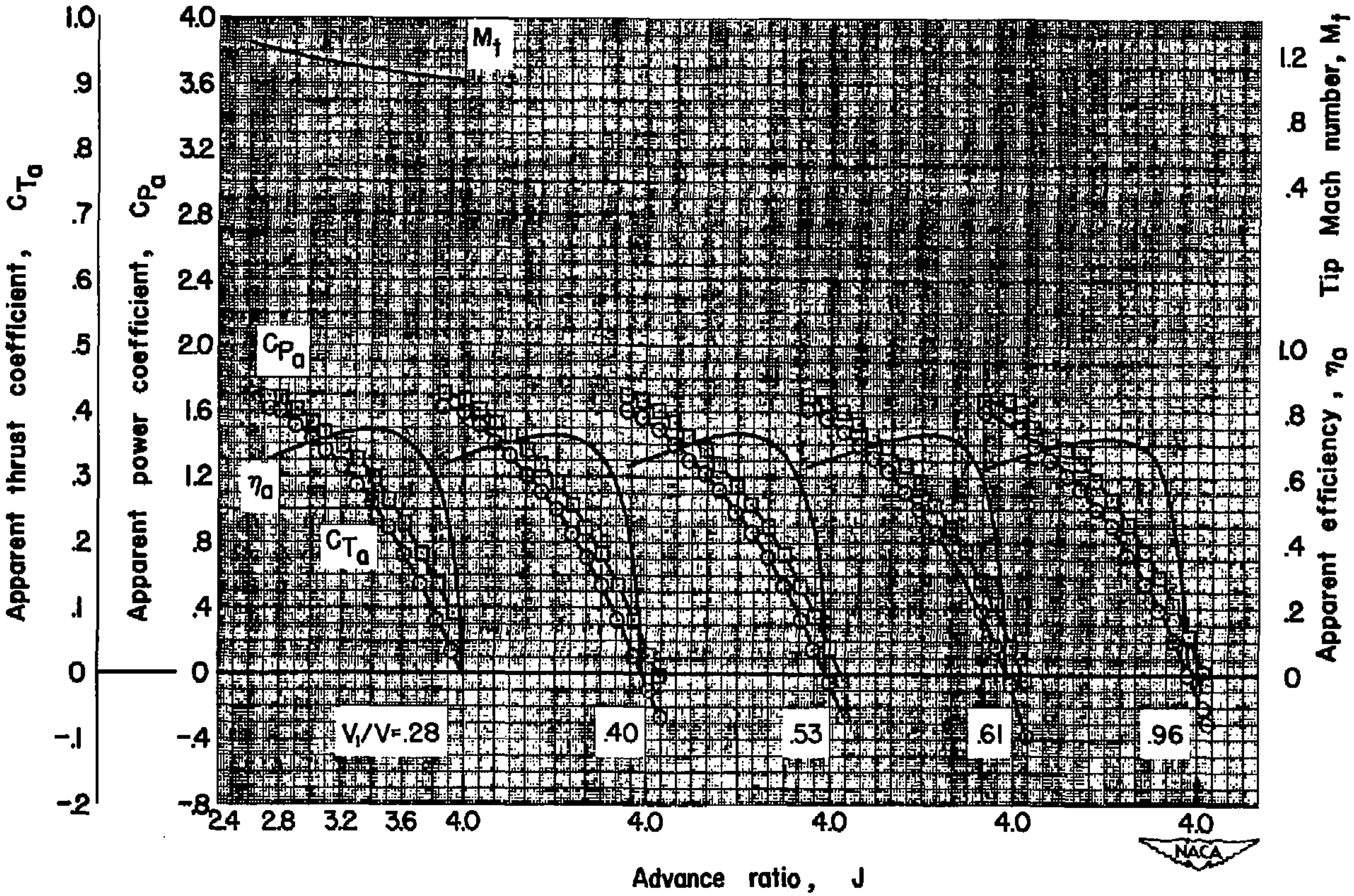

(g) $M = 0.80$, $\beta_F = 60^\circ$

Figure 16.– Continued.

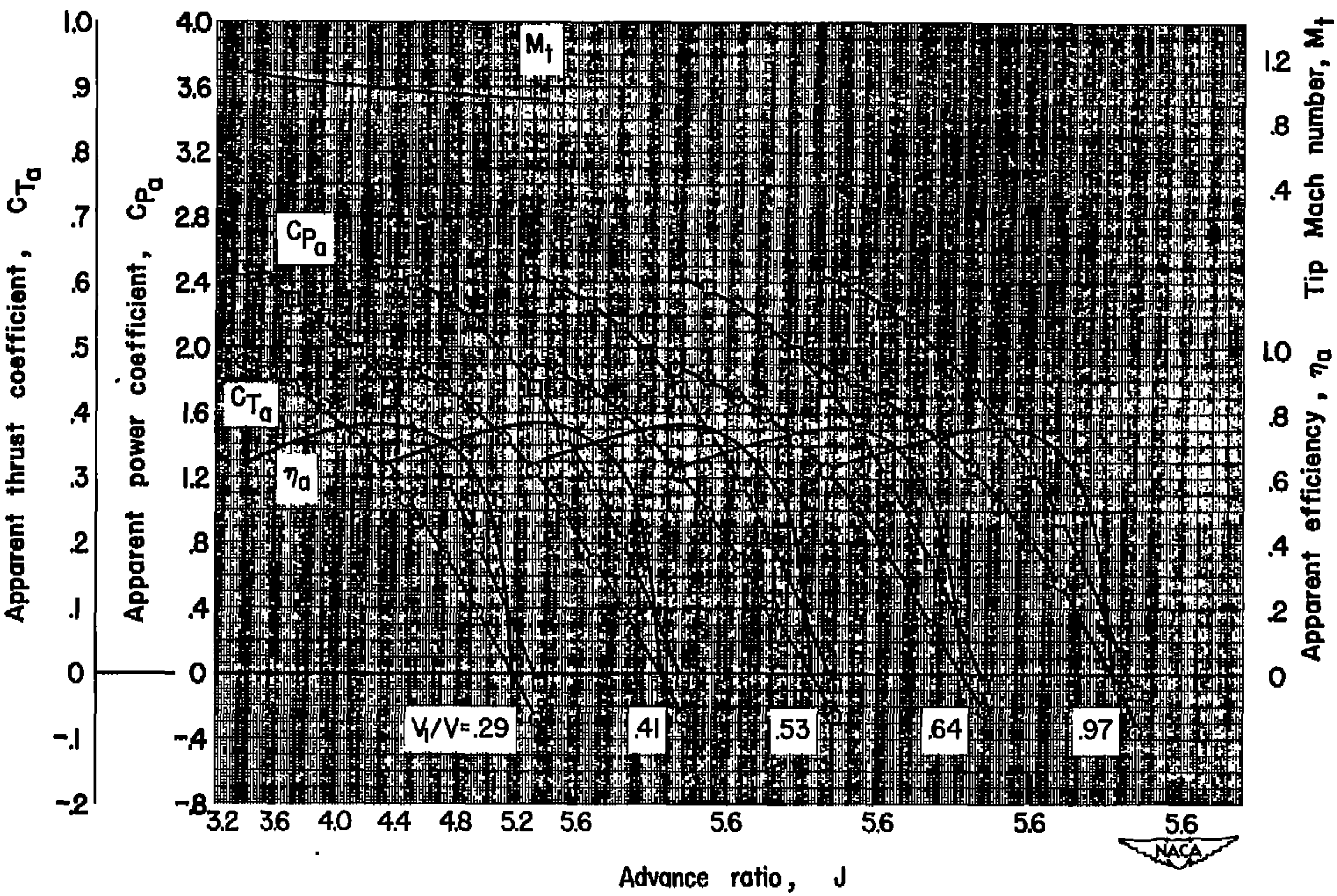

(h) M = 0.80; β_F = 65°

Figure 16.— Continued.

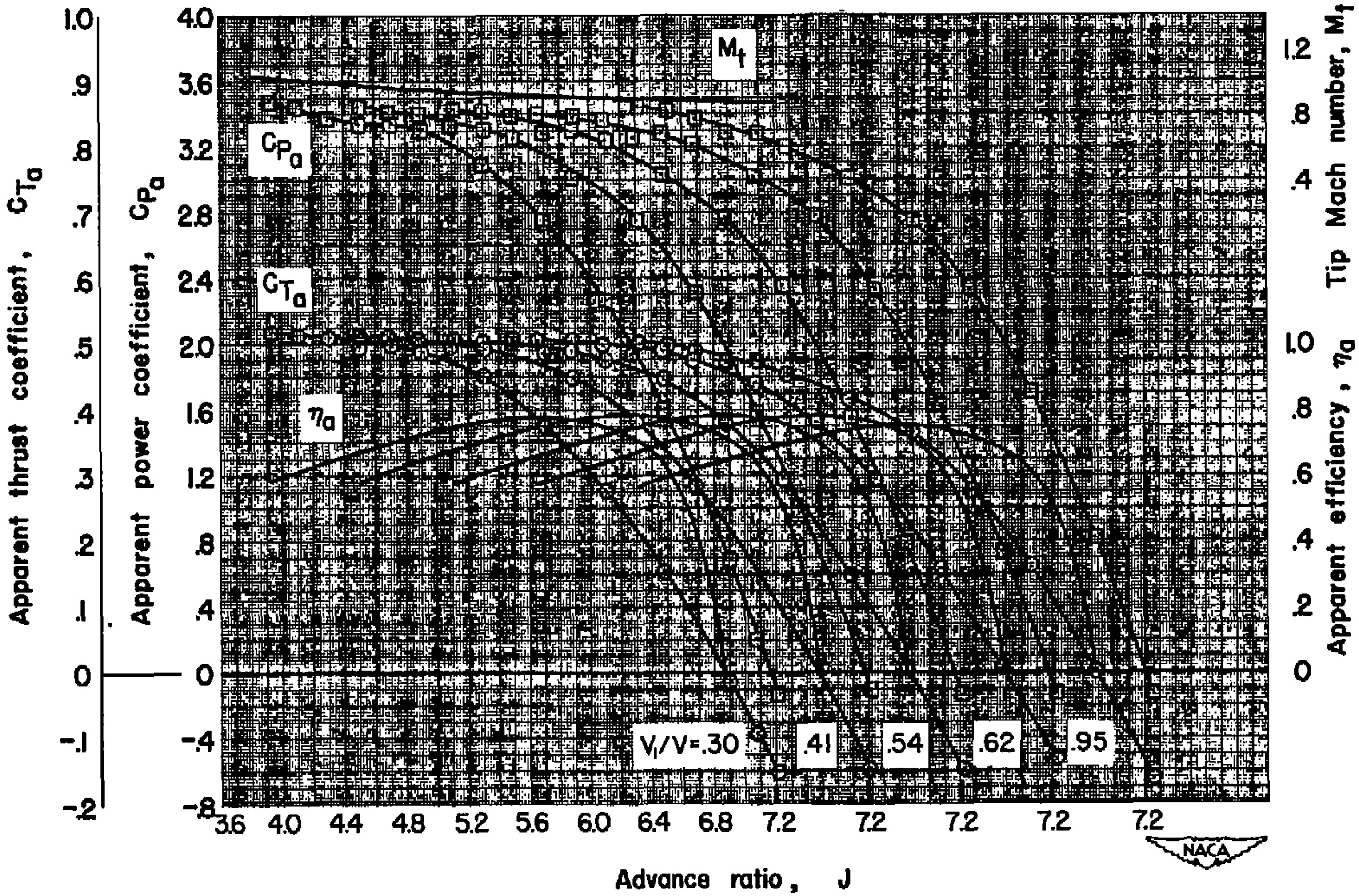

(i) $M = 0.80$; $\beta_F = 70^{\circ}$

Figure 16.– Concluded.

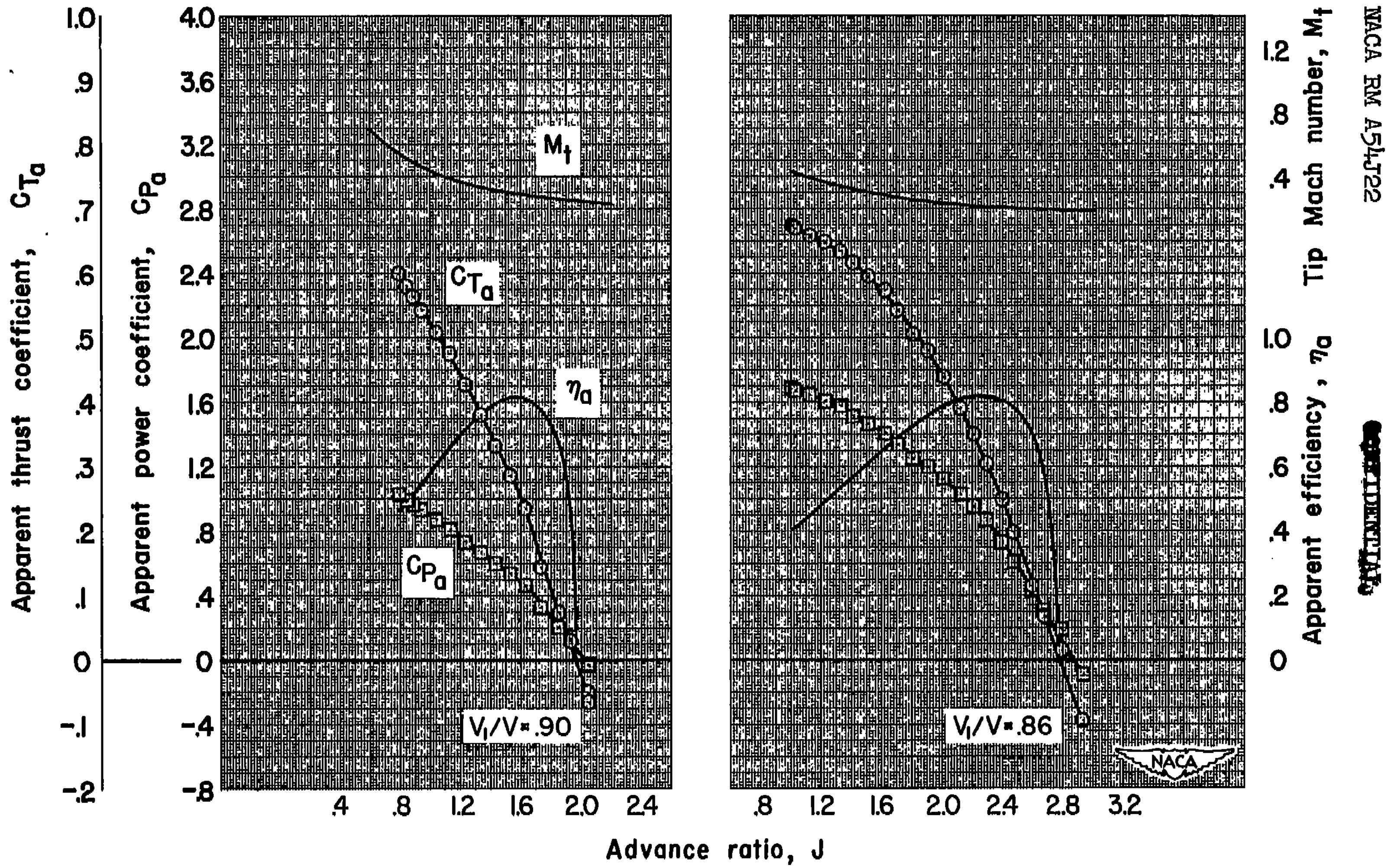

(a) M = 0.13; β_F = 40°

(b) M = 0.13; β_F = 50°

Figure 17.– Characteristics of the eight-blade dual-rotation propeller operating in the presence of the cowl.

[redacted]

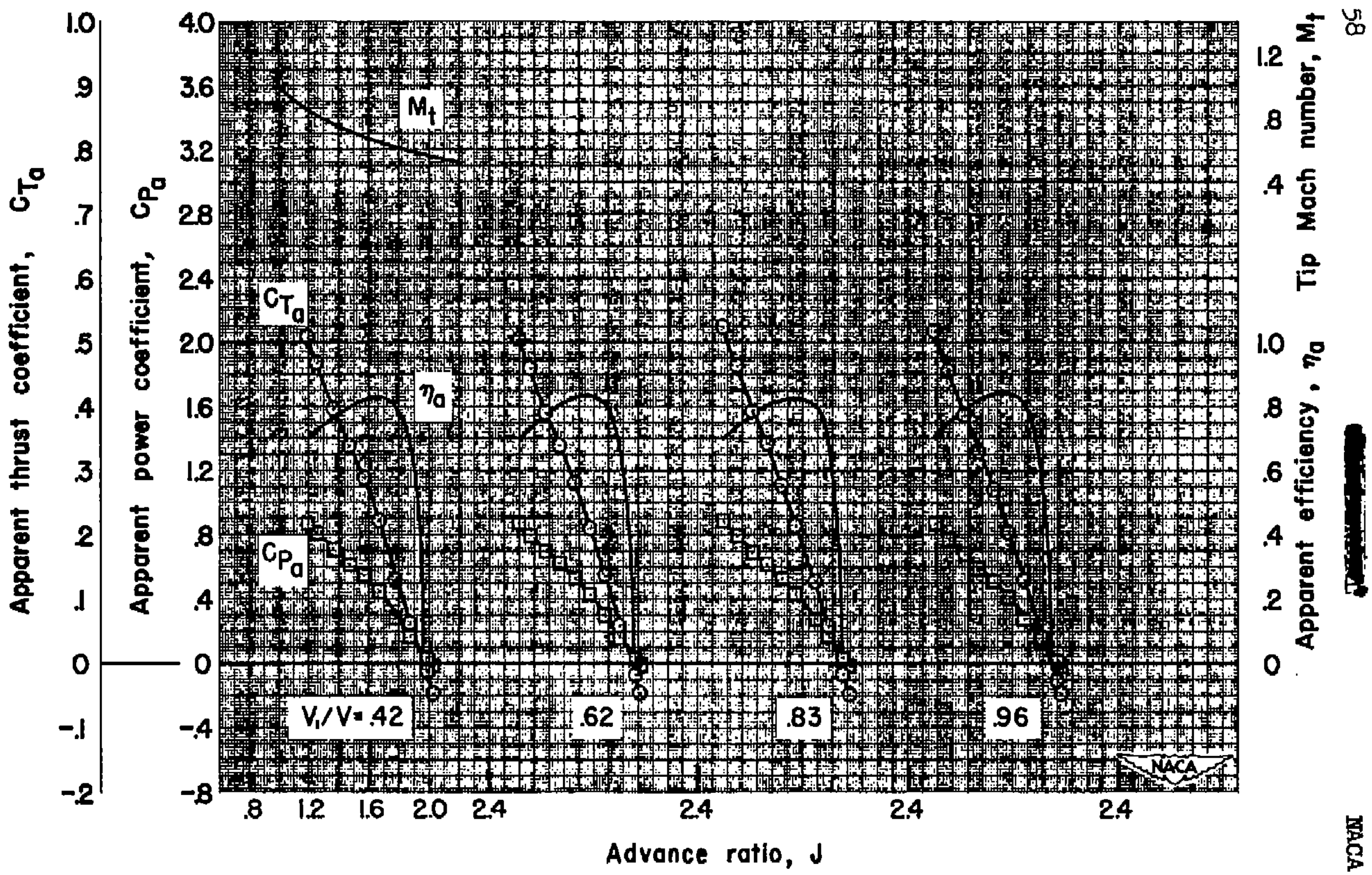

(c) $M = 0.30$; $\beta_F = 40^{\circ}$

Figure 17.– Continued.

[redacted]

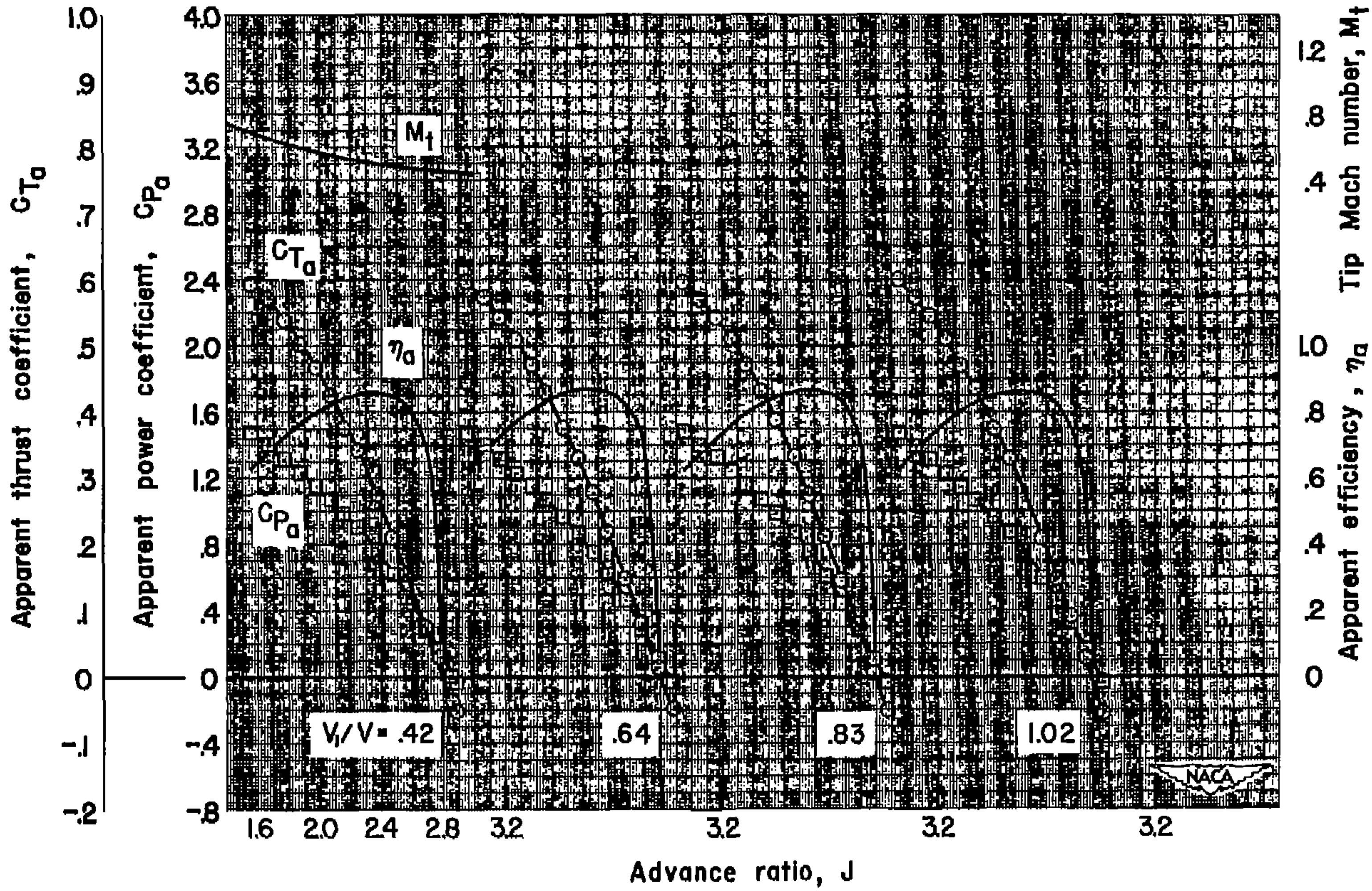

(d) M = 0.30; β_F = 50°

Figure 17.– Continued.

[redacted]

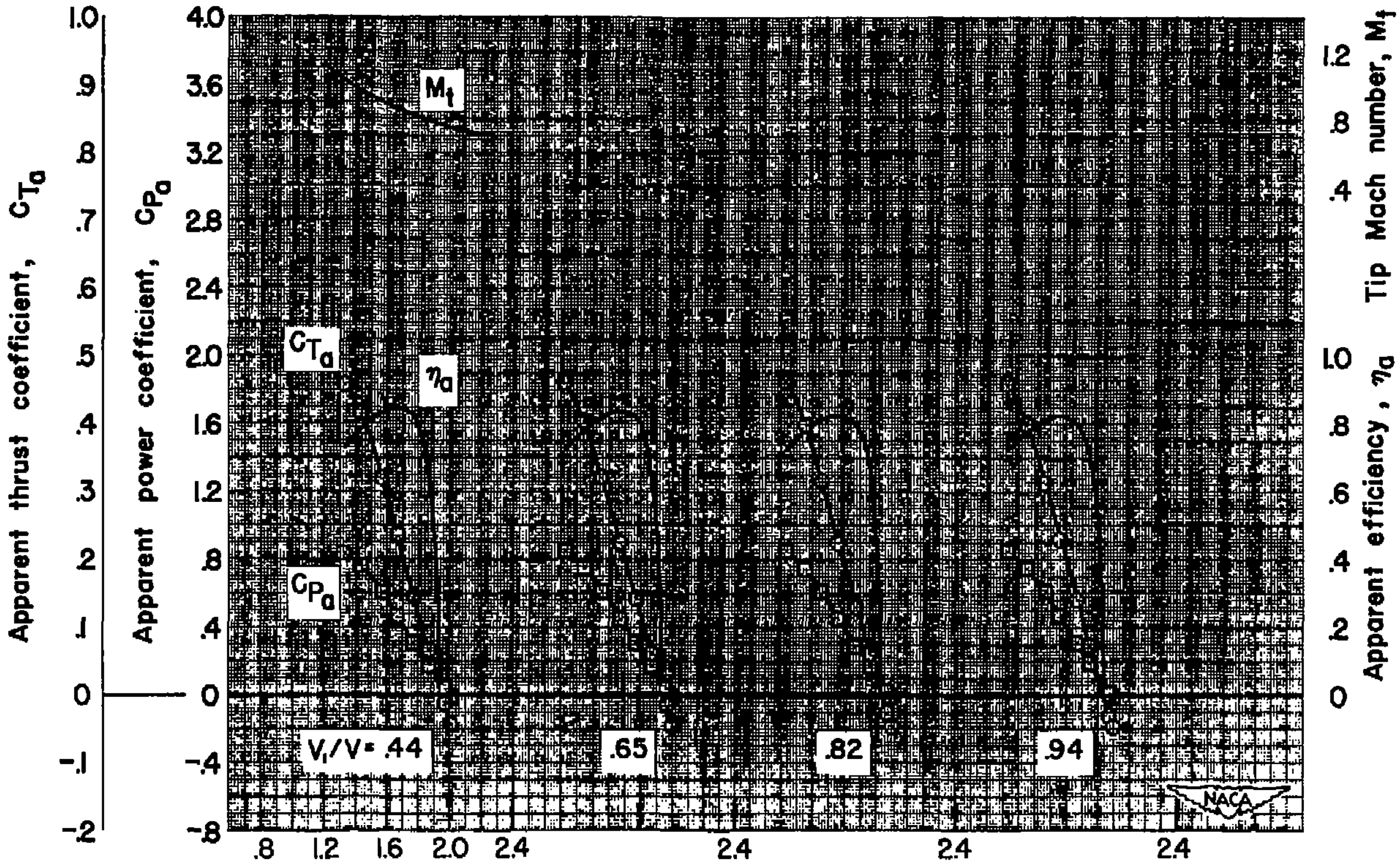

[redacted]

(e) $M = 0.40$; $\beta_F = 40^{\circ}$

Figure 17.– Continued.

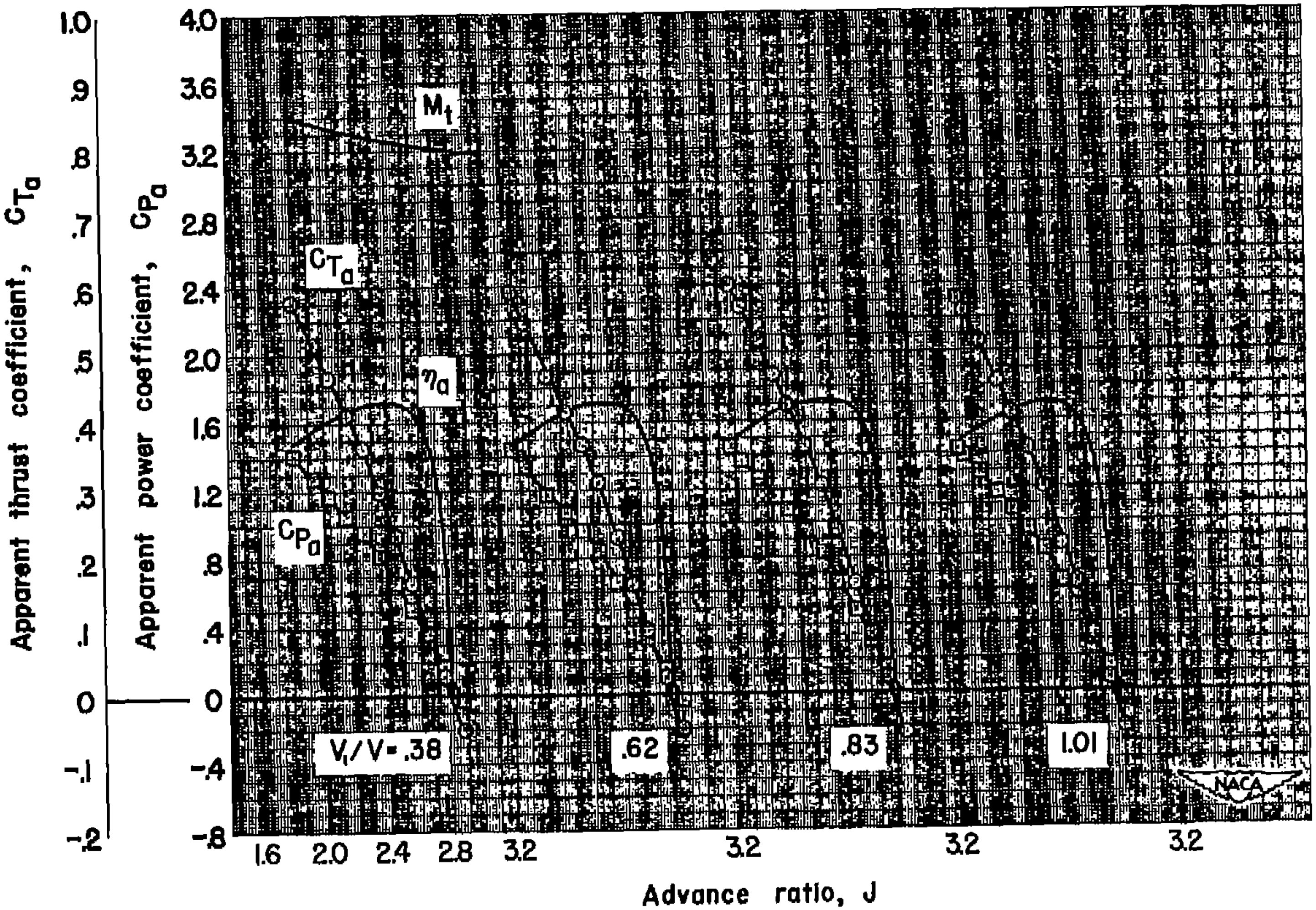

(f) $M = 0.40$; $\beta_F = 50^\circ$

Figure 17.– Continued.

[redacted]

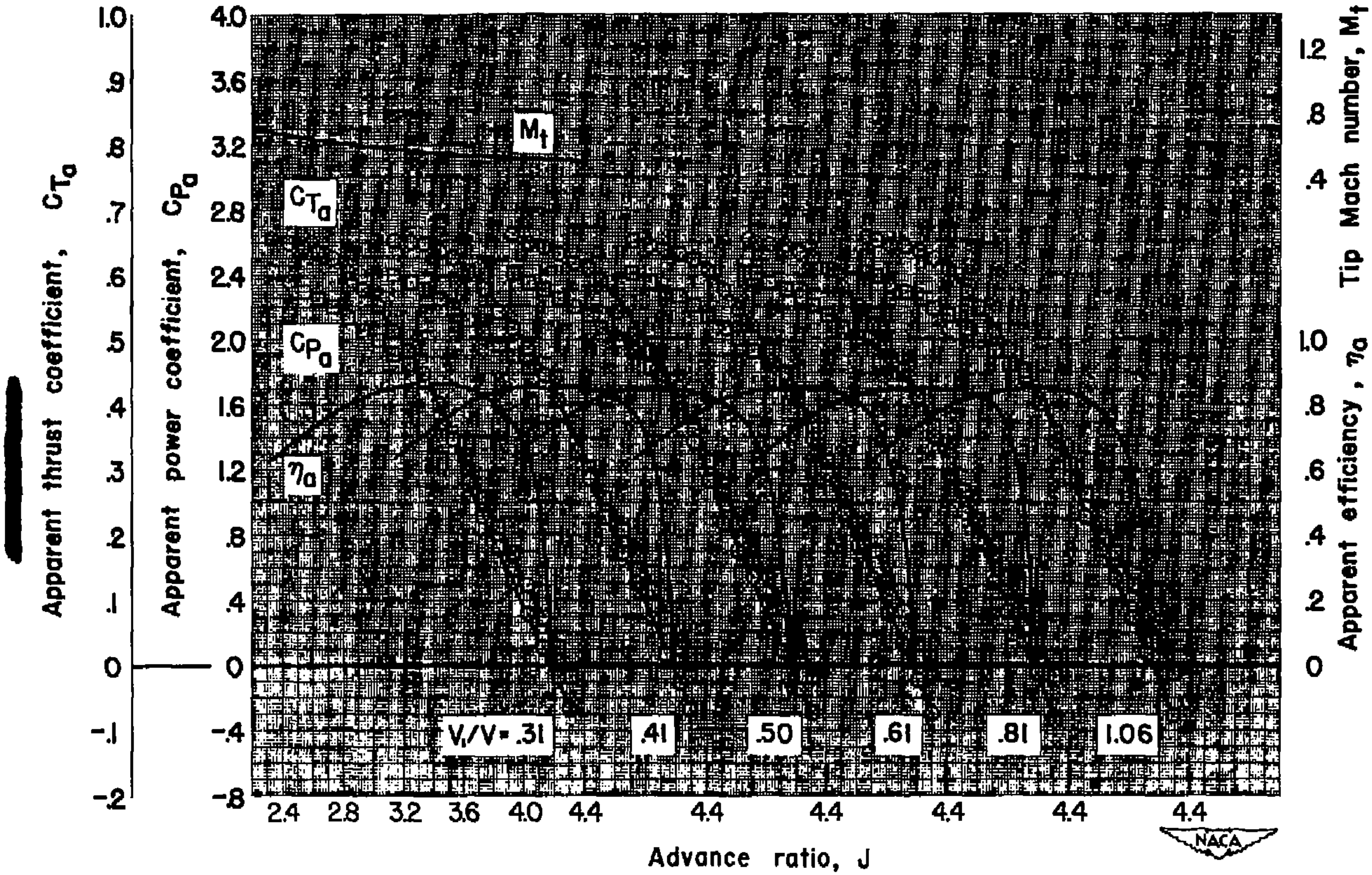

[redacted]

(g) $M = 0.40$; $\beta_F = 60^\circ$

Figure 17.– Continued.

[redacted]

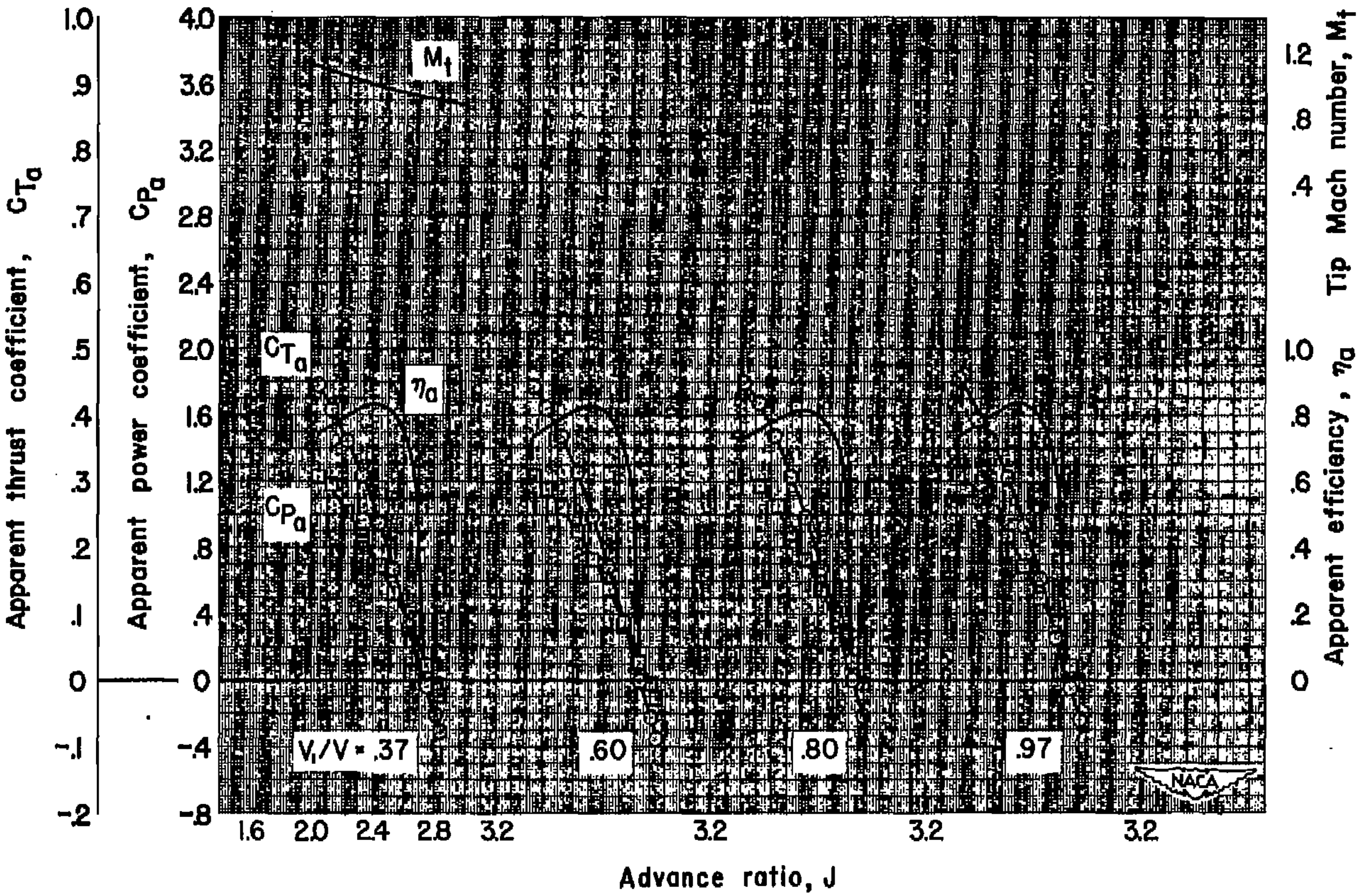

(h) M = 0.60; β_T = 50°

Figure 17.- Continued.

[redacted]

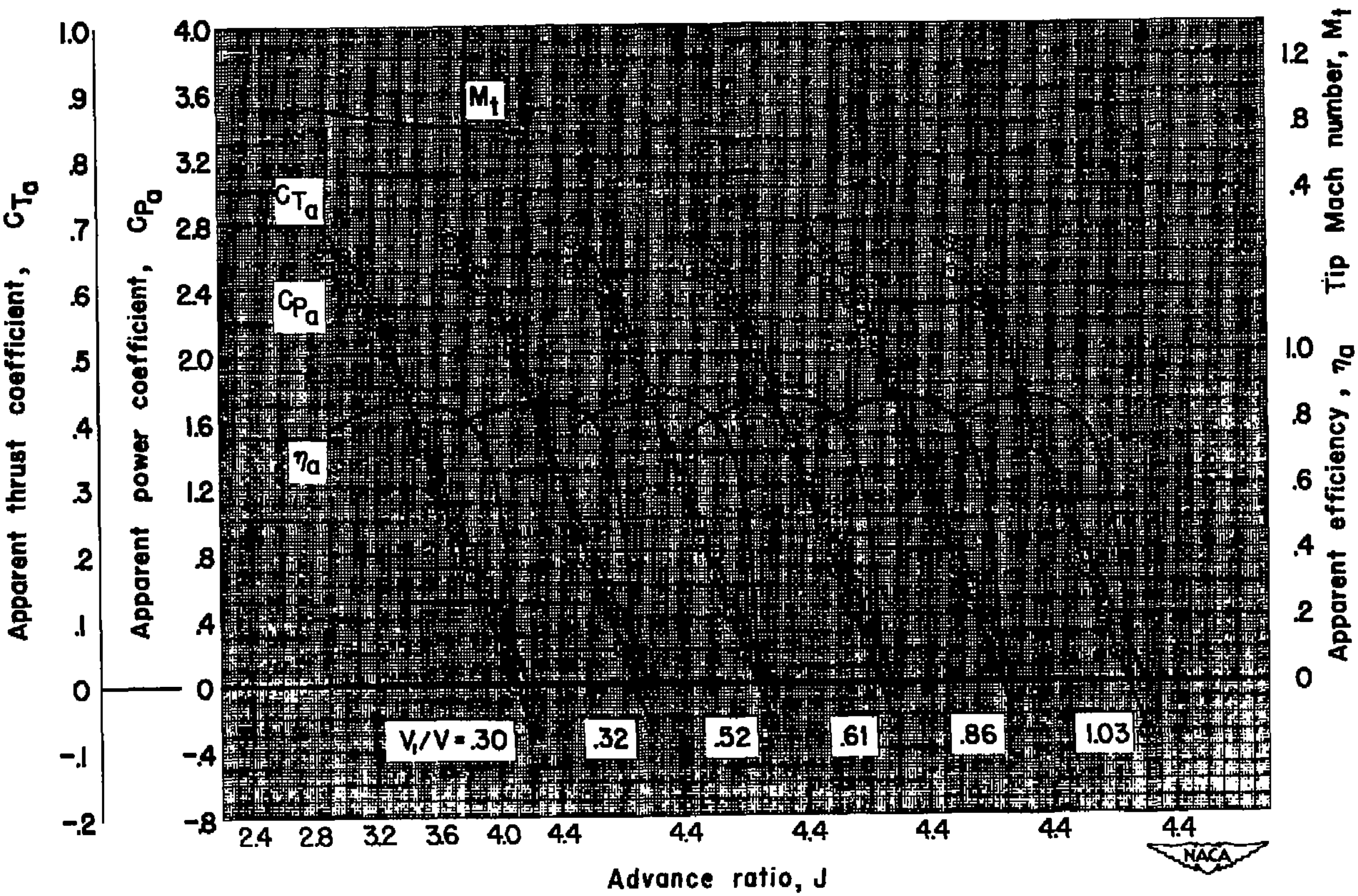

(i) $M = 0.60$; $\beta_F = 60^{\circ}$

Figure 17.- Continued.

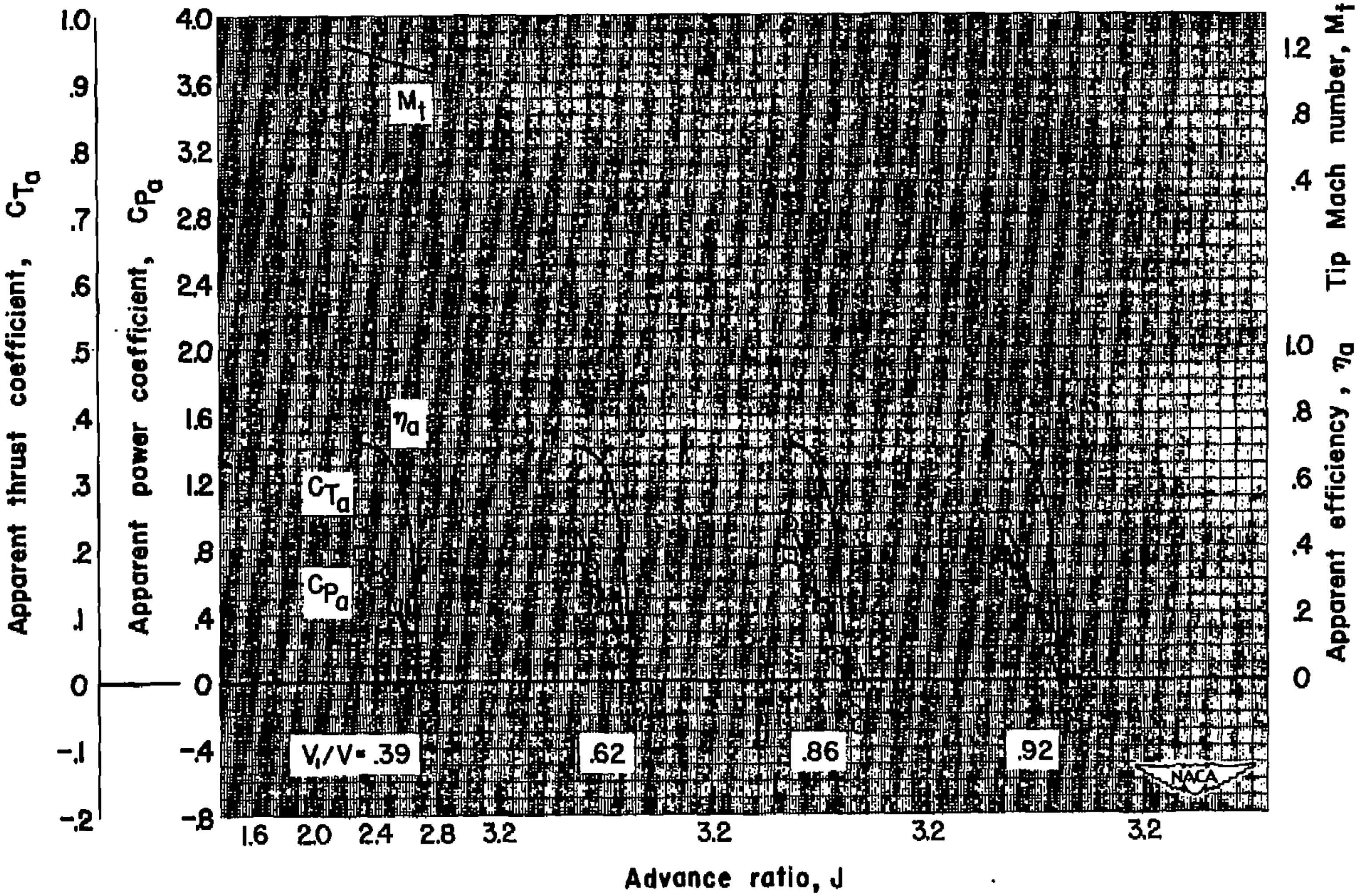

(j) M = 0.70; β_F = 50°

Figure 17.- Continued.

[redacted]

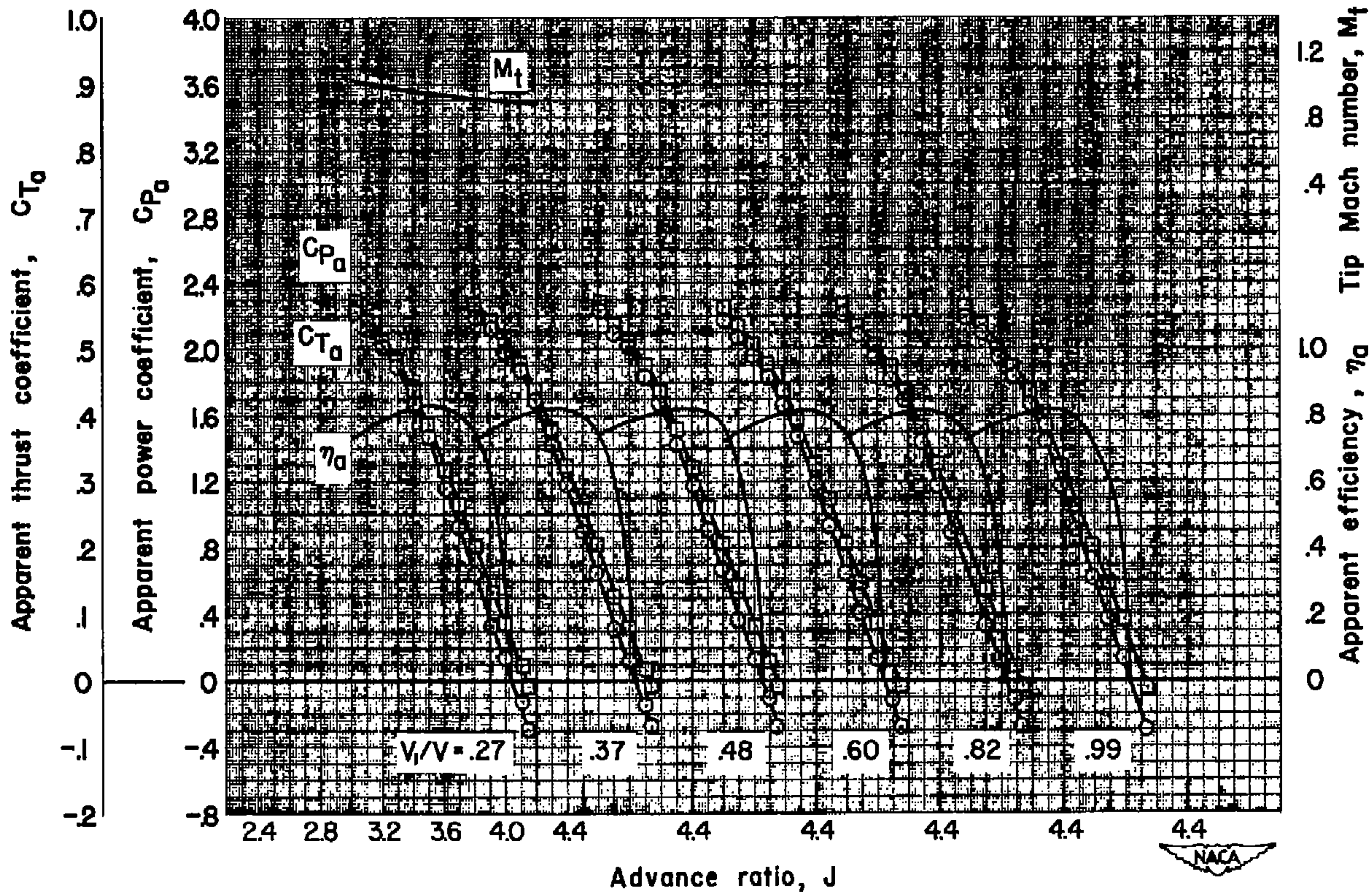

(k) $M = 0.70$; $\beta_F = 60^{\circ}$

Figure 17.– Continued.

[redacted]

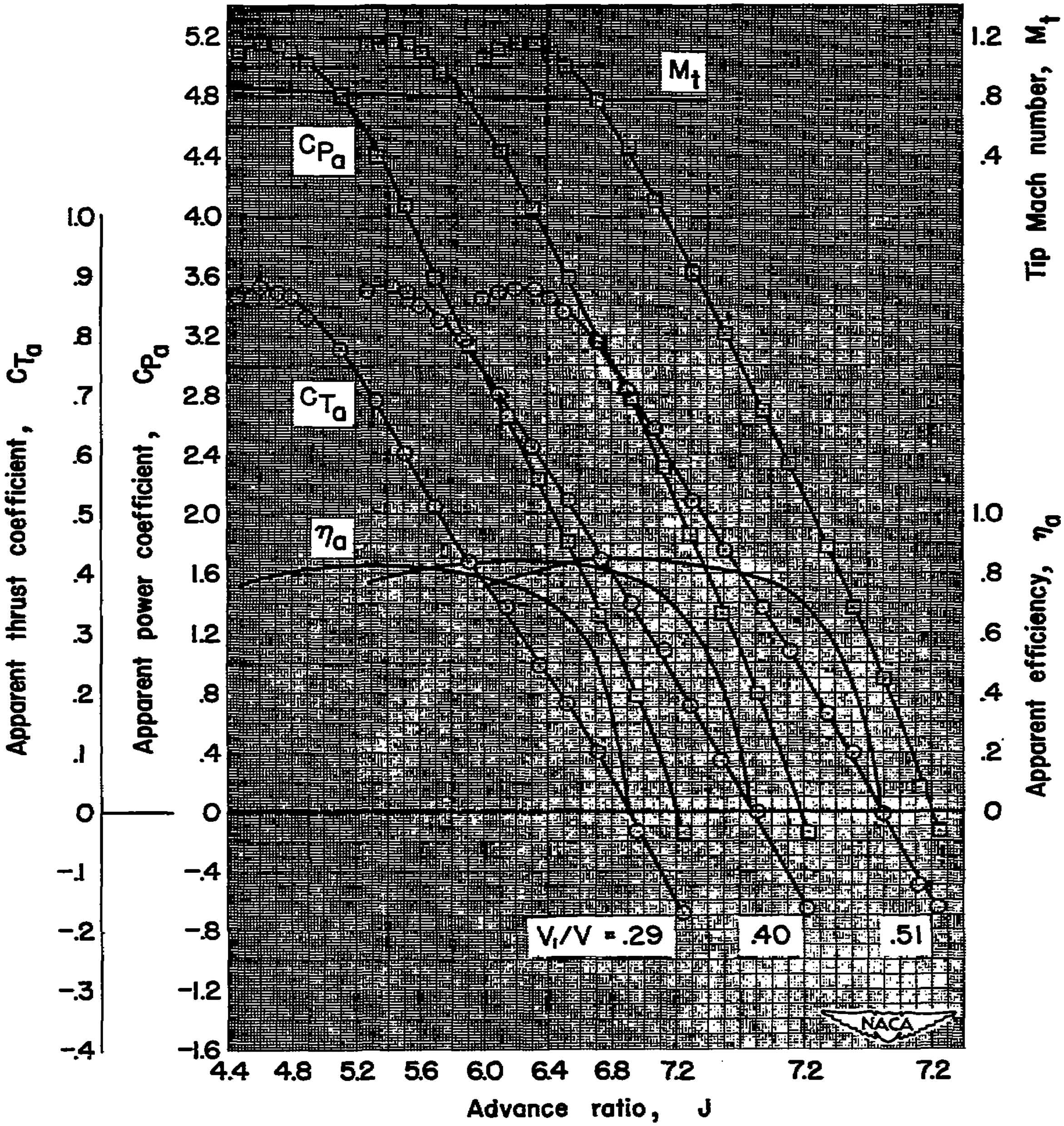

(l) M = 0.70; $\beta_F = 70^\circ$

Figure 17.— Continued.

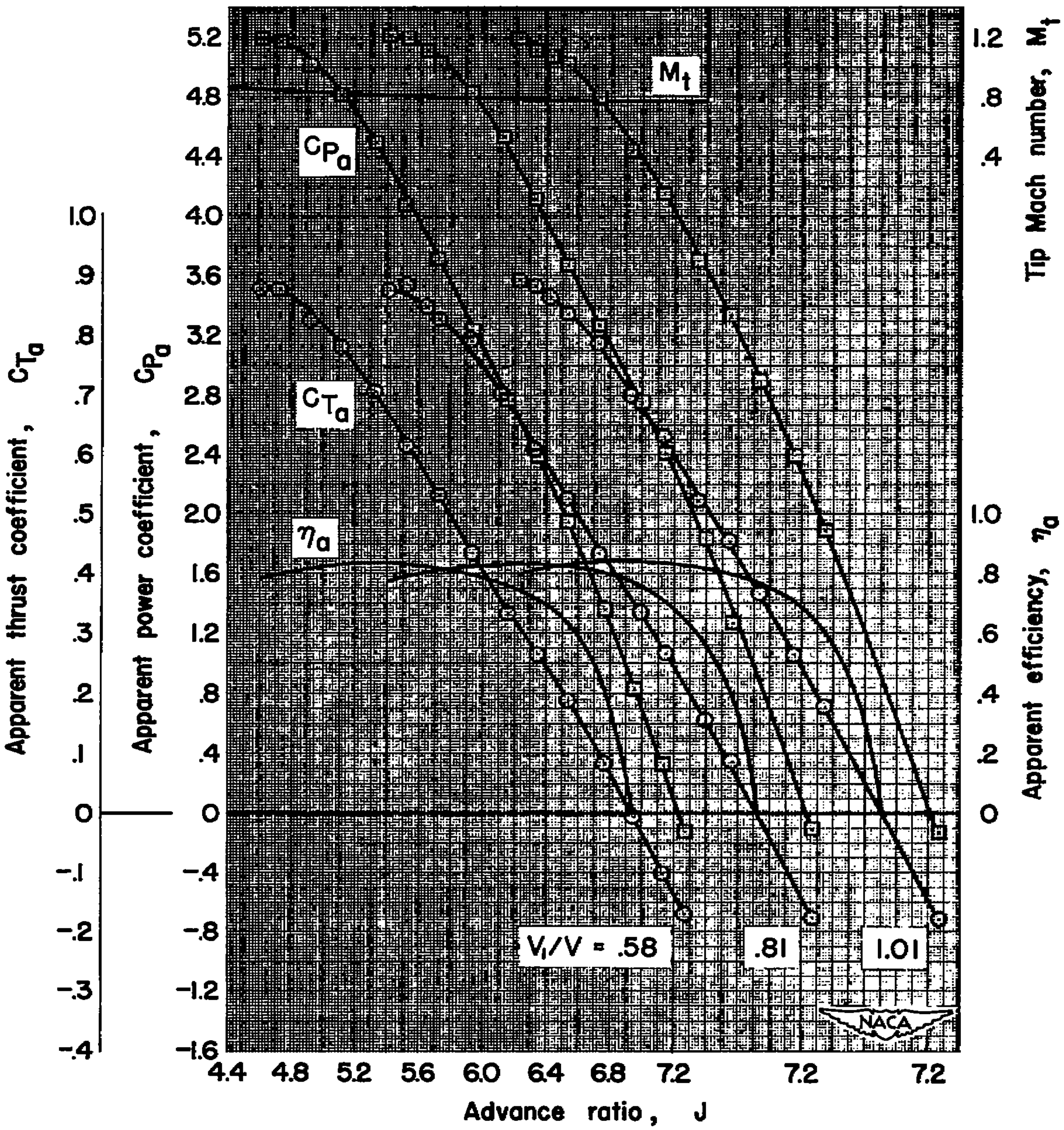

(1) $M = 0.70$; $\beta_F = 70°$ — Concluded

Figure 17.— Continued.

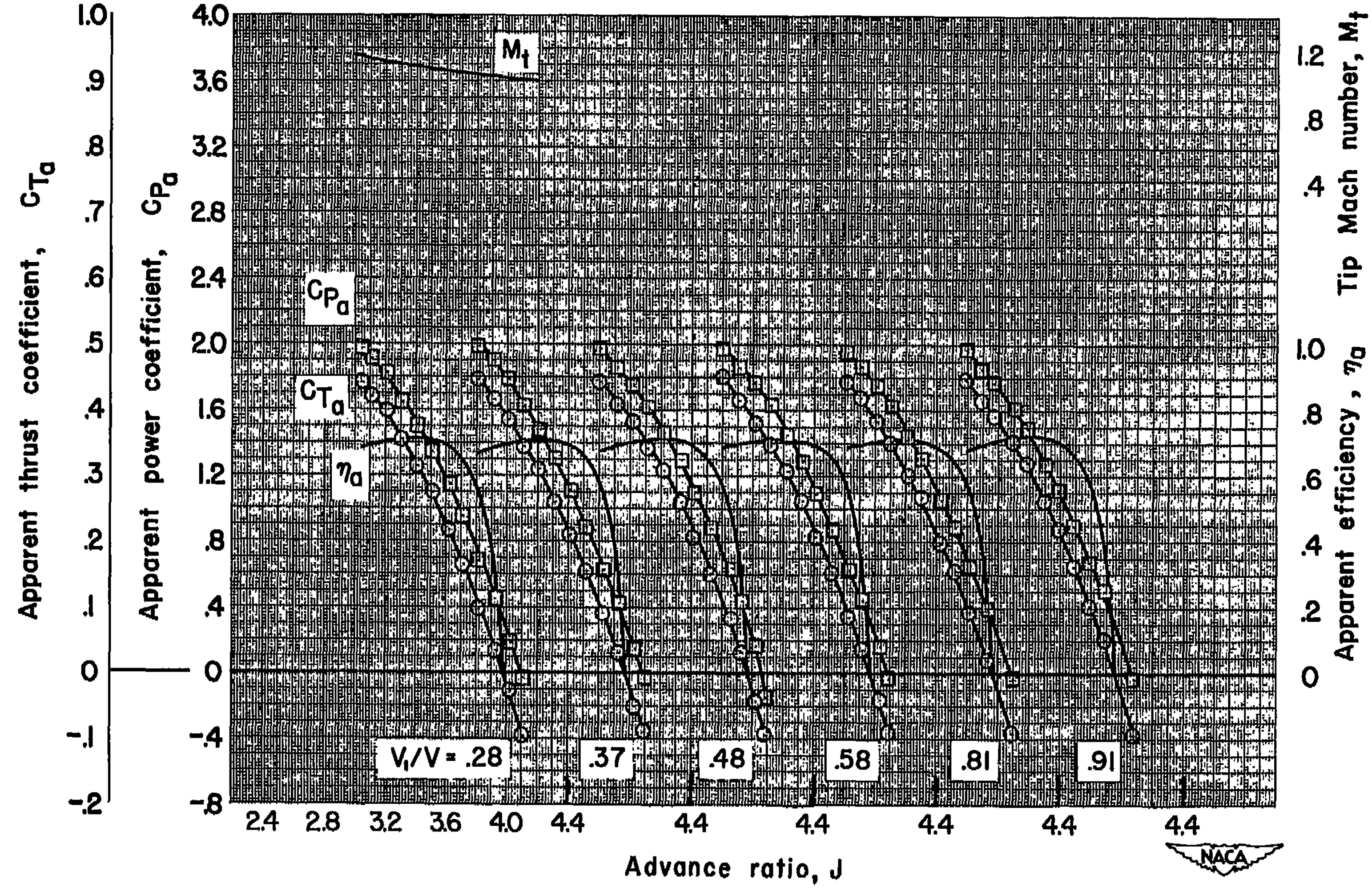

(m) $M = 0.80$; $\beta_F = 60^{\circ}$

Figure 17.– Continued.

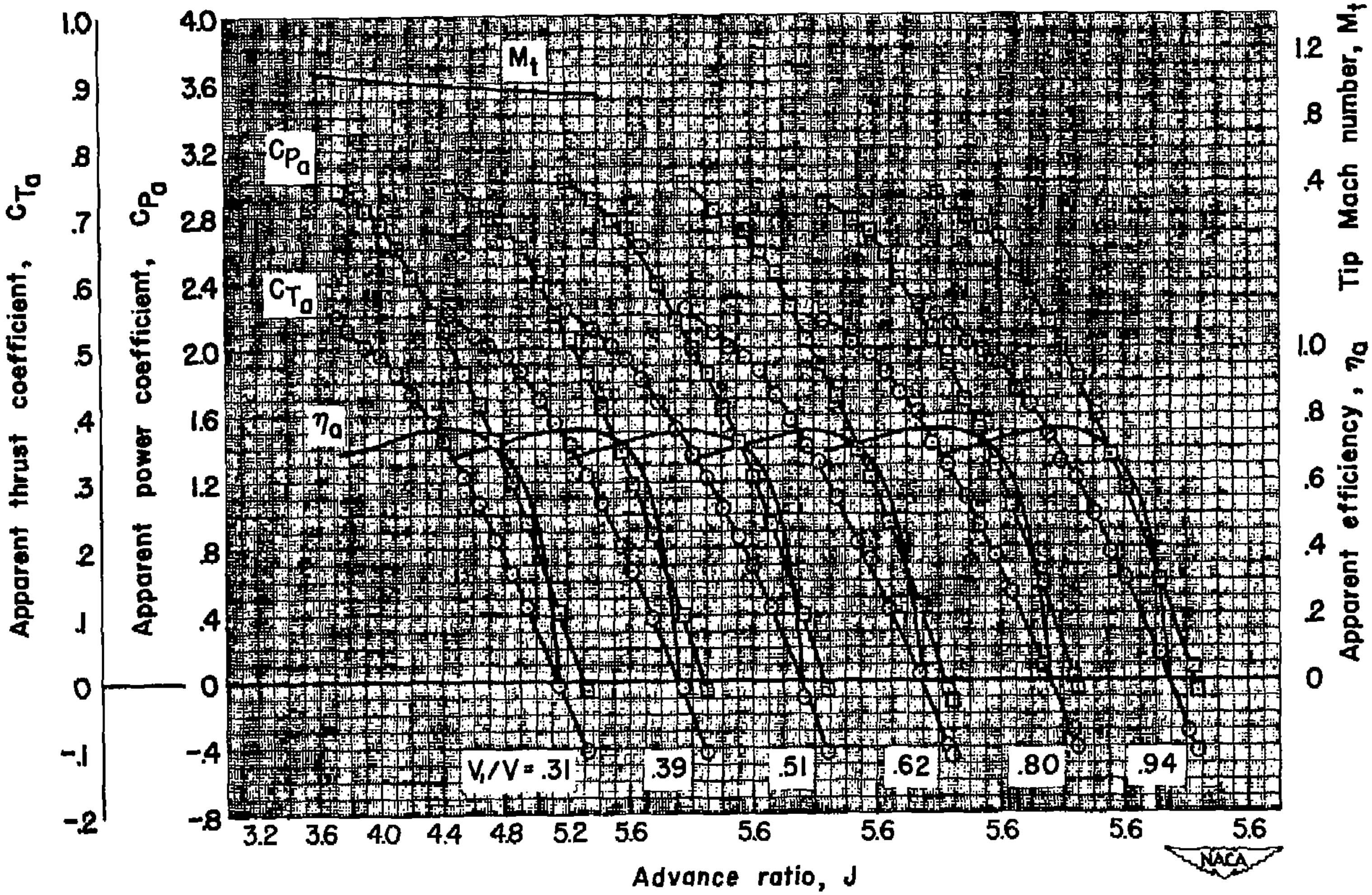

(n) $M = 0.80$; $\beta_F = 65^\circ$

Figure 17.– Continued.

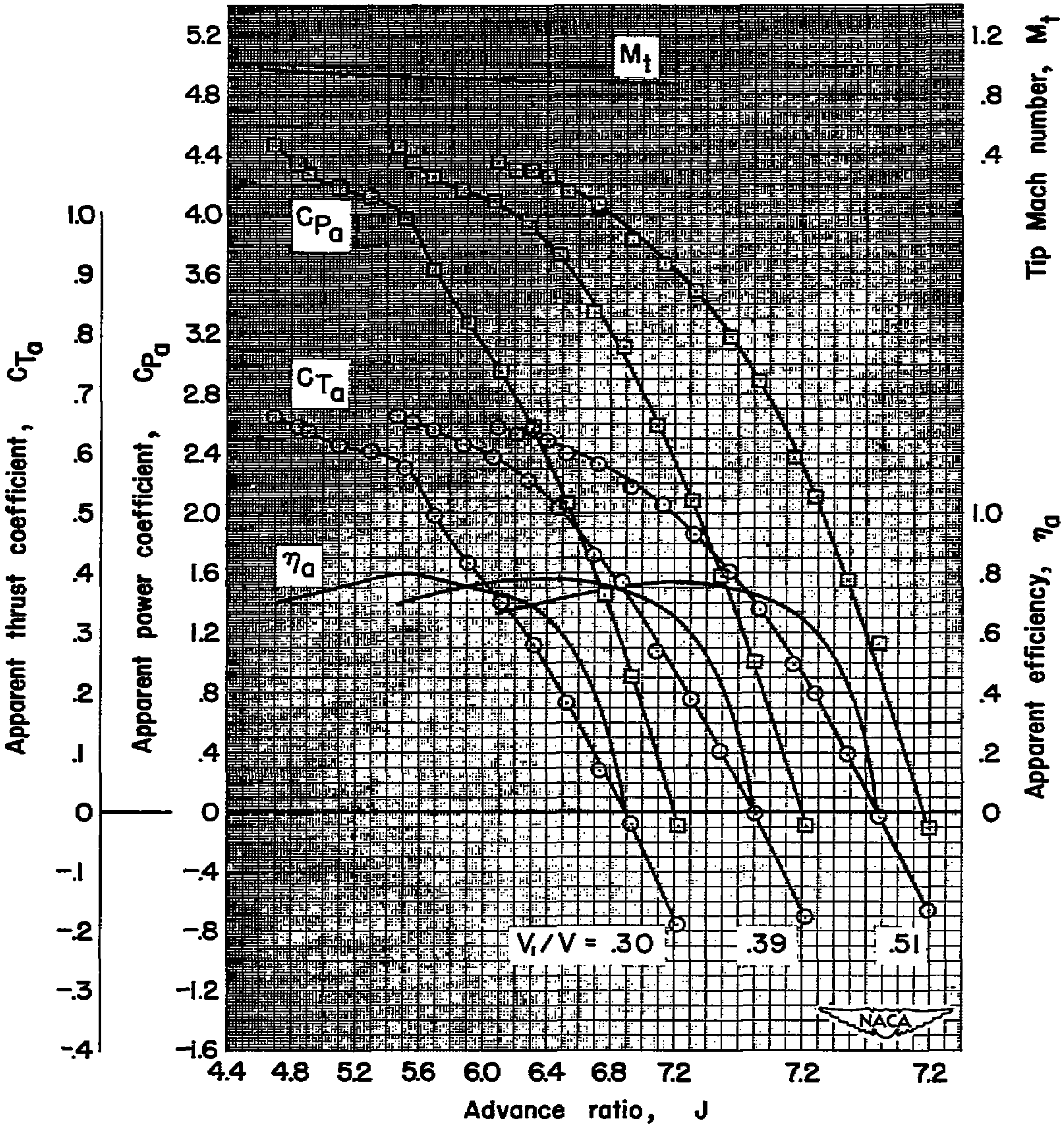

(o) M = 0.80; β_F = 70°

Figure 17.– Continued.

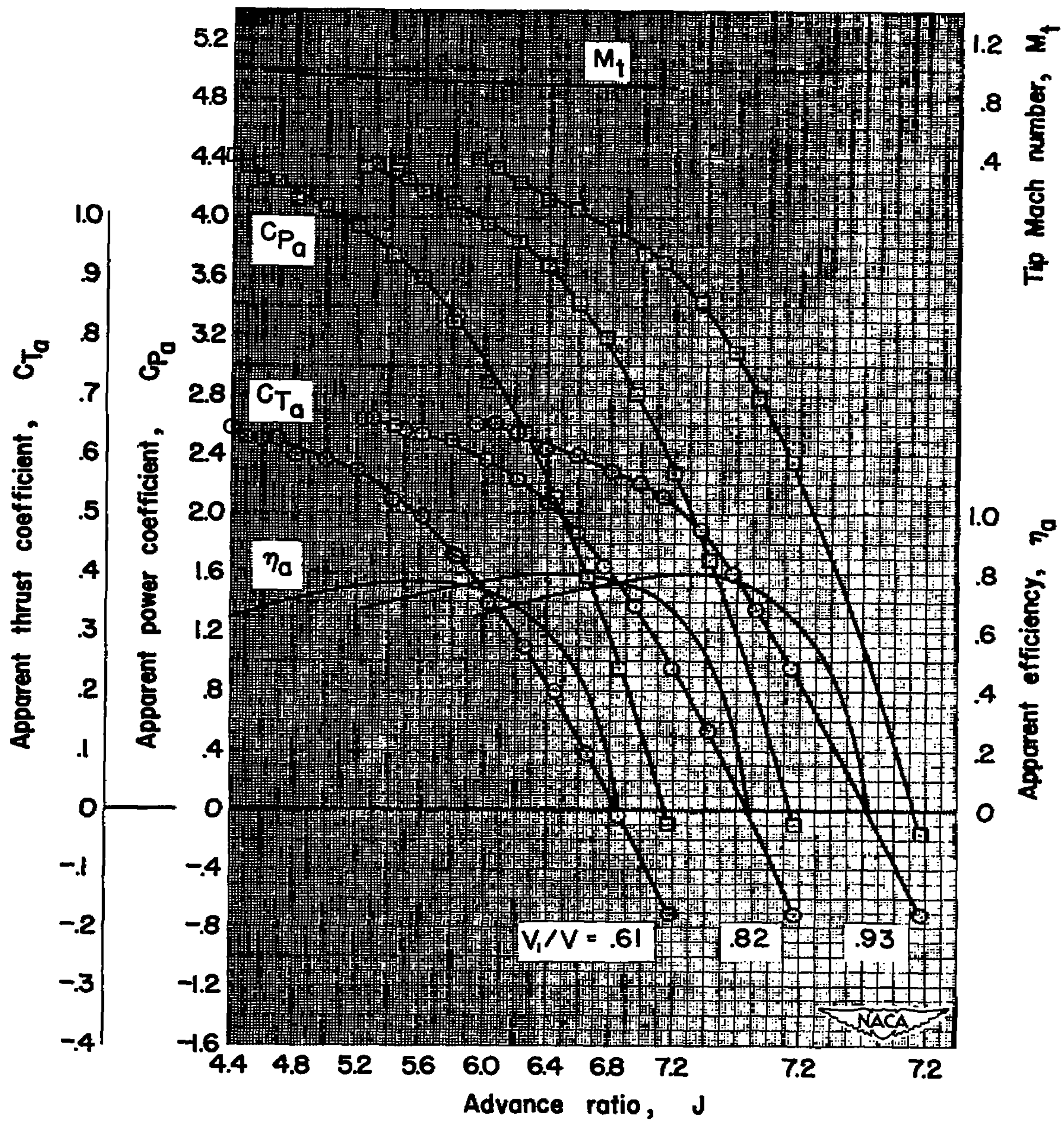

(o) M = 0.80; β_F = 70° — Concluded

Figure 17.— Continued.

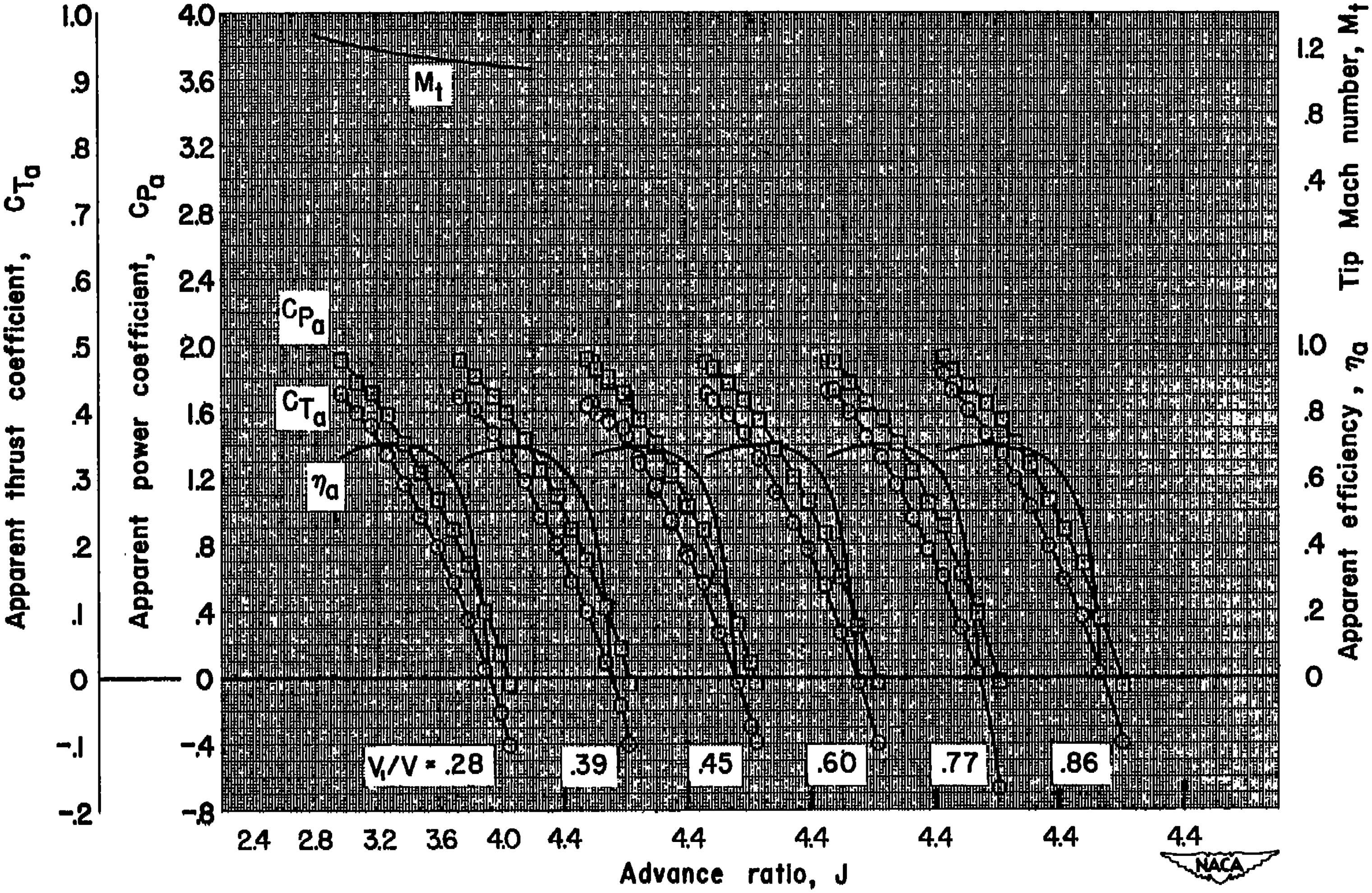

(p) $M = 0.84$; $\beta_F = 60^{\circ}$

Figure 17.- Continued.

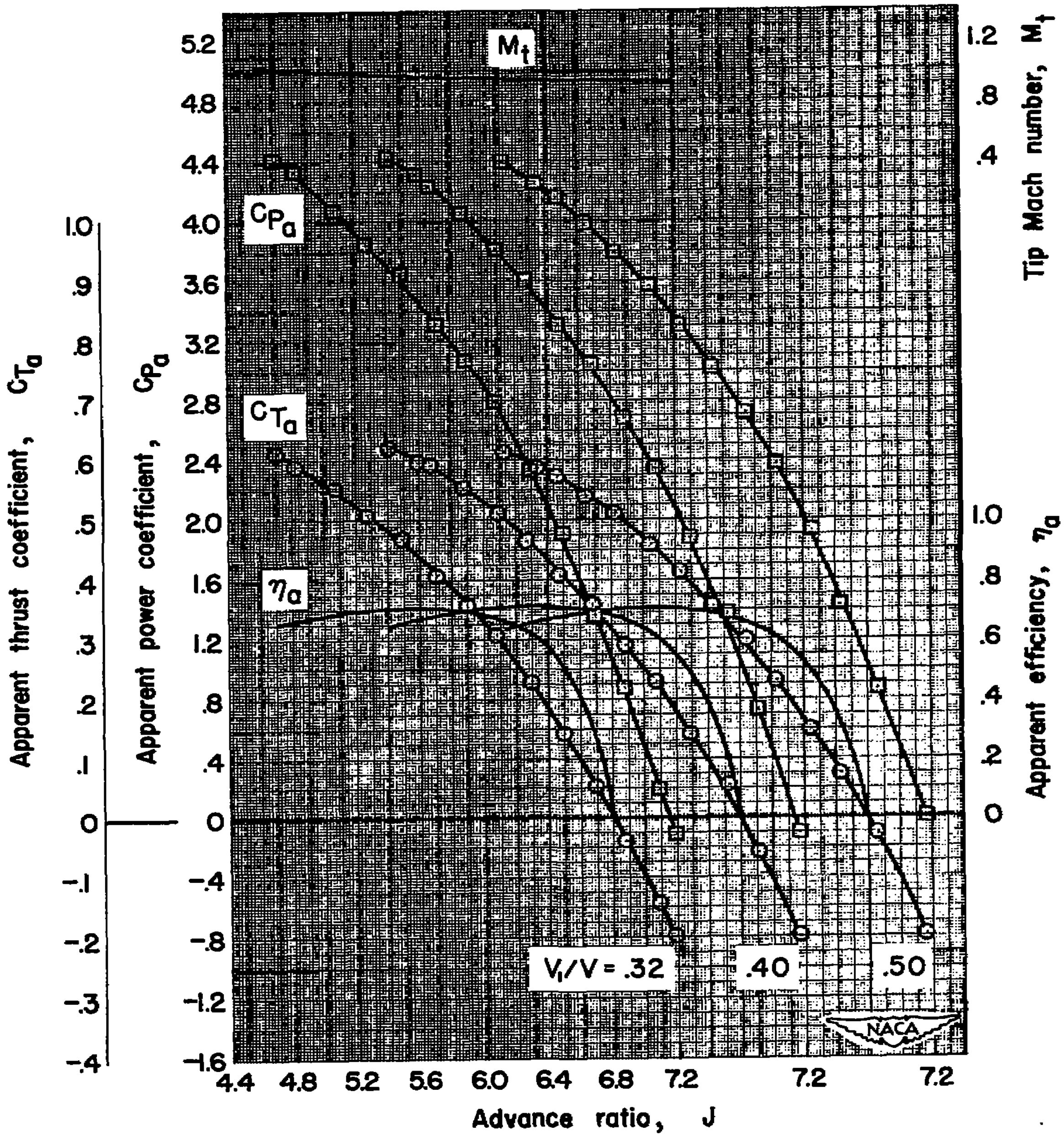

(q) $M = 0.84$; $\beta_F = 70^\circ$

Figure 17.– Continued.

[redacted]

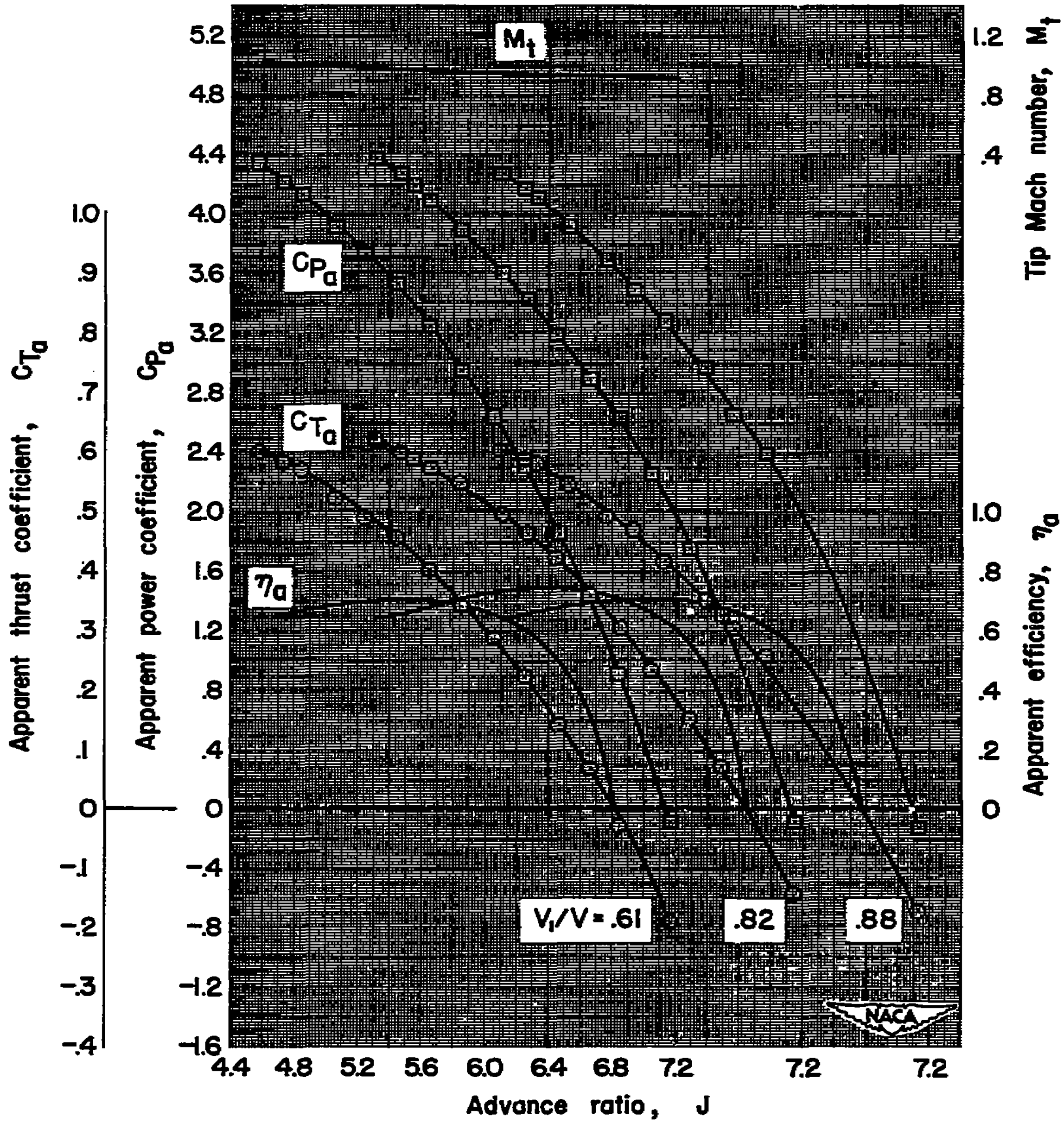

(q) $M = 0.84$; $\beta_F = 70^\circ$ — Concluded

Figure 17.— Concluded.

[redacted]

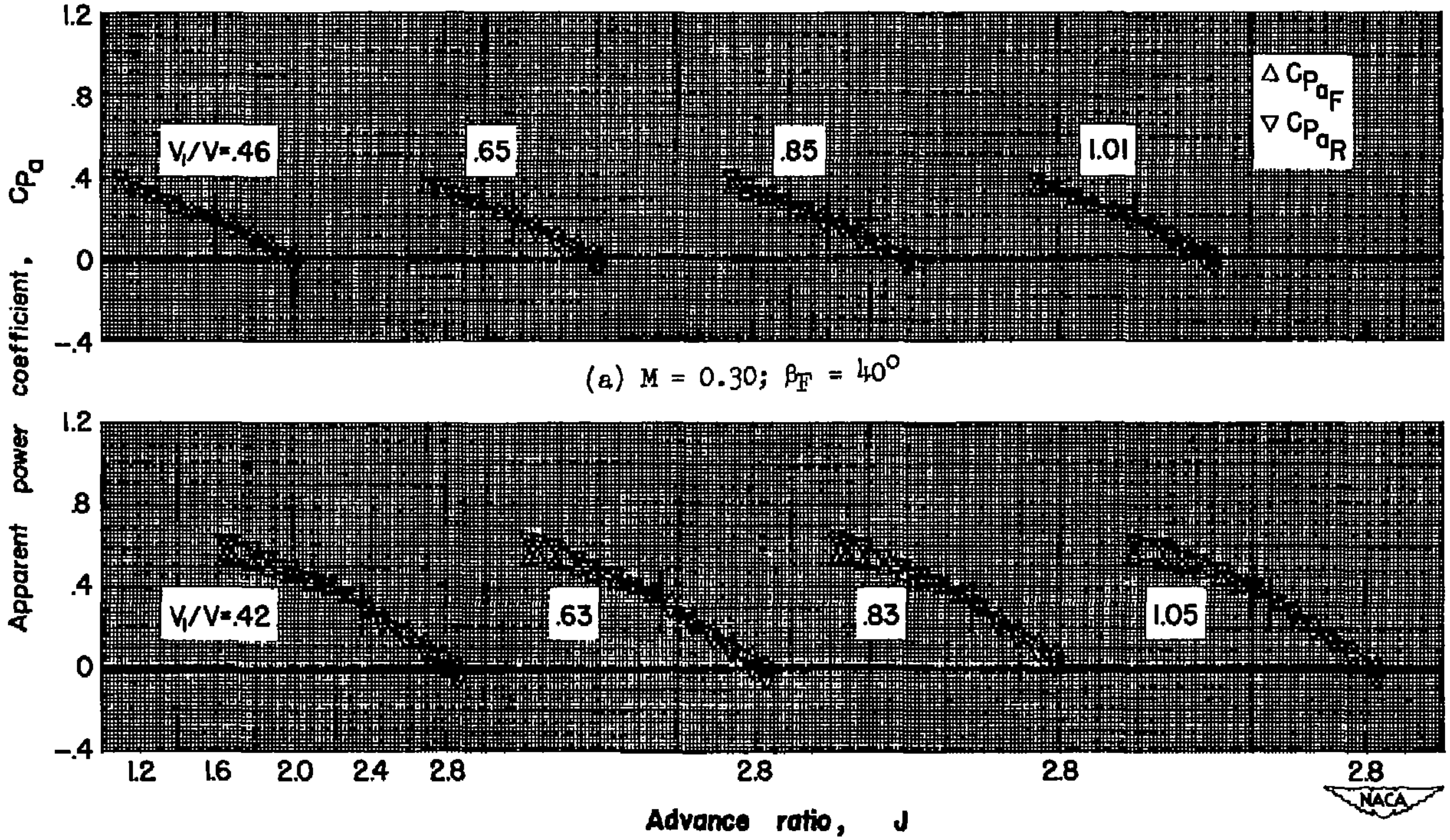

(a) $M = 0.30$; $\beta_F = 40^\circ$

(b) $M = 0.40$; $\beta_F = 50^\circ$

Figure 18.- Effect of advance ratio on the power coefficients for the front and rear components of the six-blade dual-rotation propeller. (Tick marks on curves represent J for $\eta_{a_{max}}$.)

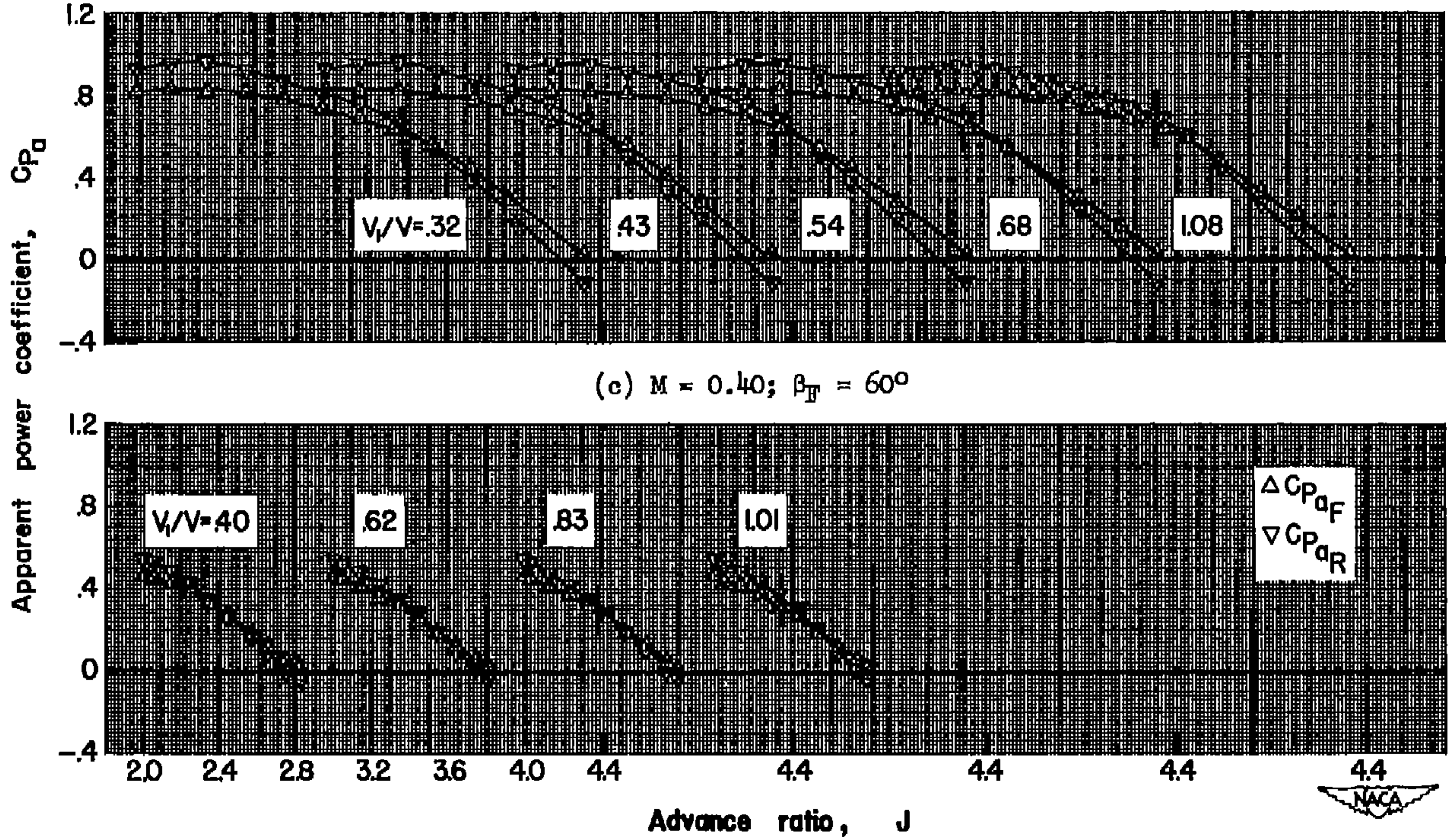

(c) M = 0.40; β_F = 60°

(d) M = 0.60; β_F = 50°

Figure 18.- Continued.

[redacted]

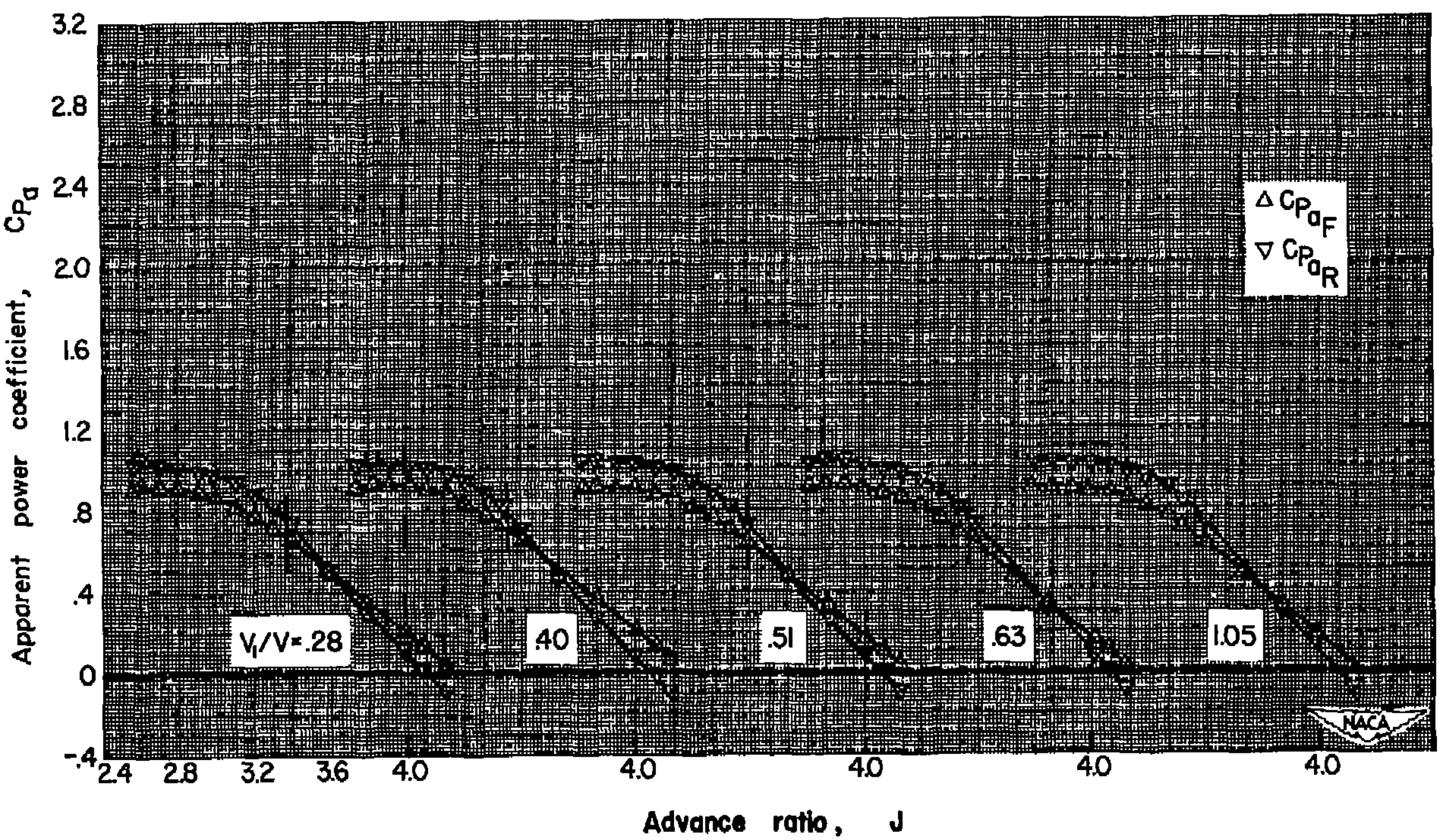

(e) M = 0.60; β_F = 60°

Figure 18.— Continued.

[redacted]

[redacted]

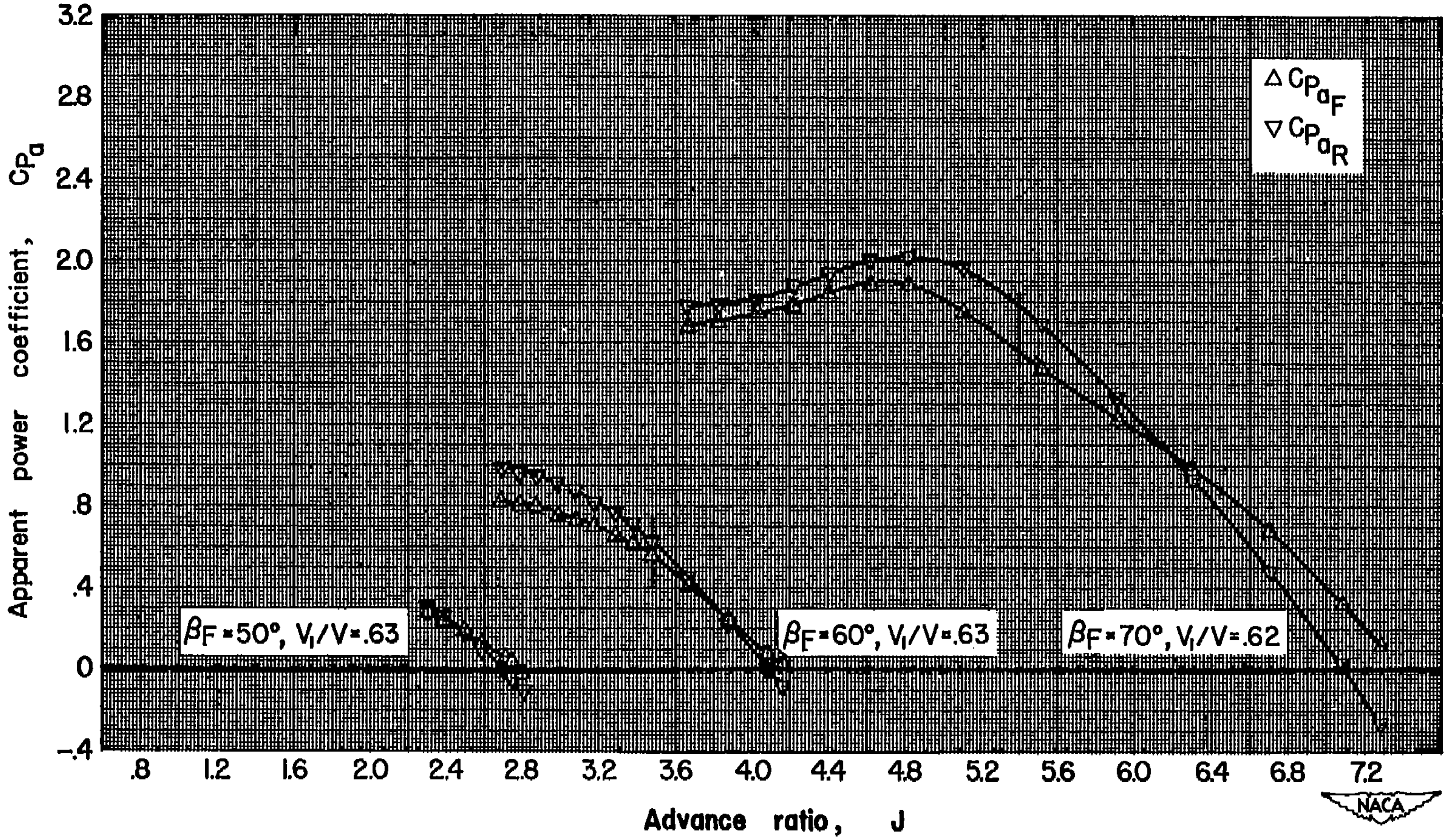

(f) M = 0.70; β_F = 50°, 60°, 70°

Figure 18.– Continued.

[redacted]

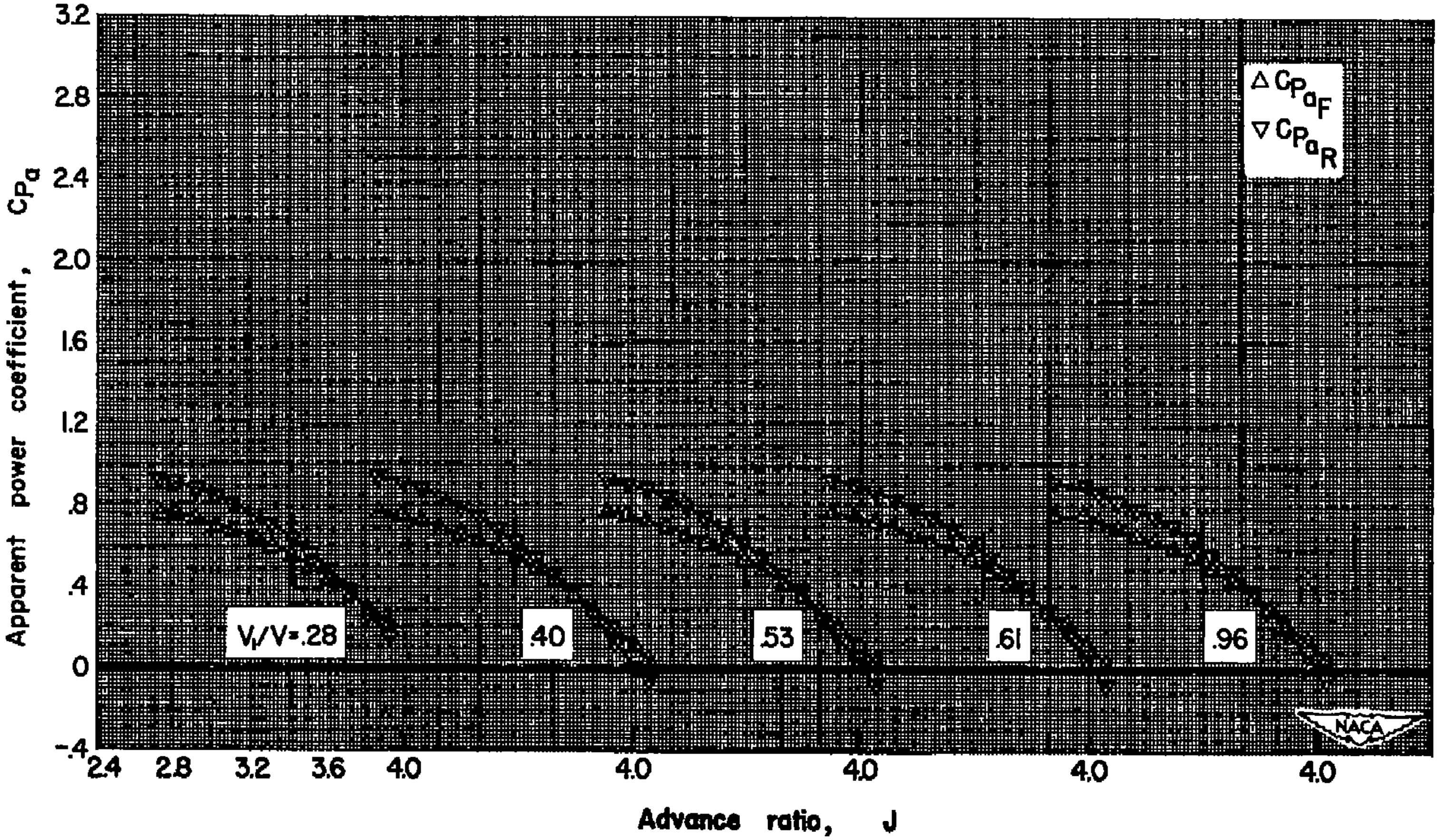

(g) $M = 0.80$; $\beta_F = 60^\circ$

Figure 18.– Continued.

[redacted]

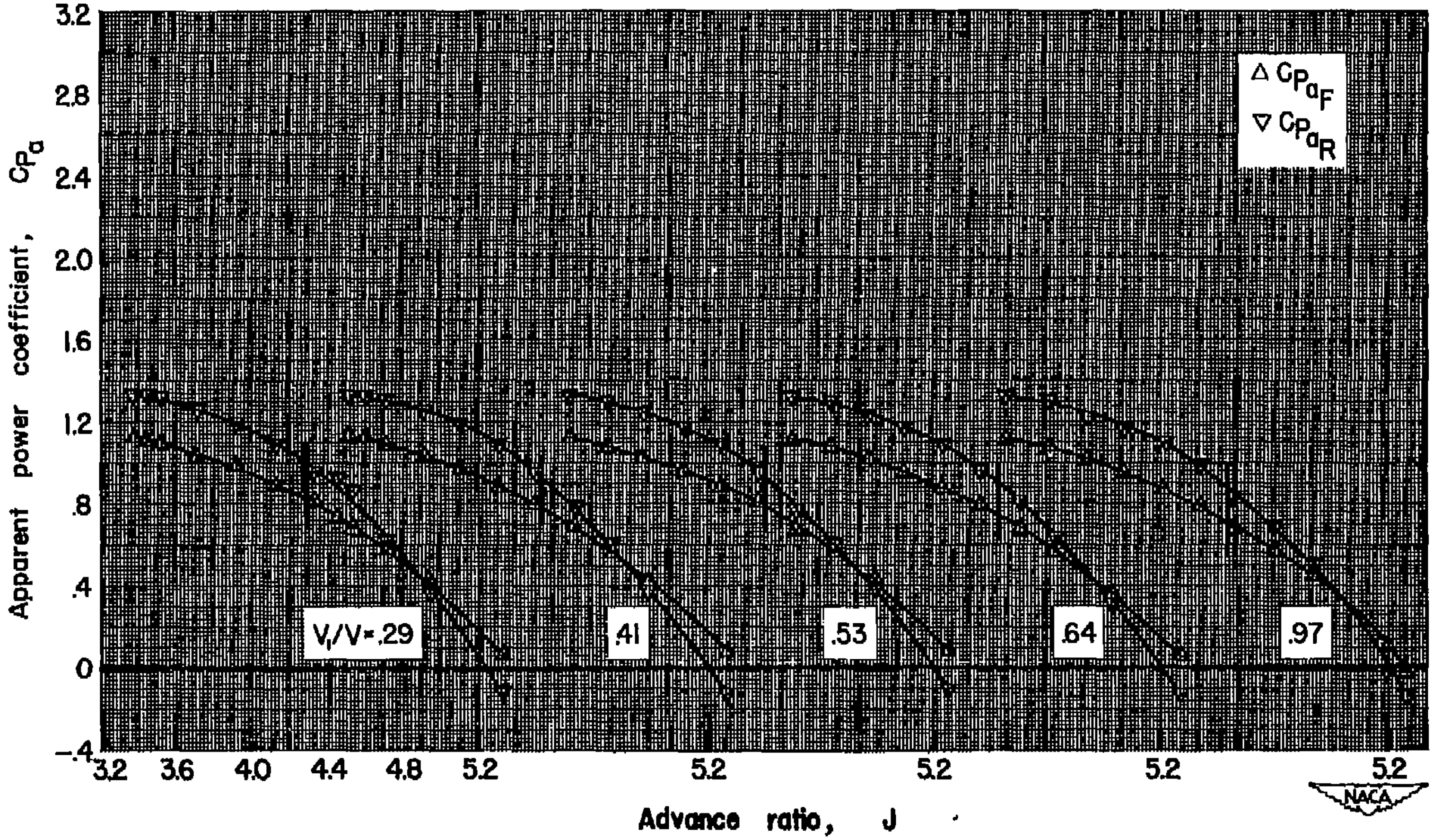

(h) $M = 0.80$; $\beta_F = 65^{\circ}$

Figure 18.– Continued.

[redacted]

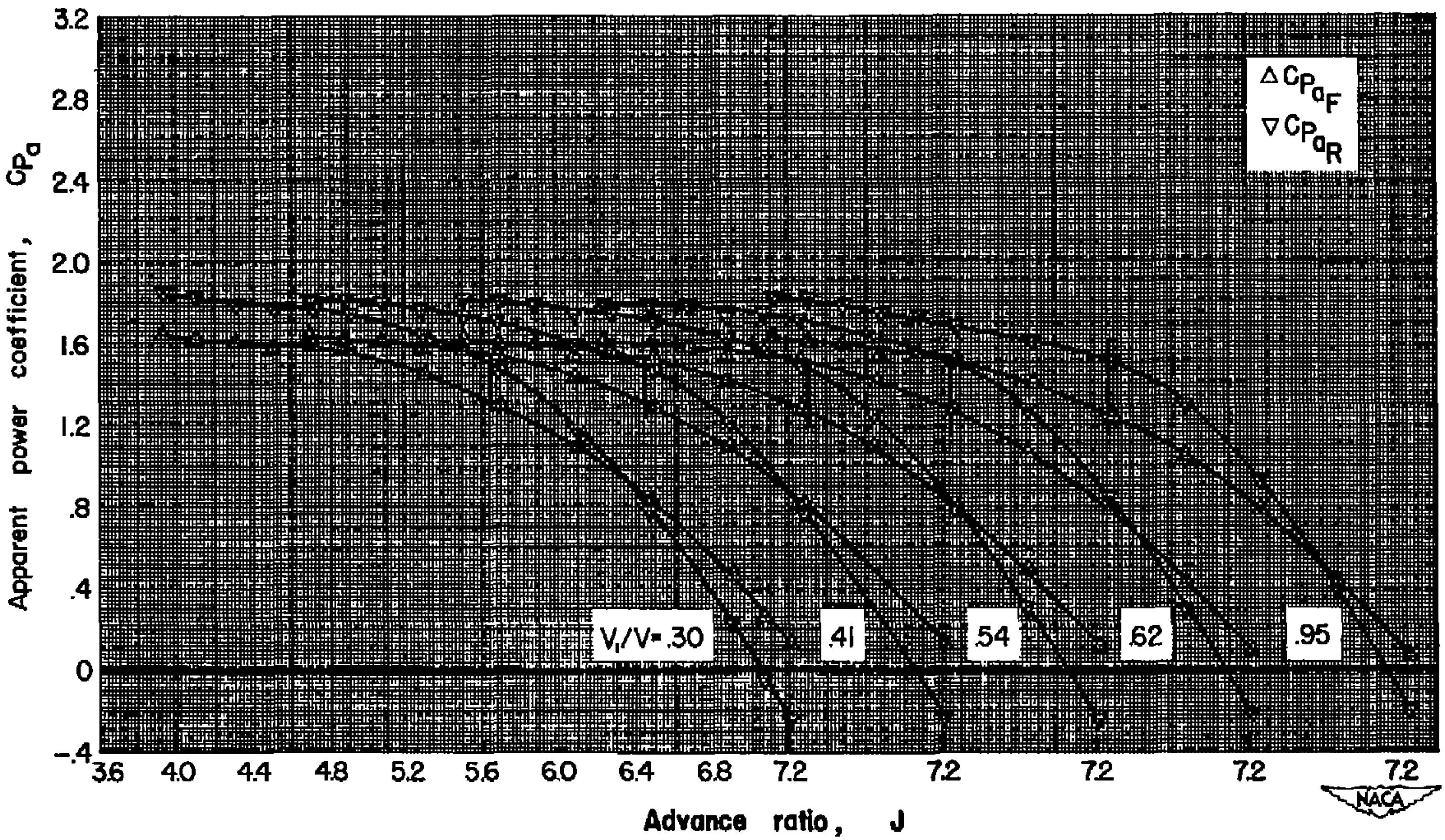

(i) $M = 0.80$; $\beta_F = 70^\circ$

Figure 18.– Concluded.

[redacted]

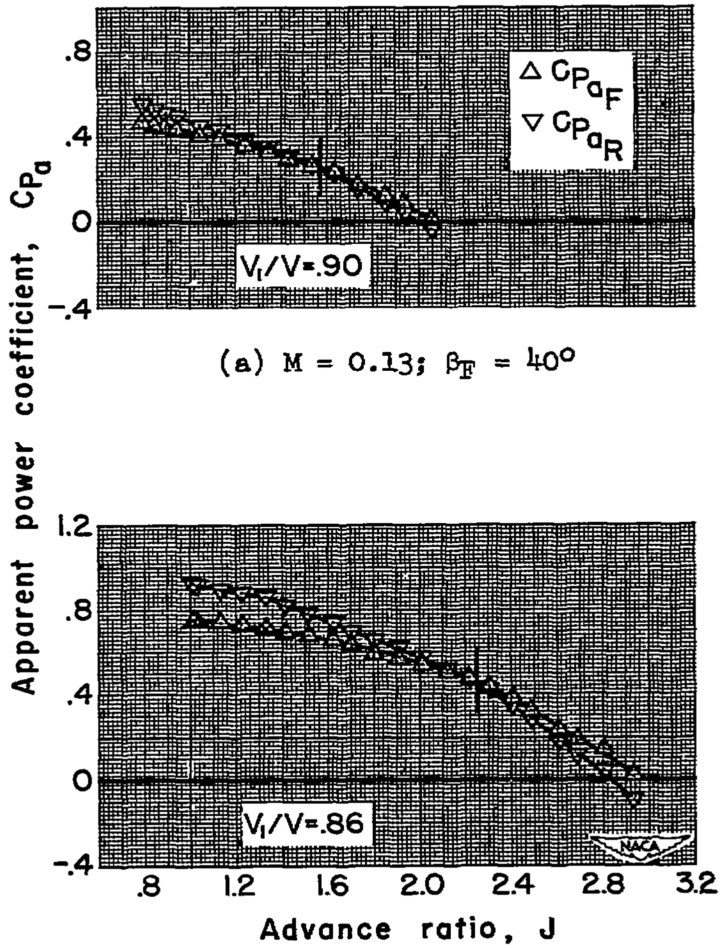

(b) M = 0.13; β_F = 50°

Figure 19.– Effect of advance ratio on the power coefficients for the front and rear components of the eight-blade dual-rotation propeller. (Ticks marks on curves represent J for $\eta_{a_{max}}$.)

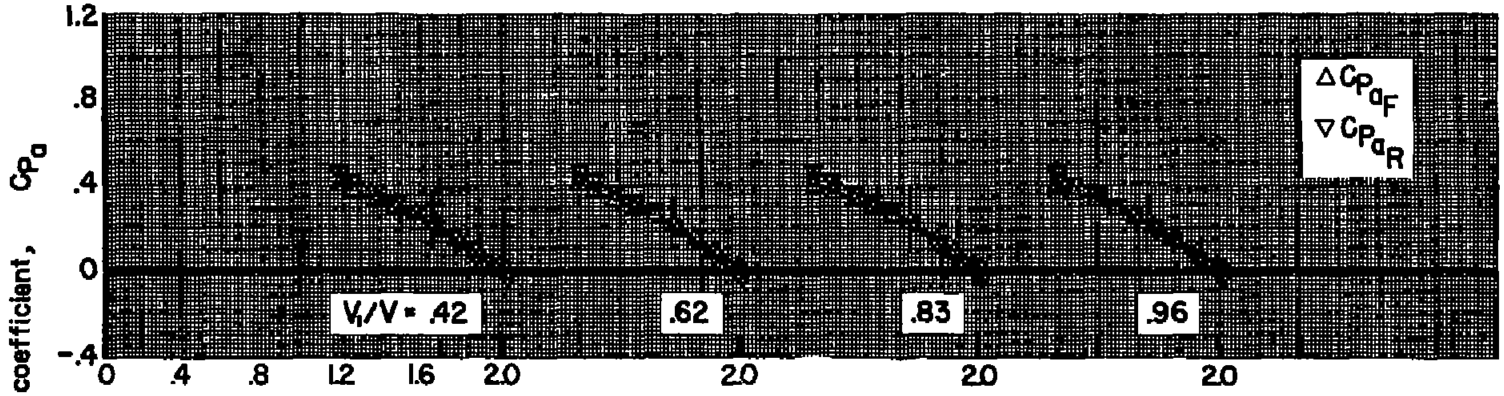

(c) M = 0.30; β_F = 40°

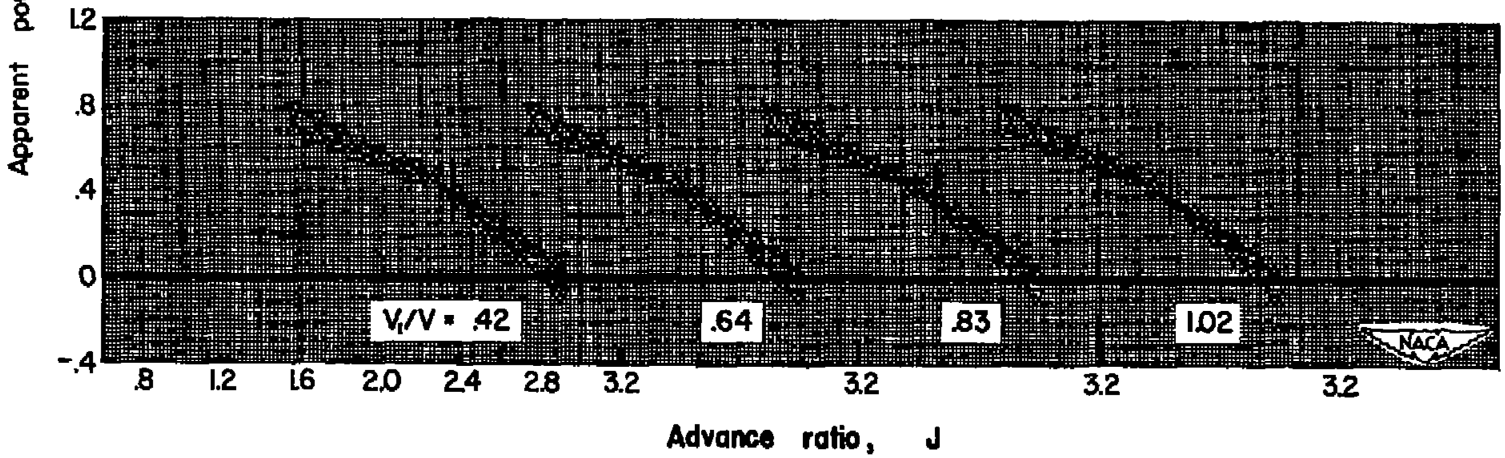

(d) M = 0.30; β_F = 50°

Figure 19.— Continued.

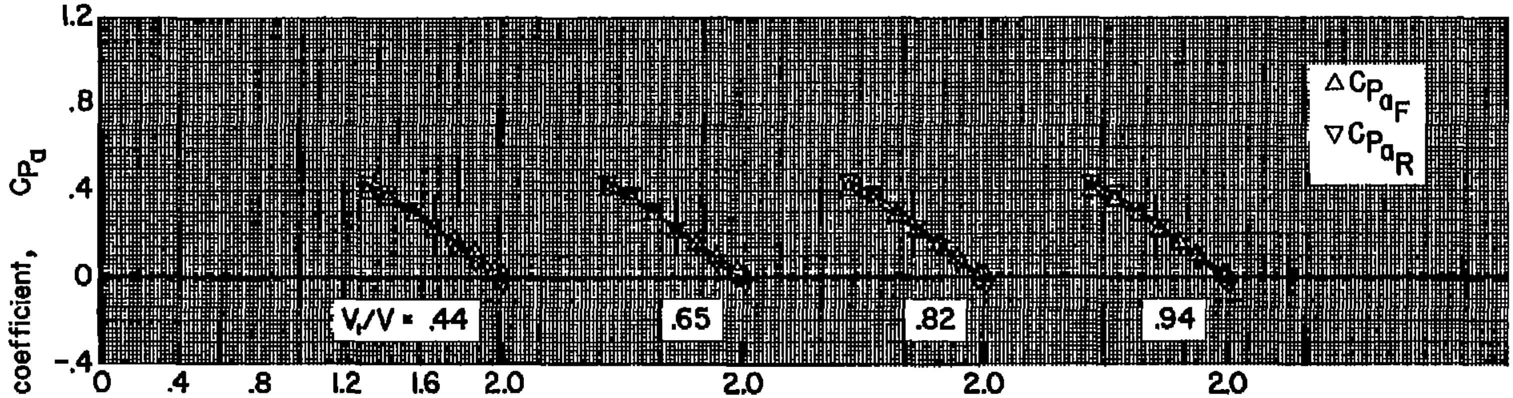

(e) M = 0.40; β_F = 40°

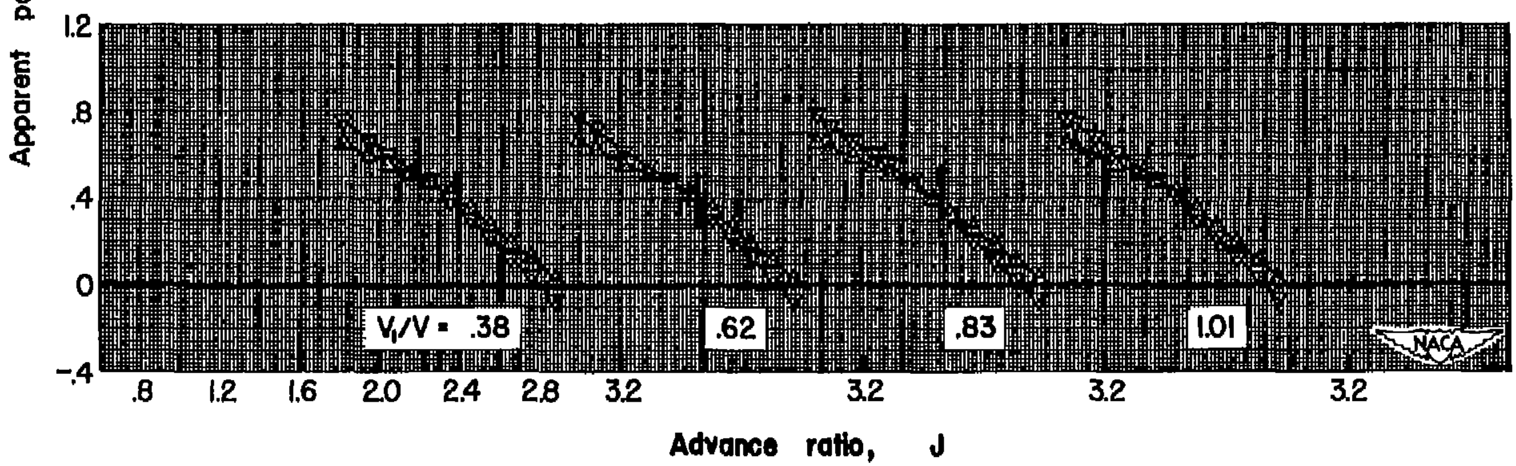

(f) M = 0.40; β_F = 50°

Figure 19.— Continued.

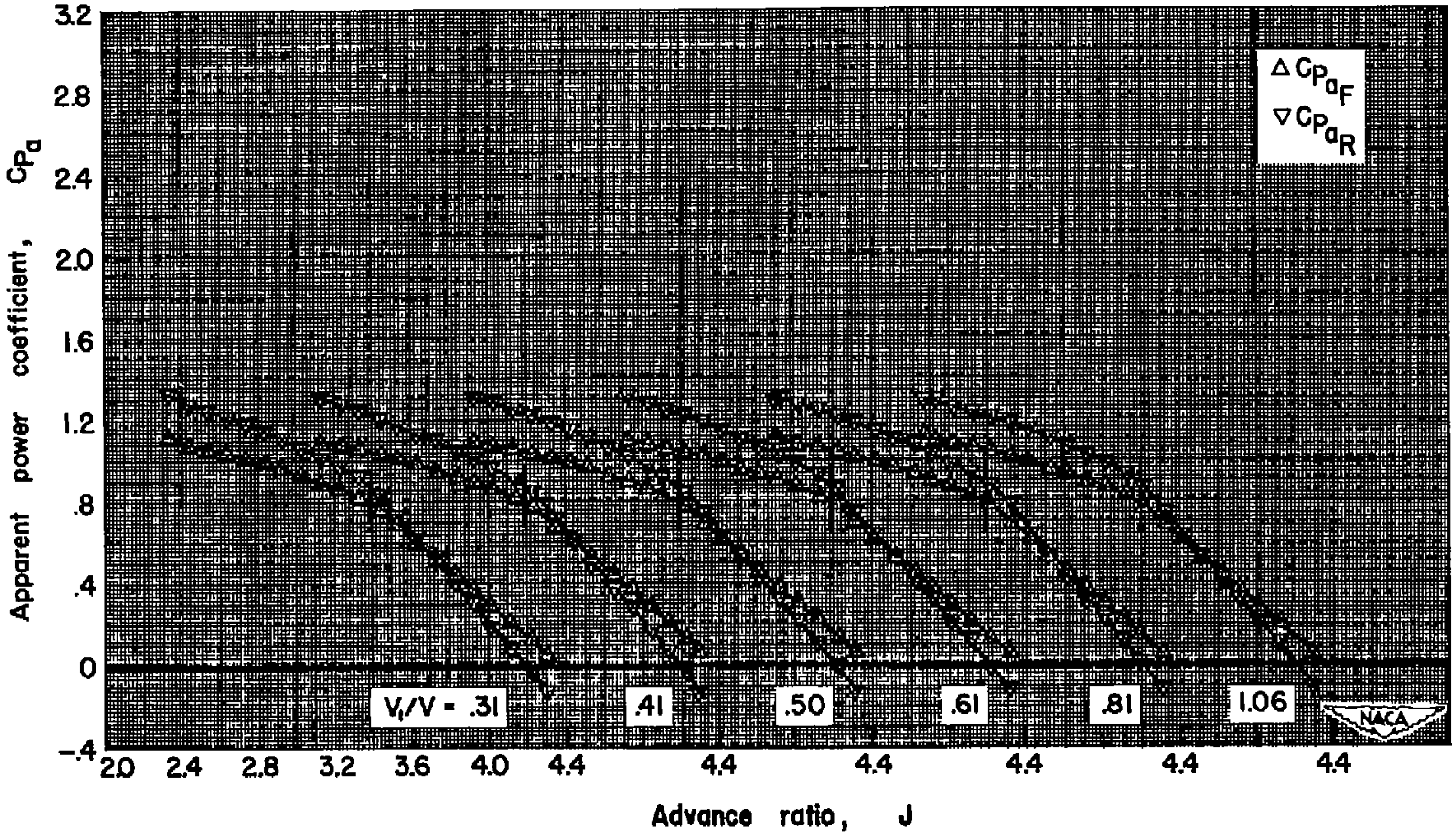

(g) $M = 0.40$; $\beta_F = 60^\circ$

Figure 19.– Continued.

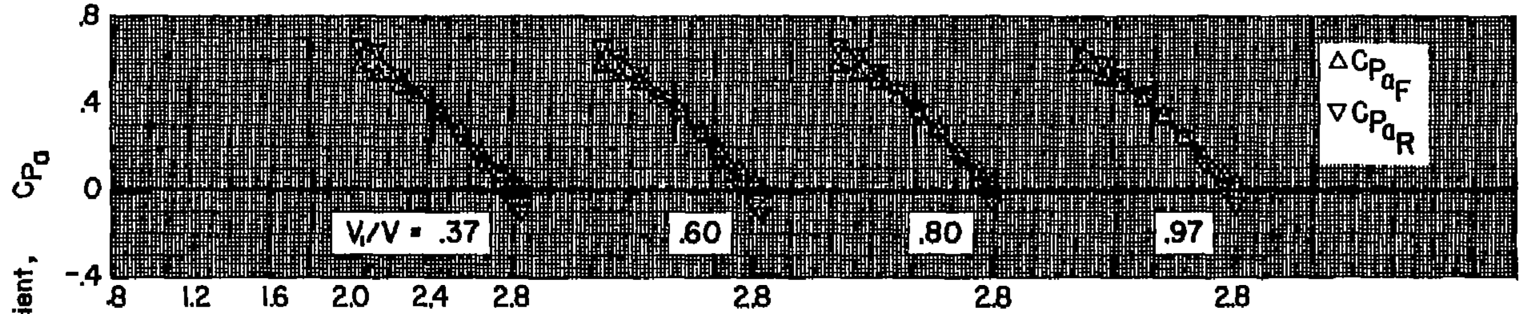

(h) M = 0.60; $\beta_F = 50^o$

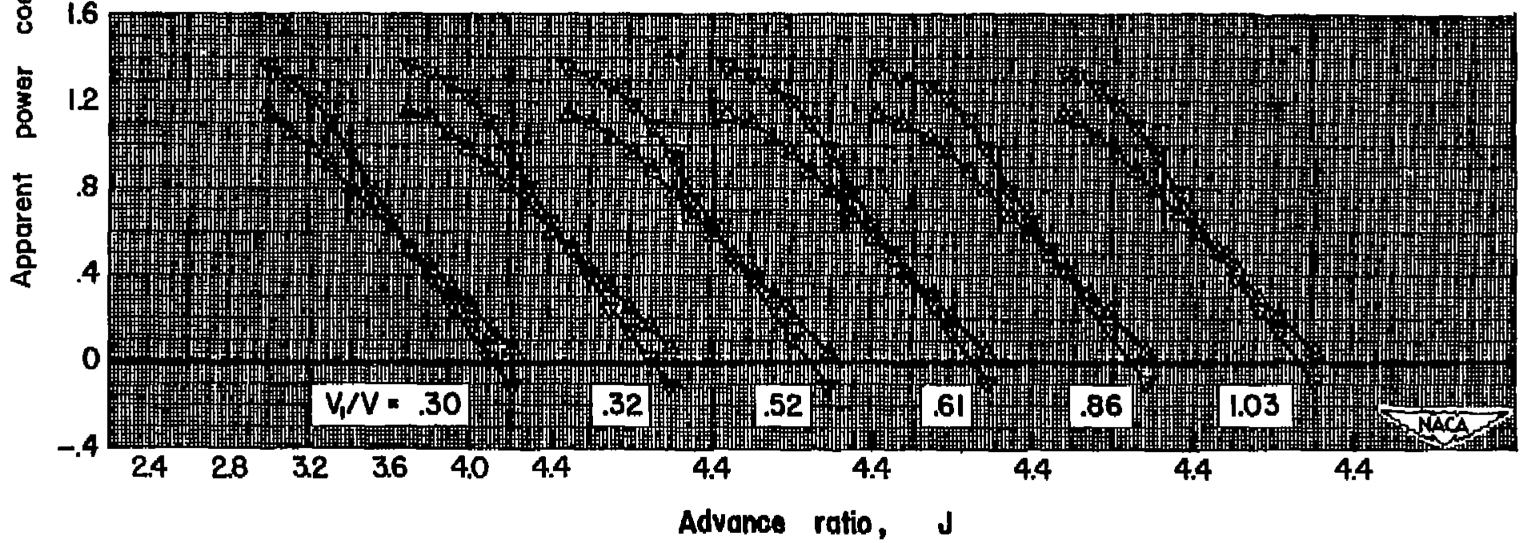

(i) M = 0.60; $\beta_F = 60^o$

Figure 19.– Continued.

[redacted]

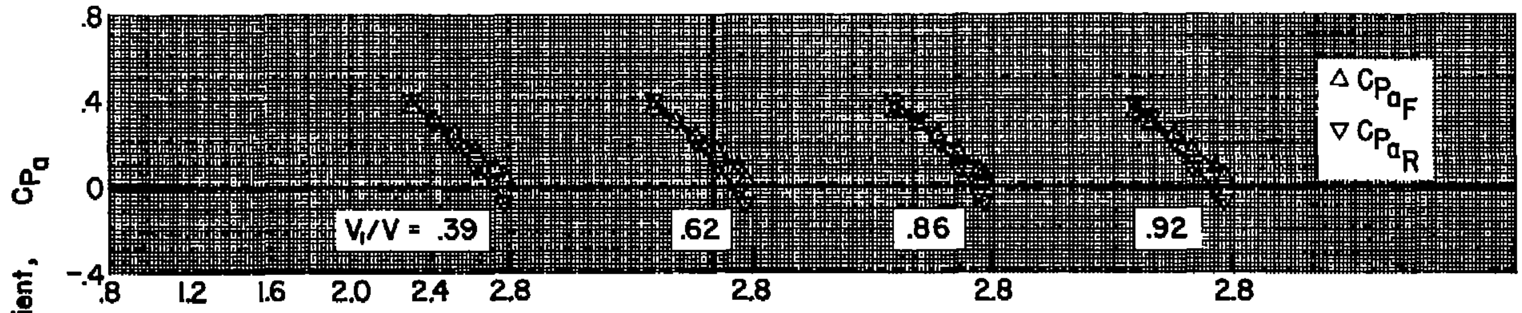

(j) M = 0.70; β_F = 50°

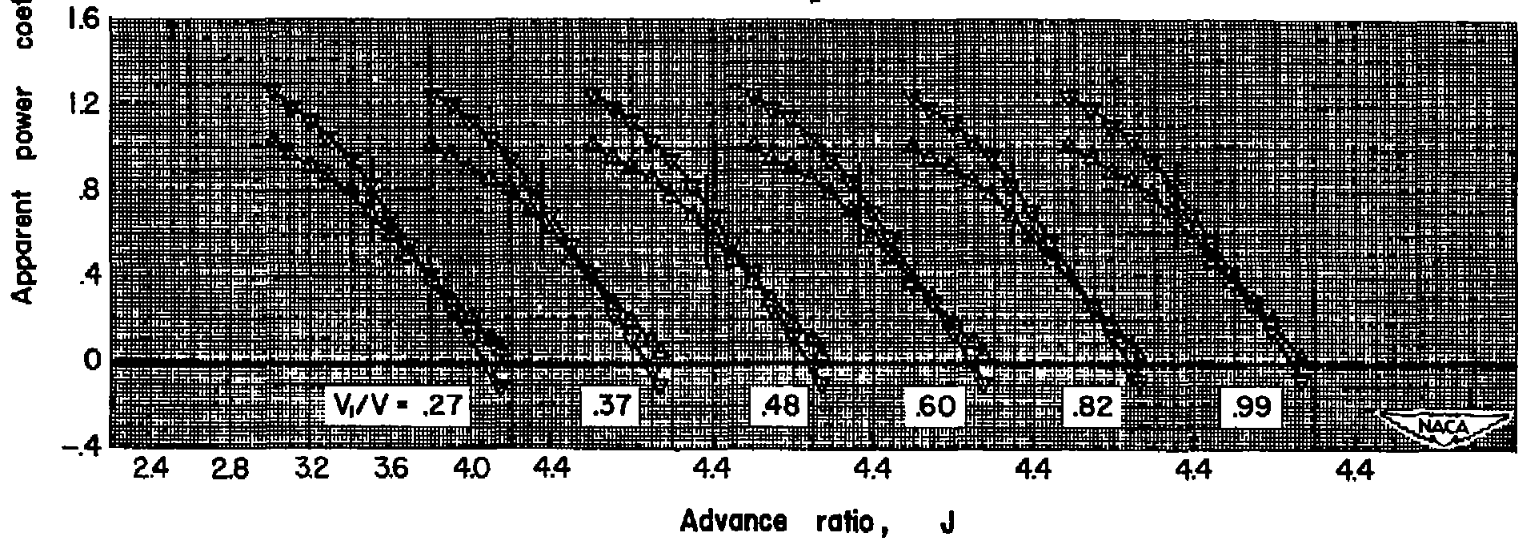

(k) M = 0.70; β_F = 60°

Figure 19.– Continued.

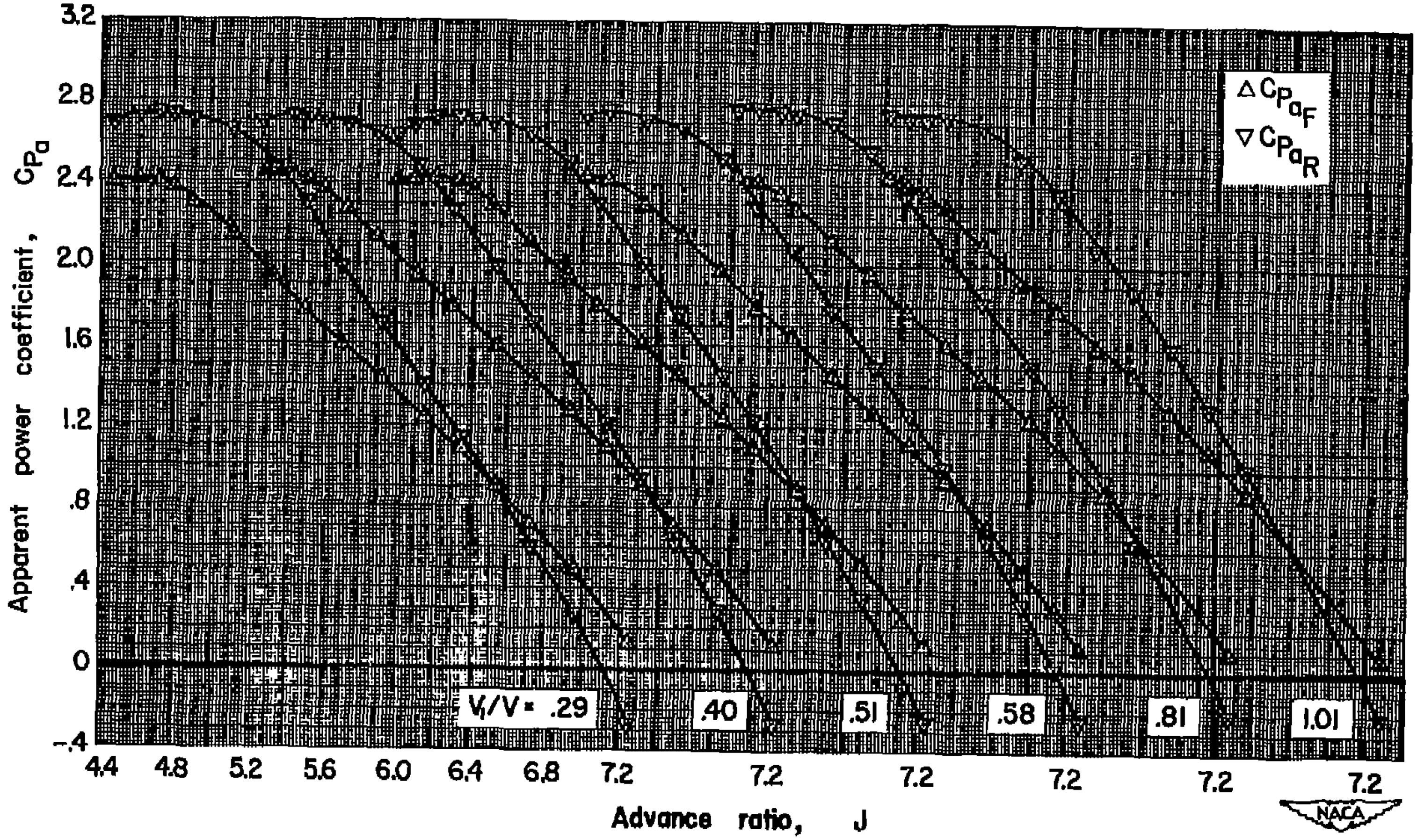

(l) M = 0.70; β_F = 70°

Figure 19.– Continued.

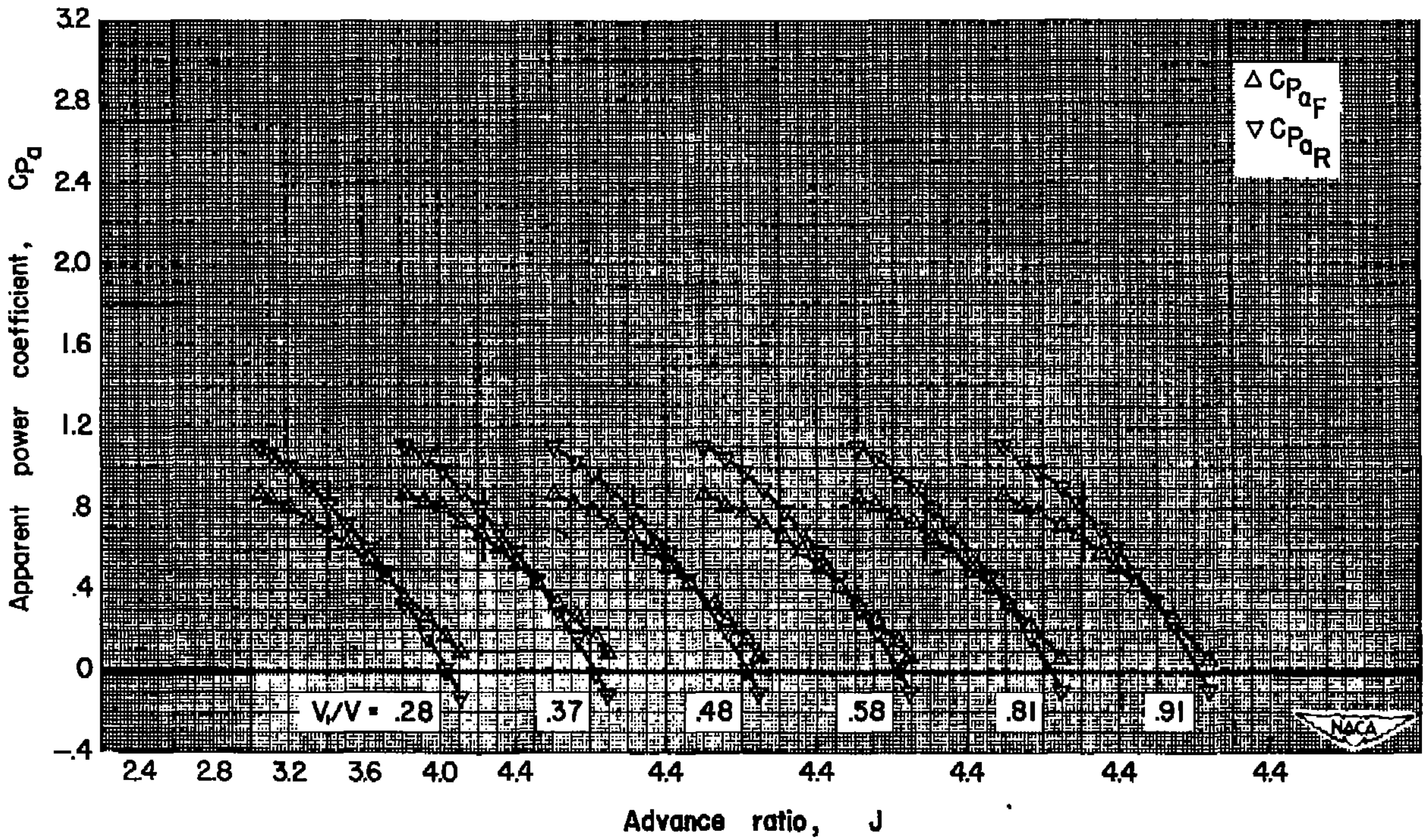

(m) $M = 0.80$; $\beta_F = 60^{\circ}$

Figure 19.– Continued.

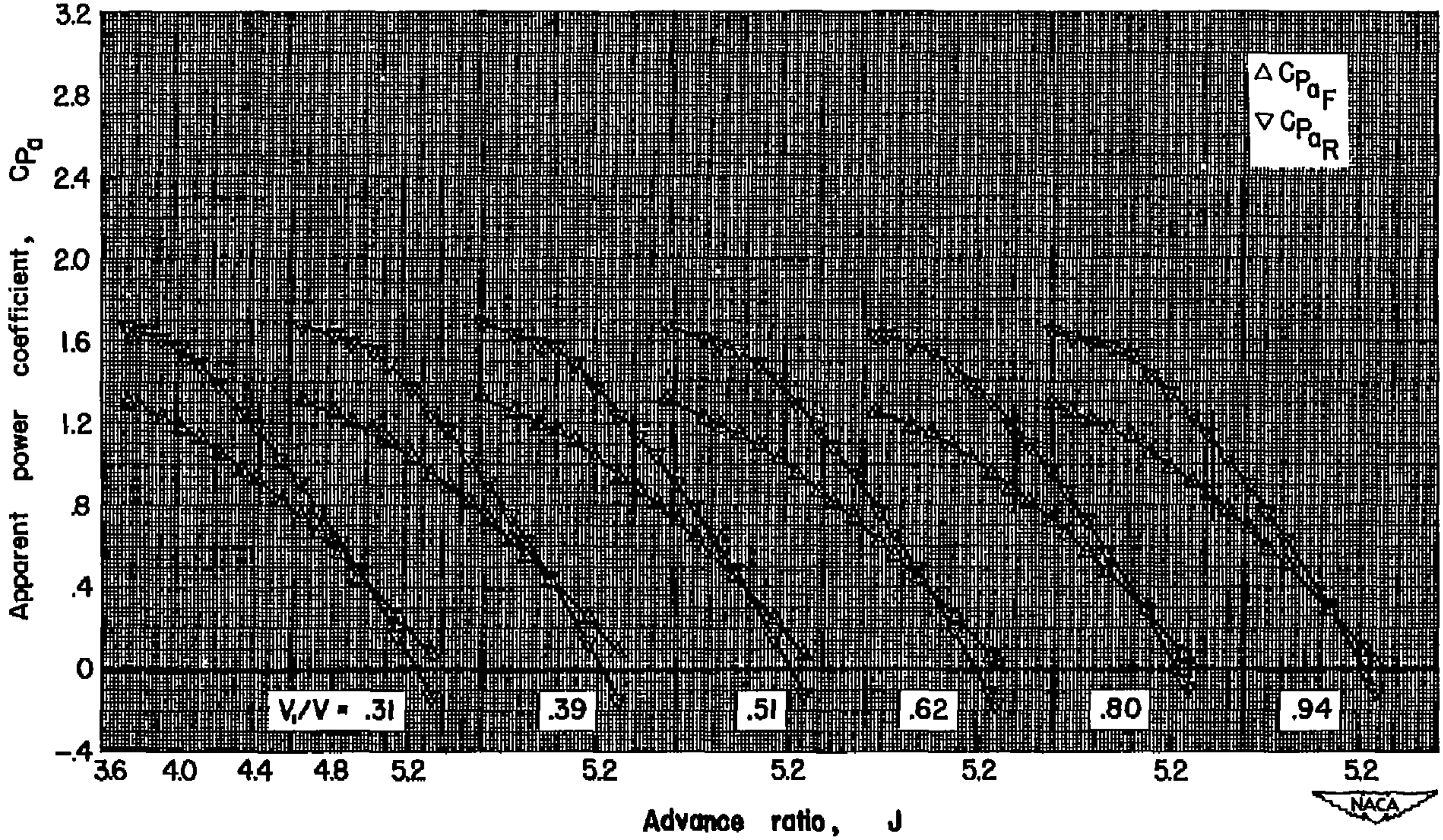

(n) $M = 0.80$; $\beta_F = 65^\circ$

Figure 19.– Continued.

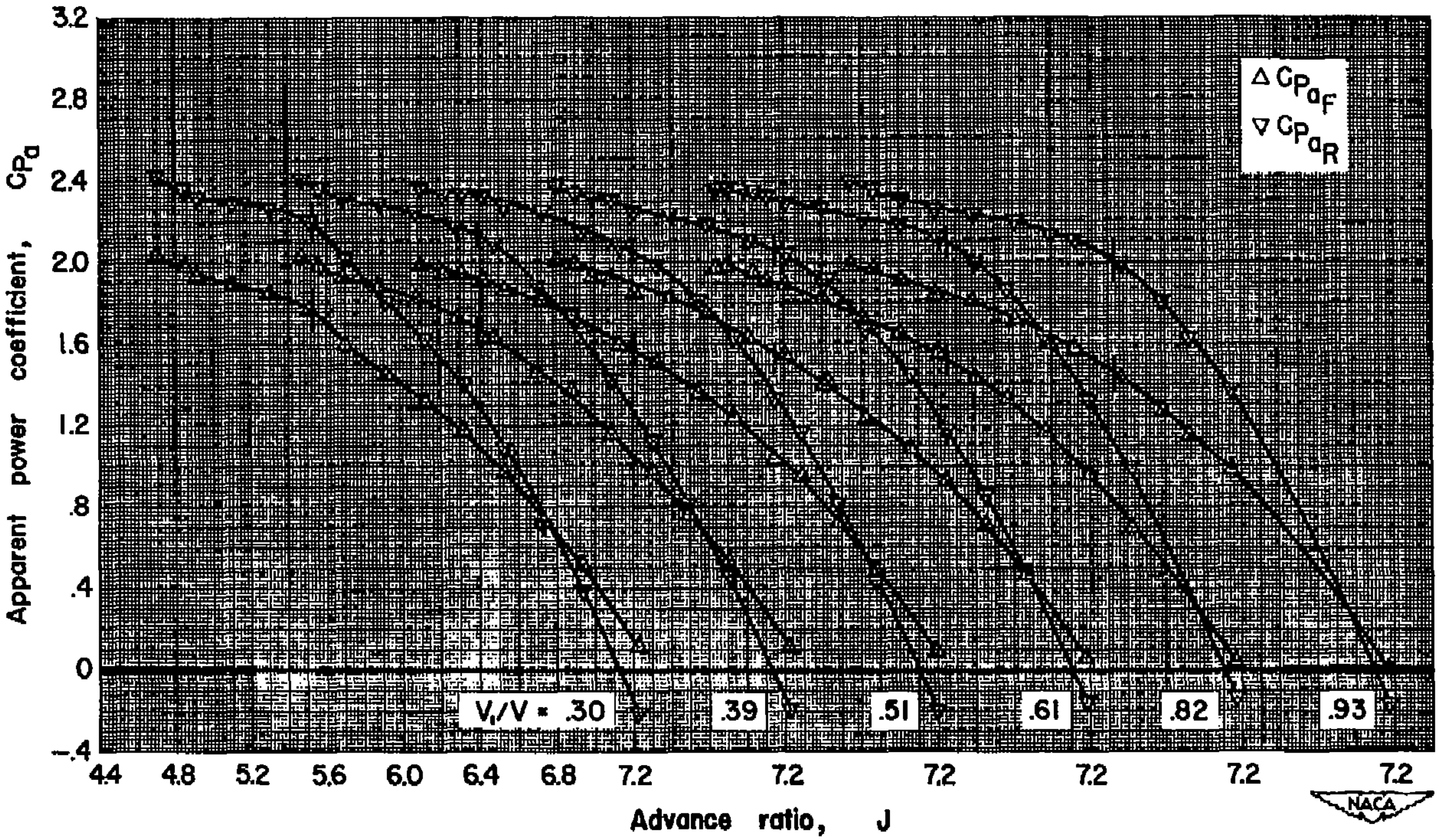

(o) $M = 0.80$; $\beta_F = 70^\circ$

Figure 19.– Continued.

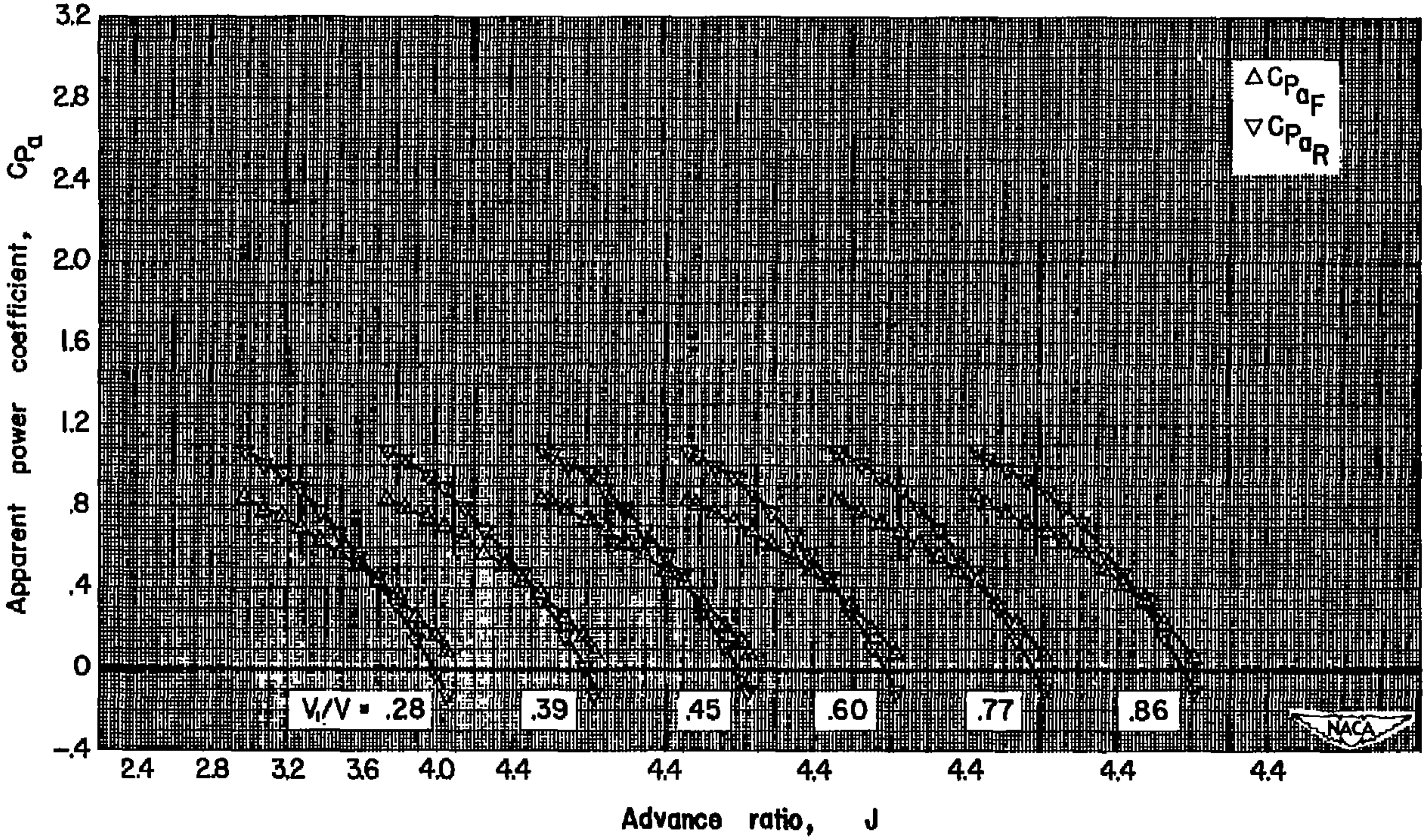

(p) $M = 0.84$; $\beta_F = 60^{\circ}$

Figure 19.– Continued.

[redacted]

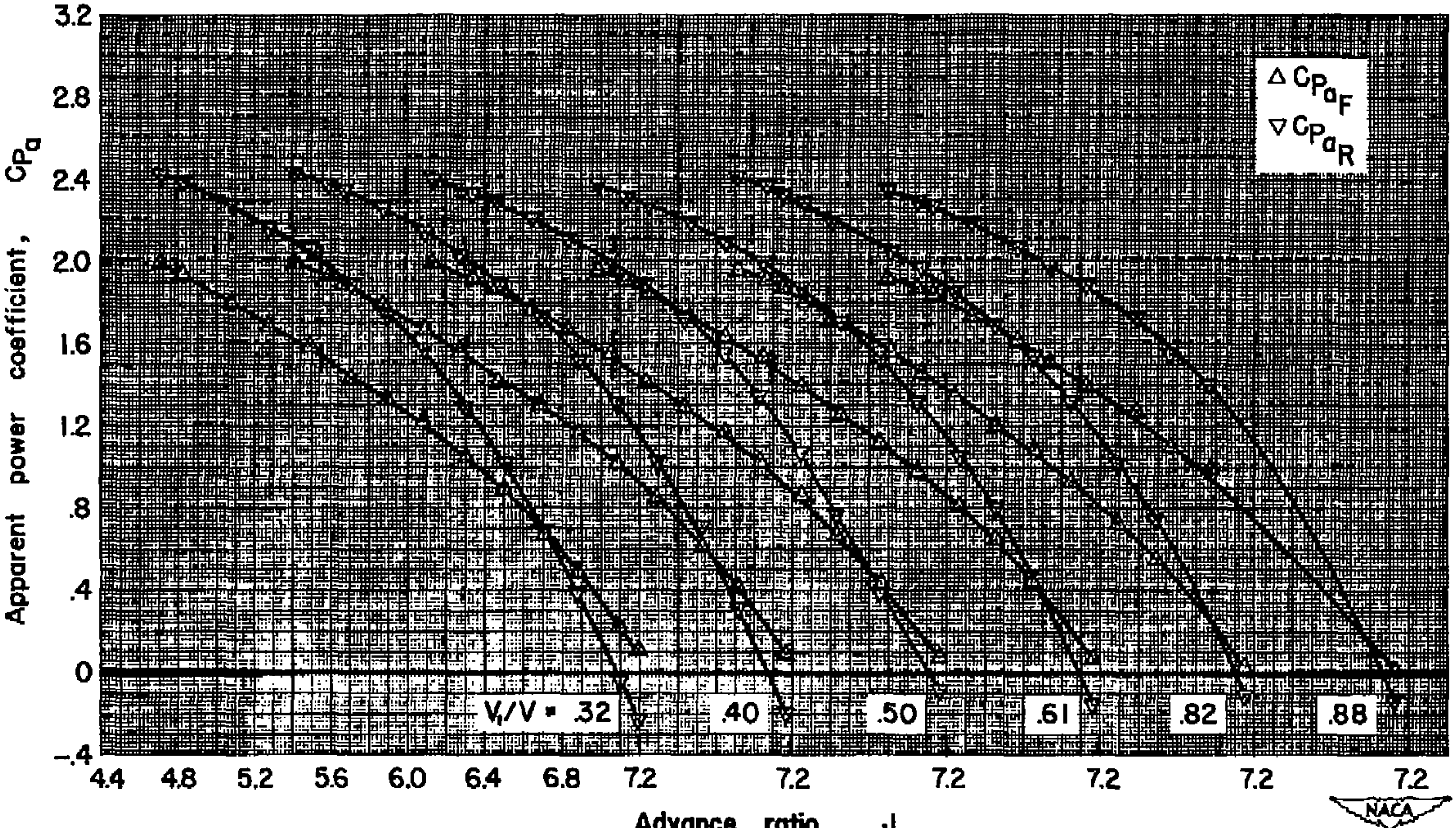

(q) $M = 0.84$; $\beta_F = 70^{\circ}$

Figure 19.– Concluded.

[redacted]

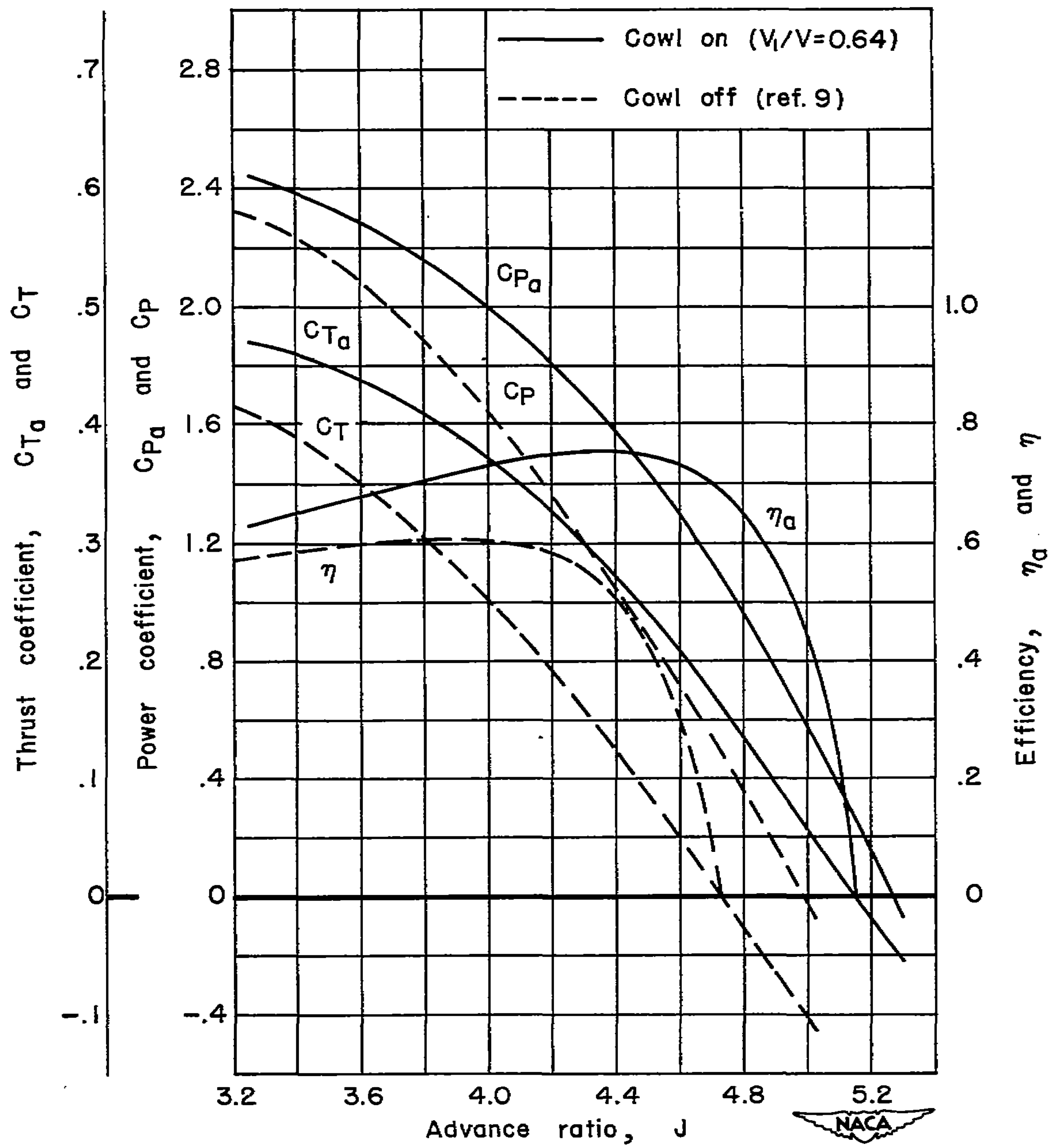

Figure 20.- The effect of the cowl on the basic characteristics of the six-blade dual-rotation propeller; M = 0.80, β_F = 65°.

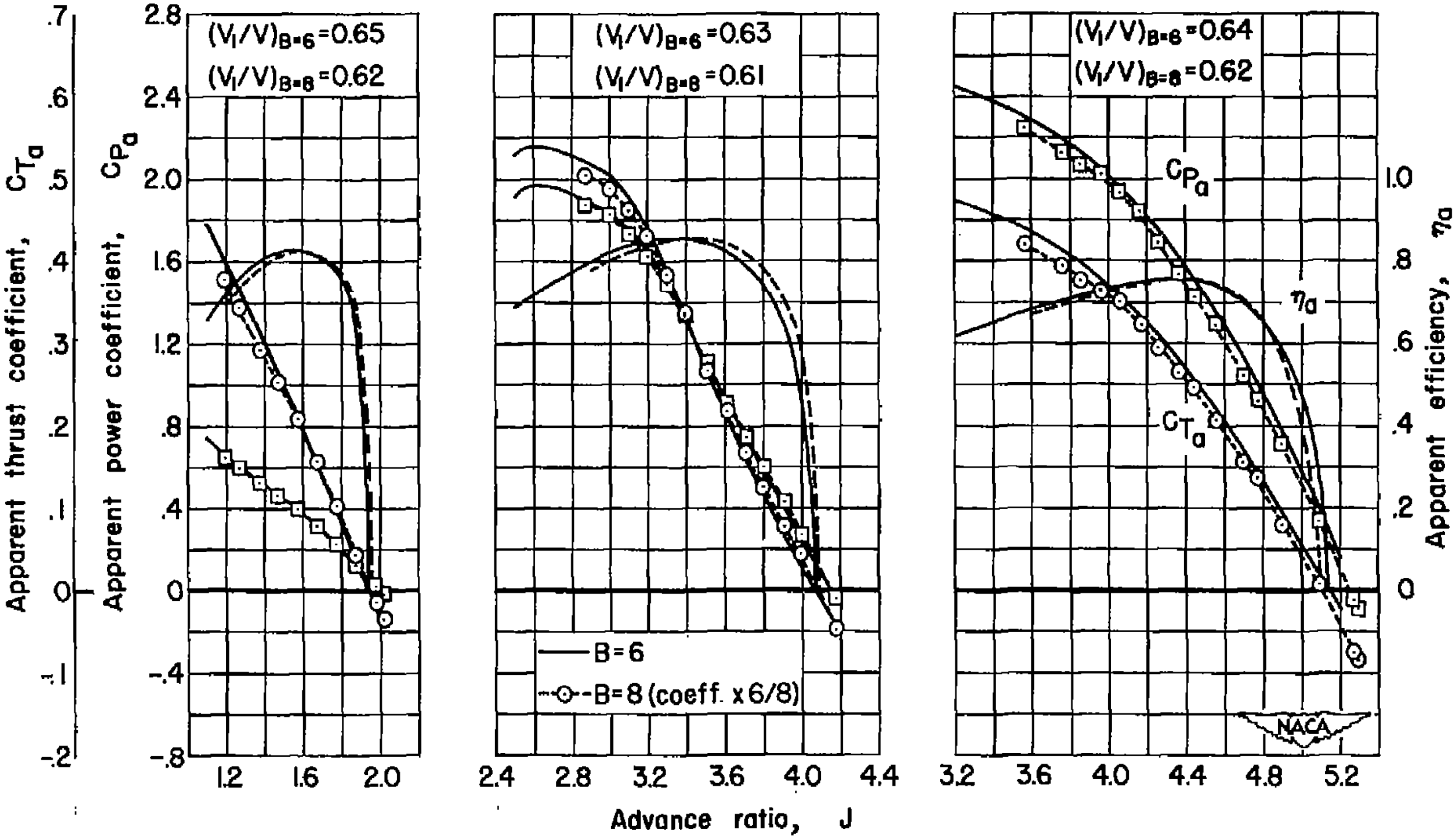

(a) M = 0.30; β_F = 40°

(b) M = 0.60; β_F = 60°

(c) M = 0.80; β_F = 65°

Figure 21.– Comparison of the characteristics of the six- and eight-blade dual-rotation propellers operating in the presence of the cowl.

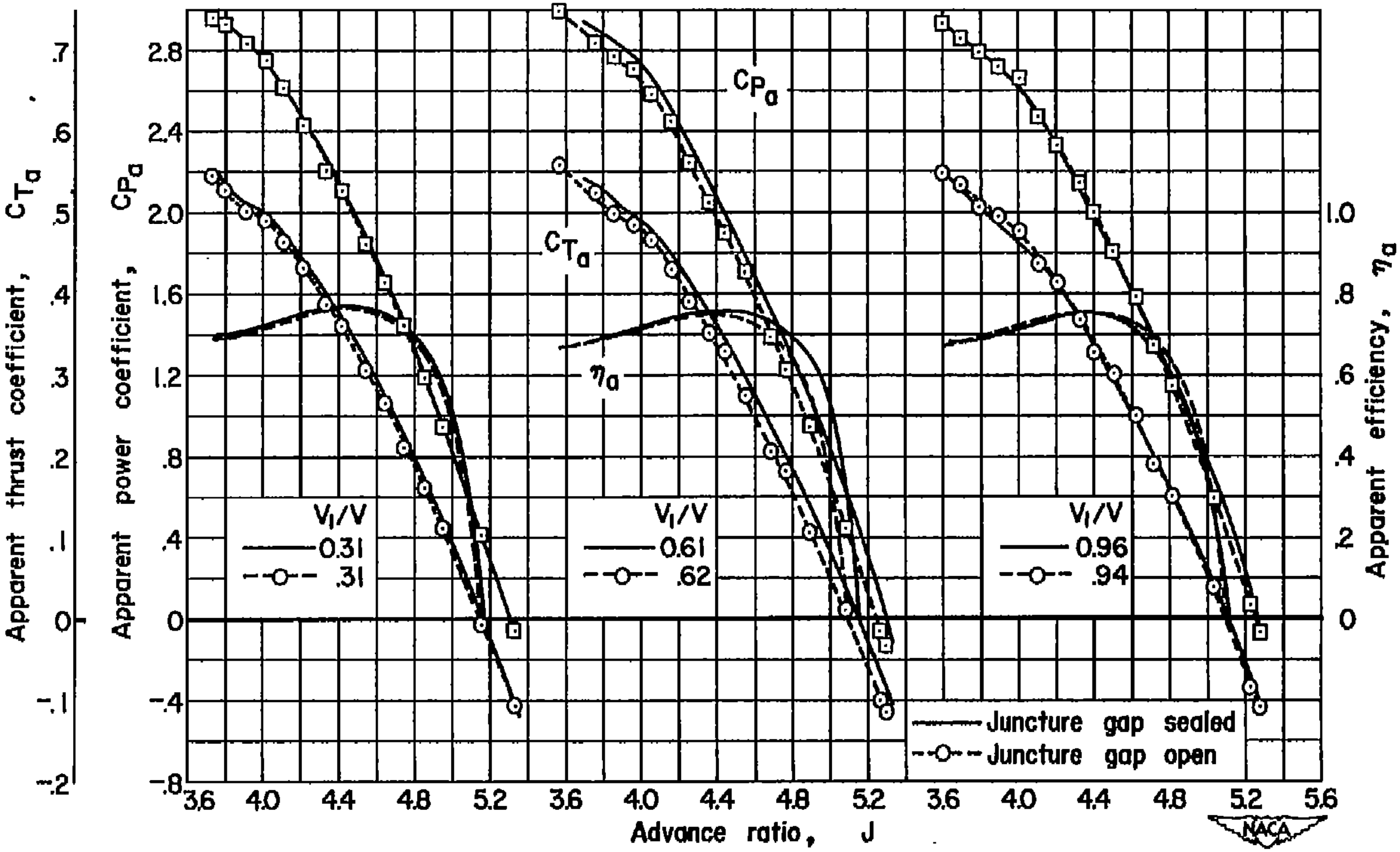

Figure 22.- The effect of sealing the propeller-platform gap on the characteristics of the eight-blade dual-rotation propeller; M = 0.80; β_F = 65°.

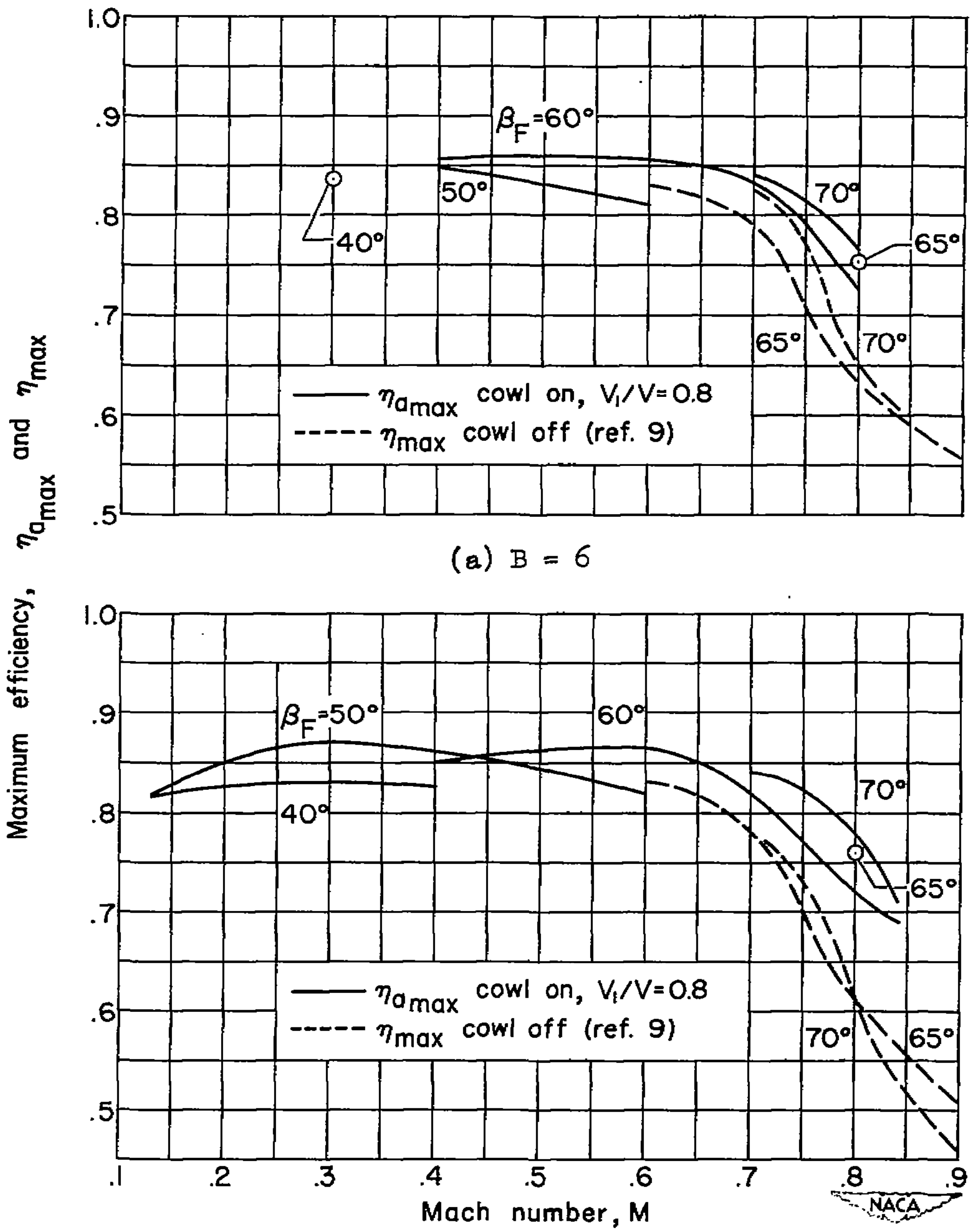

(a) B = 6

(b) B = 8

Figure 23.– Effect of Mach number on the maximum efficiency of the propellers.

[redacted]

[redacted]

[redacted]